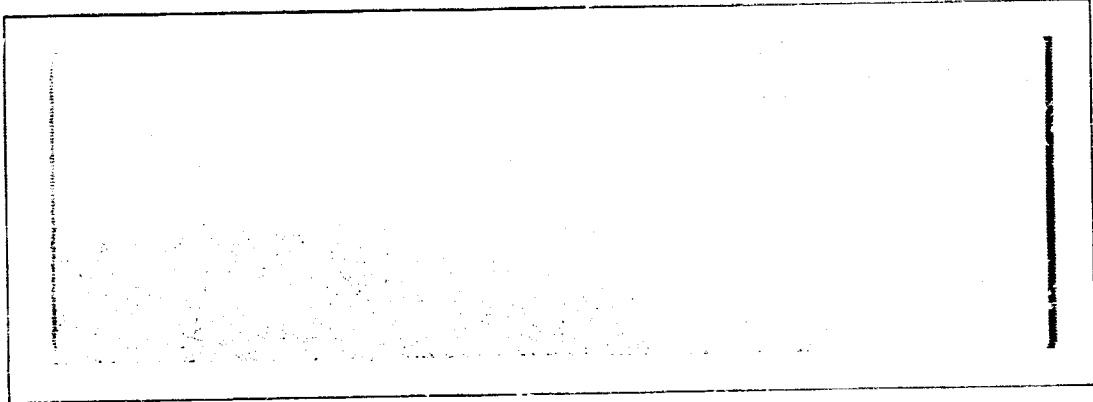
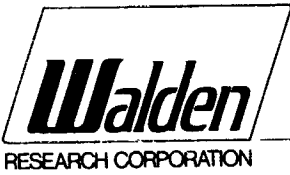


General Disclaimer

One or more of the Following Statements may affect this Document

- This document has been reproduced from the best copy furnished by the organizational source. It is being released in the interest of making available as much information as possible.
- This document may contain data, which exceeds the sheet parameters. It was furnished in this condition by the organizational source and is the best copy available.
- This document may contain tone-on-tone or color graphs, charts and/or pictures, which have been reproduced in black and white.
- This document is paginated as submitted by the original source.
- Portions of this document are not fully legible due to the historical nature of some of the material. However, it is the best reproduction available from the original submission.



FACILITY FORM 602

N71-15533

(ACCESSION NUMBER)

135

(PAGES)

CR-115895

(NASA CR OR TMX OR AD NUMBER)

(THRU)

RS

(CODE)

B

(CATEGORY)



MULTIVARIATE REGRESSION ANALYSIS OF
ATMOSPHERIC DENSITY IN THE REGION
30 TO 110 km

Paul Morgenstern and Ronald G. Orner

October 1970

Prepared under Contract No. NAS12-2125
DEVELOPMENT OF MODEL ATMOSPHERES
FOR THE REGION 30 TO 200 km

WALDEN RESEARCH CORPORATION
Cambridge, Massachusetts

Prepared for
Electronics Research Center
NATIONAL AERONAUTICS AND SPACE ADMINISTRATION
Cambridge, Massachusetts

TABLE OF CONTENTS

	<u>Page</u>
SUMMARY	1
INTRODUCTION	1
DATA SOURCE AND PRELIMINARY PROCESSING STEPS	3
Data Sample	3
Preliminary Data Processing	8
DIURNAL VARIATIONS IN ATMOSPHERIC DENSITY	23
Description of Stratification Scheme	23
Statistical Calculation	30
Plotted Results	31
METHOD OF ANALYSIS	65
Multiple Regression	66
Computer Programming	70
SELECTION OF BASIC VARIABLES	70
DISCUSSION OF RESULTS	72
Initial Analysis	72
Second Analysis	75
Third Analysis	80
Fourth Analysis	82
CONCLUSIONS	87
RECOMMENDATIONS	88
REFERENCES	89
APPENDIX A	92
B	93
C	97
D	112

MULTIVARIATE REGRESSION ANALYSIS OF ATMOSPHERIC DENSITY IN THE REGION 30 TO 110 km

by Paul Morgenstern and Ronald G. Orner

Walden Research Corporation
Cambridge, Massachusetts

SUMMARY

Density-altitude profiles from 437 rocket soundings for various portions of the altitude interval 30 to 200 km have been statistically studied for the detection of systematic time and space variations. The investigation also considered possible relationships between upper atmospheric density changes and variations in electromagnetic and corpuscular solar radiation. Multivariate regression analysis techniques were used to test for significant independent variables and to develop empirical prediction equations.

Below 65 km, seasonal effects weighted by latitude account for almost all significant density variations. There is a mid-region at about 65 km where diurnal as well as seasonal effects explain most of the variation, and at the high altitude region above 75 km, extra-terrestrial effects appear to become more important. The seasonal variations show a lag effect which decreases with height from 30 to 65 km. The diurnal variations near 65 km indicate a latitude dependence with peak densities near midnight at high latitudes and near midday at low latitudes.

INTRODUCTION

A knowledge of time and space variations in atmospheric properties above 30 km (about 100,000 feet) altitude is becoming increasingly important in the planning of various scientific experiments and the design of aerospace vehicles. The basic means of obtaining such knowledge is to study the atmospheric data gathered at various times and locations about the earth. Of the three thermodynamic properties of the atmosphere observed at high altitudes - temperature, pressure and density - temperature is commonly the more directly observed property up to about 60 km, while the density (mass density or number density) is more commonly directly observed above 60 km, particularly at altitudes above 100 km (about 300,000 feet). In addition, density is the atmospheric property which more directly influences certain space operations, such as reentry of space vehicles. Consequently, the study of the variability of this atmospheric property is of prime practical importance.

The objective of the current study program is to provide more comprehensive estimates of the space and time variations of atmospheric

density in the height region 30 to 200 km than have heretofore been available. The upper half of this region, that is the height interval 90 to 200 km, is conspicuously deficient in observational evidence to support existing models. Below 90 km the atmosphere is known to exhibit important latitudinal and seasonal density variations with evidence of an isopycnic layer in the vicinity of 90 km. Diurnal variations between 30 and 90 km have not been clearly identified although there are reasons to suspect that they do exist. Thus, it is evident that substantial gaps exist in our knowledge of the 30 to 200 km region and further investigation is required.

The region above 200 km has been shown to exhibit systematic latitudinal, seasonal, and diurnal density variations (Ref. 1). Analyses of satellite drag-acceleration data above 200 km also have shown a dependence of density on both solar and geomagnetic activity (Ref. 1). The present study is designed to search for similar relationships at the lower altitudes.

Several recent model atmosphere studies have used the technique of stratifying the total data sample of upper atmospheric soundings into discrete space and time intervals based on a selected set of classification criteria (Refs. 2 and 3). These quasi-homogeneous data cells then were statistically analyzed for systematic variations by permitting one factor to change while holding all others constant.

The analysis technique of sub-classification, although simple in its application, possesses several fundamental limitations, the most serious of which is the large number of cases required for establishing conclusive results. For example, to test the significance of only three independent variables such as season, time of day, and latitude, which are stratified into four, two and four groupings, respectively, yields a total of 32 subclasses. Testing for significant differences between these classifications necessitates that each contain sufficient sample sizes to provide reliable statistical estimates. This problem is particularly troublesome if the differences to be detected are small, such as in the case of diurnal variations. As other factors are added to the analysis problem, the total data sample required rapidly increases beyond practical bounds.

A second disadvantage of the sub-classification method is that the class limits must be established in advance on the basis of generally incomplete information. The principal physical mechanisms operating in the upper atmosphere to produce density changes are not fully identified and, thus, the establishment of class intervals must be made in a somewhat arbitrary manner. Although Minzner and Morgenstern (Ref. 2) have suggested a complex scheme for classifying atmospheric density from rocket launches by season, time of day and latitude of the launch site, this system was subject to the validity of the assumptions on the time delays in atmospheric effects.

Finally, the method of subclassification has the shortcoming that it provides no functional relation between the independent variables and density variations which can be used for prediction or interpolation purposes.

For these reasons, the method of sub-classification does not serve as a satisfactory analysis technique where many variables are involved. At the same time it is important to note that the method does possess the advantage that no a priori assumption on the form of the cause-effect relationship is required. In particular this fact simplified the task of including non-linear processes in the analysis.

Many of the limitations inherent in the stratification method described above for analyzing the density data may be overcome by using an alternate method of analysis. In particular multiple regression methods present several features which are attractive to the current application. One of the principal advantages multiple regression analysis techniques possess is that the entire sample can be considered simultaneously as opposed to the method of partitioning the data into subsets. This feature facilitates extracting all the statistical information contained in a given sample. Multiple regression techniques also permit analysis of the data by considering the independent variables to be continuous ones rather than discrete variables. This characteristic is decidedly more desirable in dealing with the interpretation of geophysical parameters. Finally, the adaptation of multiple regression techniques to automatic data processing systems coupled with a stepwise screening procedure permits a rapid evaluation of the statistical significance of many different independent variables in terms of their utility in explaining observed upper altitude density variations.

The current study is very much analogous to the work reported by DeVries, Friday and Jones (Ref. 4). These authors considered the problem of analyzing density data derived from tracking information of several low altitude satellites in the height region 160 to 210 km. Multiple regression analysis techniques in conjunction with a stepwise screening procedure were used to investigate the existence of significant periodic relationships as well as the influence of other geophysical variables. The current study has been designed to follow a similar research plan only the application is to data obtained by rocket soundings over the 30 to 200 km height region.

The authors wish to acknowledge the assistance of Professor E. N. Lorenz for his valuable suggestions during the course of this study.

DATA SOURCE AND PRELIMINARY PROCESSING STEPS

Data Sample

A total of 437 soundings covering the period 1947 to early 1965, assembled previously under earlier study programs (Ref. 5), were used for the current analysis. This basic data was originally collected from 45 different sources including journal articles, institutional reports and private communications. Table I gives an inventory of the soundings showing

TABLE I

INVENTORY OF ATMOSPHERIC DATA BY SITE

Site Name	Code	Lat.	Long.	LST Hrs.	Number of Soundings
Albuquerque, N. Mexico	AQ	35.05N	106.40W	GMT-07.0	26
Ascension I., Atl. Ocean	AI	07.98S	014.42W	GMT-00.0	44
Barking Sands, Hawaii	BS	22.05N	159.78W	GMT-10.0	6
Carnarvon, W. Australia	CA	24.82S	113.87E	GMT+08.0	9
Eglin AF Base, Florida	EG	30.38N	086.70W	GMT-06.0	74
Ft. Churchill, Manitoba	FC	58.73N	093.82W	GMT-06.0	49
Guam, Mariana Is.	GM	13.62N	144.85E	GMT+10.0	7
Heiss I., Franz Jos. Land	HI	80.62N	058.13E	GMT+05.0	25
Holloman AFB, N. Mexico	HA	32.85N	106.10W	GMT-07.0	6
Kapustin Yar, USSR	KY	48.6 N	045.8 E	GMT+04.0	2
Kwajalein I., Marshall Is.	KW	08.73N	167.73E	GMT+12.0	23
McMurdo Sound, Antarctica	MC	77.88S	166.73E	GMT+11.0	20
Point Mugu, California	PM	34.12N	119.12W	GMT-08.0	3
Ship A, Eq. Pacific Ocean	SA	00.18N	161.42W	GMT-11.0	1
Ship B, N. Atlantic Ocean	SB	62.06N	063.92W	GMT-04.0	1
Ship C, Lancaster Sound	SC	74.57N	094.48W	GMT-05.0	1
Ship D, N. Atlantic Ocean	SD	54.0 N	053.33W	GMT-04.0	2
Ship E, N. Atlantic Ocean	SE	58.43N	055.06W	GMT-04.0	2
Ship F, N. Atlantic Ocean	SF	49.0 N	048.4 W	GMT-03.0	2
Ship G, N. Atlantic Ocean	SG	57.8 N	046.7 W	GMT-03.0	2
Ship H, N. Atlantic Ocean	SH	65.6 N	058. W	GMT-04.0	2
Thule, Greenland	TH	76.55N	068.82W	GMT-04.0	5
Wallops I., Virginia	WI	37.83N	075.48W	GMT-05.0	59
White Sands, New Mexico	WS	32.28N	106.48W	GMT-07.0	25
Woomera S. Australia	WO	31.11S	136.97E	GMT+09.5	41

the number available from each of 25 different launch sites. With the exception of three flights, data published in the reports of the Meteorological Rocket Network (MRN) (Ref. 6) were not taken as the basic source of data in this study. MRN reports do, however, contain the same or revised forms of data for a considerable number of soundings used in this study.

Measurement techniques.- Table II lists several of the measurement techniques that have been used to obtain the soundings contained in the current sample, indicating the altitude range of applicability of the technique and giving estimates of the associated measurement errors (Ref. 7). The primary thermodynamic parameter sought differs between these various methods, but if this property is determined over an extended altitude region, the altitude profile of the parameter measured can be used to derive altitude profiles of the other properties (see Ref. 2). Profiles of density versus altitude alone generally are sufficient to perform the requisite mathematical operations to deduce the other variables. The conversion of temperature-altitude profiles requires an additional piece of information containing a reference-level value of pressure (or of density). This information is normally obtained by means of a balloon borne radiosonde which is released in conjunction with the rocket probe. The information derived from the balloon radiosonde not only yields a reference value for processing the rocket derived observations, but also provides a mechanism for extending the thermodynamic profile of the atmosphere over the entire balloon-rocket observation range. This procedure is widely used in current applications by the stations of the Meteorological Rocket Network.

To preserve the integrity of the observations, atmospheric sounding data most frequently are published for the actual altitudes of the measurements. The current statistical study, however, requires that those data be normalized to a common set of altitudes. The procedures used to interpolate the basic source data into density profiles at successive integer geopotential altitudes has been described by Schultz (Ref. 8). These interpolated records were the initial data base for the current investigation.

Distribution of the soundings in time and space.- The frequency distribution of the 437 soundings as a function of time of year and launch site location is present in Table III. A discussion of the diurnal distribution of the soundings as well as a description of the special seasonal, latitudinal, and diurnal classification scheme used to categorize the soundings are given in the next section. The summaries in Table III, however, clearly indicate that the predominate source of these data are from launch sites located in sub-tropical latitudes. The seasonal distribution of these soundings shows a peak during the autumn months and a minimum during the winter months.

TABLE II

HIGH-ALTITUDE MEASUREMENT OF ATMOSPHERIC PARAMETERS (See Ref. 7)

Basic Methods and Measurement	Primary Data Sought	Error	Secondary Data	Range of Altitude
Pressure Gauge (side of rocket) (nose cone)	Pressure	Below 75 km; error less than 10% Above 75 km; error may be 100%	Density Temperature	30-120 km
Pressure Stagnation (nose tip of rocket)	Density	Error less than: 20%	Pressure Temperature	30-100 km
Supersonic flow around a right circular cone	Temperature	Below 50 km, $\pm 5K^\circ$ Above 50 km, $\pm 7-15K^\circ$	Pressure Density	30-90 km
Pressure Modulations on rolling rocket	Density	Errors varied between 20% and 100%		above 120 km
Rocket Grenades (transit time of sound wave)	Temperature Winds Speed Direction	Less than 3% ($\pm 5K^\circ$) ± 10 m/sec $\pm 18^\circ$		30-80 km 30-80 km
Falling Sphere Drag Acceleration	Density	Less than 10%	Temperatures Pressure	30-100 km
Anomalous Sound; Sound Wave Refraction	Winds Temperature	$\pm 5K^\circ$		25-50 km
Searchlight-Probing	Density	1 to 5%	Temperature Pressure	10-65 km

NOTE: Rocket experimental data may contain one or more errors due to: wind, yaw, outgassing, and spin.

TABLE III
 DISTRIBUTION OF SAMPLE SIZE WITH
 LATITUDE AND SEASON

	W I N T E R	A U T U M N	S U M M E R	S P R I N G	TOTAL
ARCTIC	14	8	17	12	51
SUBARCTIC	19	16	16	7	58
MIDLATITUDE	15	13	21	14	63
SUBTROPICAL	23	75	41	45	184
TROPICAL	10	29	20	22	81
TOTAL	81	141	115	100	437

The variety of instrumentation techniques used to obtain these soundings also introduces a heterogeneity in the altitude region over which the observations are available. A review of the effective altitude range for these measurement techniques as given in Table II, shows the degree of overlap between the various systems. The distribution of sample size as a function of altitude for the 437 soundings is given in Table IV and illustrates a marked maximum near 55 km with a rapid drop in measurements above 85 km. The frequency distribution given in Table IV reflects the editing of the original data which was performed in this study, and is discussed in detail below.

Preliminary Data Processing

Several preliminary operations were performed on the basic sounding data in preparation for the statistical analysis part of the study. The objective of this preliminary work was three-fold: (1) to check the quality of the data by screening the observations and applying appropriate editing to suspect values, (2) to merge the density-altitude profiles with supplementary information to be used as independent variables in the multiple regression analysis, and (3) to format the records into a structure convenient for the subsequent statistical processing. A brief description of the procedures used for each of these steps is presented in the following sections.

Checking and editing.- The basic data set used for analysis in this investigation had been subjected to screening and editing in previous studies of related upper-atmosphere problems (Ref. 2). It is desirable to review briefly the editing performed in this earlier work before describing the additional testing conducted in the current program.

The originally published forms of the soundings used had the common feature of density-altitude profiles $\rho(z)$ in one of a number of systems of units. These were all converted to the mks system for uniformity of units. In addition, the density altitude data were used to derive new temperature altitude profiles for each sounding using a numerical integration procedure described by Minzner and Sauerman (Ref. 9). The complete set of soundings were published in separate scientific technical report by Minzner, Morgenstern and Mello (Ref. 5).

The calculated temperatures served as a basis for checking the quality of the density data and for verifying the key-punching accuracy. The procedure used consisted of comparing the computed temperatures with (1) interpolated values of the temperatures from the U. S. Standard Atmosphere (Ref. 10), and (2) with the originally published temperatures when these were available. The differences between the several temperature profiles were then reviewed noting large differences or any abrupt change in differences from one level to the next. Such situations result from abnormal vertical density gradients, and suggested keypunch errors or other difficulties in the basic data cards. The related basic data were then checked and corrected when necessary.

TABLE IV
DISTRIBUTION OF SAMPLE SIZE WITH ALTITUDE

HEIGHT (km)	SAMPLE SIZE	HEIGHT (km)	SAMPLE SIZE
30	145	120	13
35	197	125	13
40	220	130	13
45	277	135	13
50	298	140	12
55	303	145	12
60	285	150	13
65	215	155	10
70	171	160	10
75	155	165	10
80	131	170	12
85	104	175	12
90	66	180	11
95	57	185	10
100	41	190	10
105	38	195	10
110	23	200	9
115	22		

Some observed density data were shown by the temperature test to have a very erratic behavior, which most likely was not real but probably represented the uncertainty in some phase of the measurement. Where such erratic observations resulted in density inversions, i.e., density increasing with increasing altitude, the data were either eliminated or smoothed in one of two ways: (1) in a selective smoothing process, individual data points were adjusted to eliminate isolated density inversions, and (2) in a number of other instances where many inversions existed within a sounding, a third-order root-mean-square fit was made of the entire sounding. Soundings containing identical densities for two successive levels yielded impossible temperatures at the lowest of these levels, and these cases were eliminated by selective adjustment of density-data pairs.

The sounding profiles as modified from their original published values by the procedures described above, were subjected to further screening in the present study to identify questionable individual measurements. The reason for this emphasis on even eliminating individual erroneous data points within a sounding, was that a subsequent step in the preliminary data processing plan consisted of smoothing the profiles to remove selected wave number components. Although the amplitude of an undetected, large spurious value contained in the profiles would be reduced by this smoothing, the smoothing operation also would tend to transmit some of the error into adjacent altitudes. This effect is an undesirable one for any subsequent regression analysis of the data and, therefore, further checking of the data appeared advisable.

To facilitate the screening process each sounding was machine plotted for graphic display of the individual data points. The graphs were constructed by calculating and plotting the percent departure between the density-altitude values of the given sounding and an idealized profile based on averages for the entire set of 437 soundings. This differencing scheme both linearizes the density scale and amplifies anomalous values.

Because the number of graphs to be generated was relatively large, a special purpose computer subroutine was developed which utilized the computer system printer as a high-speed plotter. Carriage spacing on the line feed was used to generate an integer height scale while the integer value of the percent density departure determined the print position for the data points. To eliminate the possible noise effect of sampling fluctuations in the reference sounding upon the percent density departure profiles, a smoothed mean reference sounding was generated. This reference profile was derived by applying a least square polynomial regression on the observed mean density profile.* After a certain amount of numerical experimentation, the following fourth-degree polynomial was obtained which yielded a very good approximation to the mean density (ρ) up to about 135 km,

*The regression actually was performed on the logarithms of the mean density profile.

$$\rho(z) = \exp (b_0 + b_1z + b_2z^2 + b_3z^3 + b_4z^4) \quad (1)$$

where

$$\begin{aligned} b_0 &= 0.2176377E+01 \\ b_1 &= -0.2723788E+00 \\ b_2 &= 0.2810370E-02 \\ b_3 &= -0.2329382E-04 \\ b_4 &= 0.6503292E-07 \end{aligned}$$

and (z) is the geometric altitude in kilometers. Equation (1) can be used to approximate the mean density profile as a function of geopotential altitude by substituting (h) for (z) where (h) is given by

$$h = \frac{R \cdot z}{R - z} \quad (2)$$

where R is an effective mean radius of the earth and has a value 6356.766 km (Ref. 1). Above 135 km the approximation given by Equation (1) became more unreliable, but still sufficiently adequate for evaluating the relatively few soundings in the data base which exceeded this altitude.

Examples of the graphs produced by this procedure are given in Figures 1 and 2. These examples have been selected to illustrate the features of the profiles which were checked further for possible errors. Figure 1 shows two data points at 47 and 48 km which are substantially different than the values only one kilometer above and below. A subsequent check of the original publication for this data indicated a transcription error and the correction was made in the current data. Figure 2 shows a profile measured by means of light scattering techniques (Ref. 11) and indicates a very sharp gradient above 60 km. Again a subsequent review of the original publication indicated that this measurement technique tends to become unreliable at these altitudes. Consequently all soundings using this measurement technique were truncated above 60 km.

A review of all the plotted profiles indicated that 45 of them required further editing. In each case the original source was consulted for confirmation of the data. In a number of these cases, the original investigator noted those segments of the sounding for which the data were considered questionable similar to the illustration given above. This information together with considerations of consistency, and known limitations in the measurement techniques provided the basis for editing these soundings. A listing of the editing performed is given in Appendix A.

Numerical smoothing.- It is easily recognized that the numerous sources of upper-air soundings and the variety of measurement techniques which are represented in the data sample assembled for this investigation constitute a

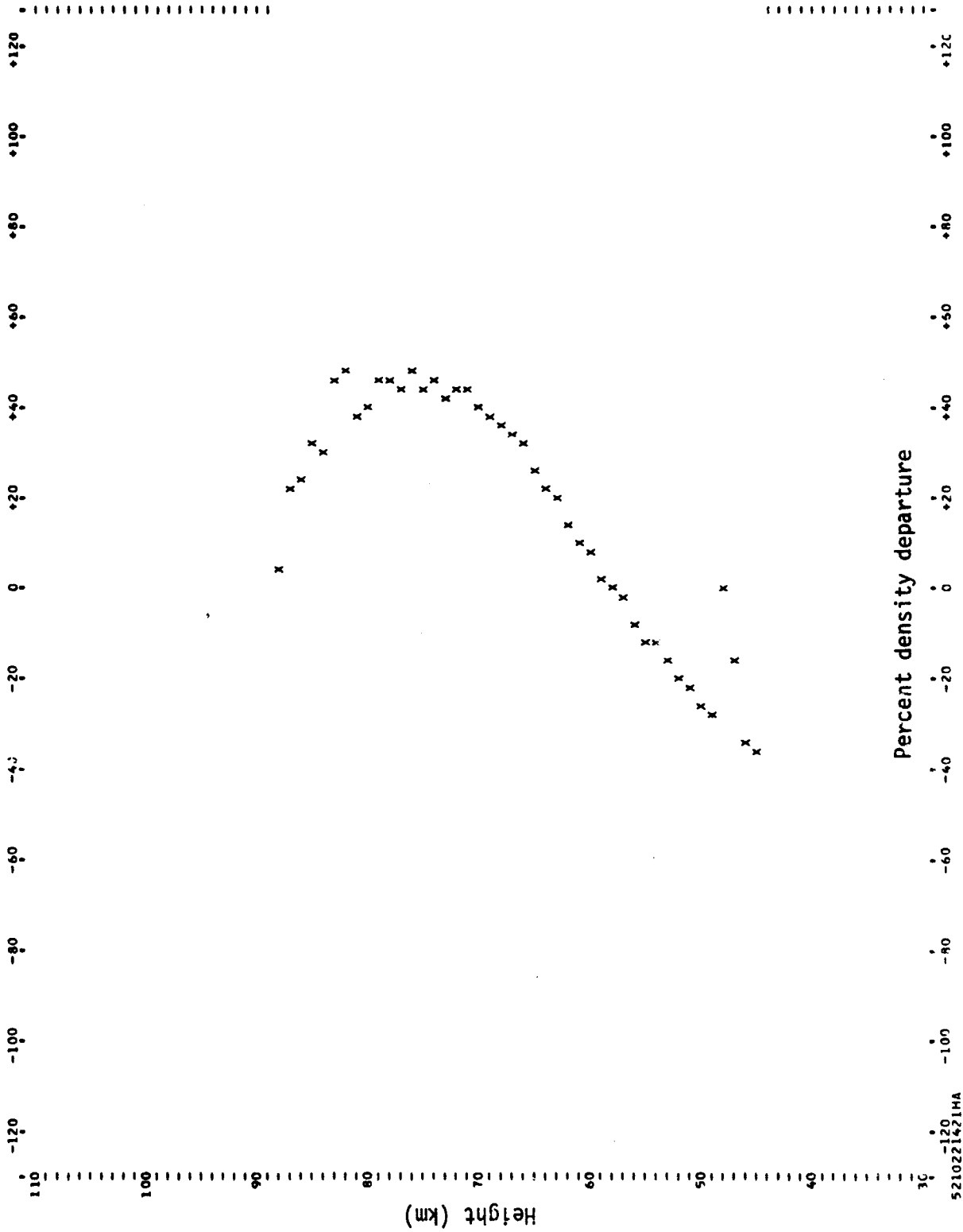


Figure 1.- Illustration of suspected errors near 50 km.

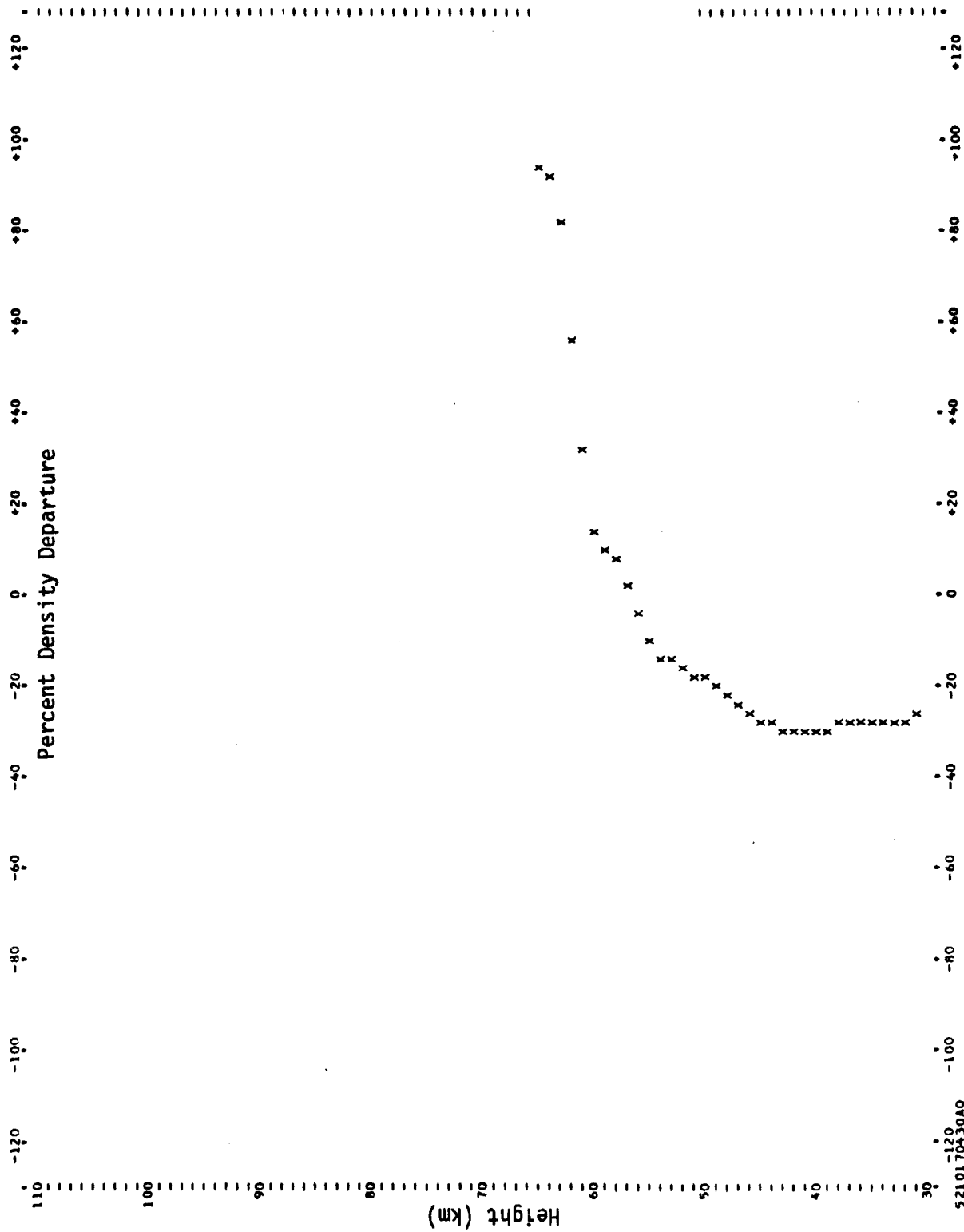


Figure 2. Illustration of suspected error near 60 km.

relatively heterogeneous data base. Not only do the measurement techniques and instrumentation differ, but in many instances data reduction procedures differ even when the same type of measurements are obtained. A preliminary smoothing of the density-altitude profiles to affect a greater degree of homogeneity of the data sample appeared highly desirable.

The methods of smoothing and filtering commonly applied to time series may be applied equally as well to space smoothing and filtering in one dimension, except, that the terms "wavelength" and "wave-number" (number of waves in a given distance) are used instead of period and frequency, respectively. Also in space smoothing in one dimension, the term "wave-number response" may be substituted for frequency response of the filter.

The objective of this smoothing is to attenuate the amplitude of high wave numbers or noise in the soundings without significantly affecting the more meaningful low frequency components. Hence, it will be necessary to prescribe a critical wave number above which the fluctuations are to be attenuated and below which they will pass unaltered.

In selecting a numerical filter or smoothing function several features of the response were considered. First, we require that the mean of the smoothed data remain unchanged from the mean of the original data. Second, it is desirable that the smoothing function does not shift the phase of waves over the range of wavelength under investigation. In addition, it is necessary to consider the effect of any side lobes which the filter possesses and, finally, we should be concerned with the computation problems of implementing the filter.

Generally, the smoothing function consists of a series of the fractional values or weights which are applied to the original data. The mean value of the data is preserved if this smoothing function is designed such that the sum of these weights is unity, while the phase of the waves will be unaltered by requiring that the smoothing function be an even one. A commonly used smoothing which satisfies these conditions is one in which the weights are proportional to the ordinates of the normal probability curve.

For greater computation convenience, the normal curve filter can be approximated rather closely by choosing the weights proportional to the coefficients in the binominal expansion of $(p+q)^m$. This follows from the well-known property that the envelope of these coefficients approaches the shape of the normal curve as (m) increases. The wave-number response of the binominal smoothing function is given by

$$R\{k\} = \cos^m(\pi k \Delta L) \quad (3)$$

where (k) is the wave number, and ΔL is the distance between consecutive data points. Brooks and Carruthers (Ref. 12) have described a very simple computational procedure for synthesizing the binominal smoothing function. This

technique is based on repeated application of the basic two-point filter consisting of the weights $1/2$ and $1/2$ to simulate higher powers of the binomial expansion. A modified form of this method was adopted in this study by using the elementary filter with normalized weights $1/4$, $1/2$ and $1/4$ corresponding to the binomial coefficients in the expansion of $(p+q)^2$. Figure 3 shows the wave-number response for a single pass and for multiple passes of this filter. The curve shows, for example, that the amplitude of oscillations with a wavelength of 5 km are reduced to 65 percent of the unfiltered value by a single pass of the filter. A triple application of the filter reduces these amplitudes to approximately 30 percent of their initial value, whereas a quintuple application reduces the amplitude of these fluctuations to only about 10 percent of their initial value. For oscillations of wavelength 20 km, corresponding to two scale heights at about 120 km altitude, the attenuations are 97, 93, and 89 percent, respectively.

As an initial test of these filters, approximately a dozen soundings were processed by a single pass and up to 10 multiple passes. Figures 4 through 6 illustrate the application of these filters to a typical atmospheric sounding derived from a falling-sphere experiment.* These graphs show the smoothed profile values plotted as percent departures from the reference mean to linearize the scale. The results from a single pass are seen still to contain substantial high wave-number components. Three passes have eliminated most of this, whereas five passes begin to effect the amplitude of some of the longer wave features of the profile. From these and other similar results, it appeared that three passes of the binomial filter removed most of the small scale fluctuations without major attenuation of the wavelengths greater than two scale heights. Hence this was the filter selected and applied to every sounding in the data set.

Merging with other parameters.- Jacchia (Ref. 13) has shown that the temperature in the atmosphere above 200 km is positively related to geomagnetic activity. Since one of the objectives of the current study is to determine whether similar relationships exist below 200 km, geomagnetic index data were collected for the current inventory of 437 soundings. The index of geomagnetic activity used is one developed by Bartels (Ref. 14). Bartels' index measures the range during a 3-hour interval of the most disturbed component (horizontal or vertical) of the geomagnetic field. His planetary index K_p is calculated as an average from 12 selected observations wherein each of the individual site values have been standardized to compensate for local anomalies. The scale of this index is a geometrically increasing one designed to correspond to the latitude variation in the intensity of magnetic disturbance. It has the range 0 to 9 in twenty-seven equal steps.

Three-hour values of the planetary geomagnetic index have been published continuously in the Journal of Geophysical Research since 1949. These data

*The filter was applied to the logarithm of the density values.

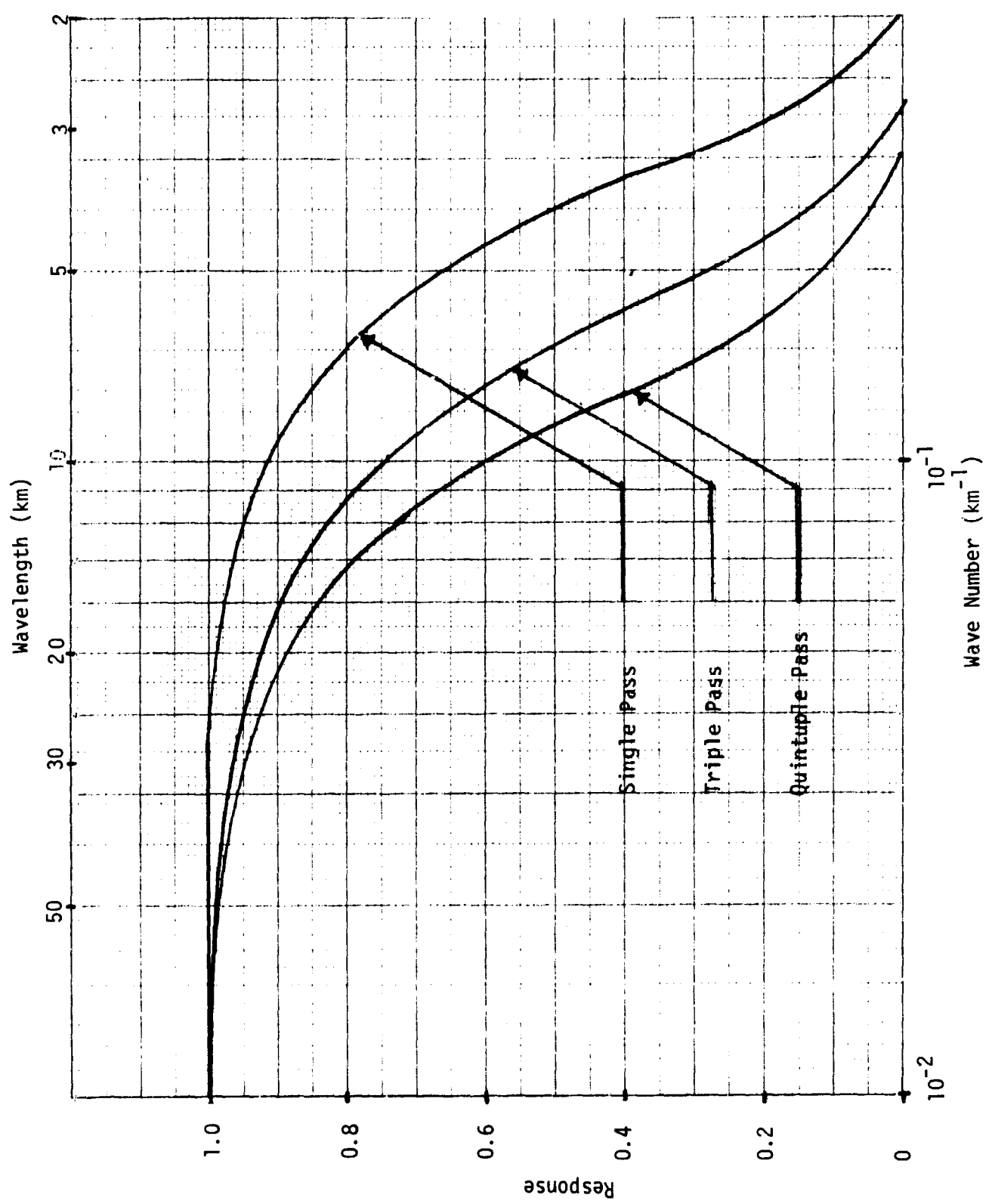


Figure 3. Wave number response of elementary (1-2-1) binomial filter for single, triple and quintuple passes.

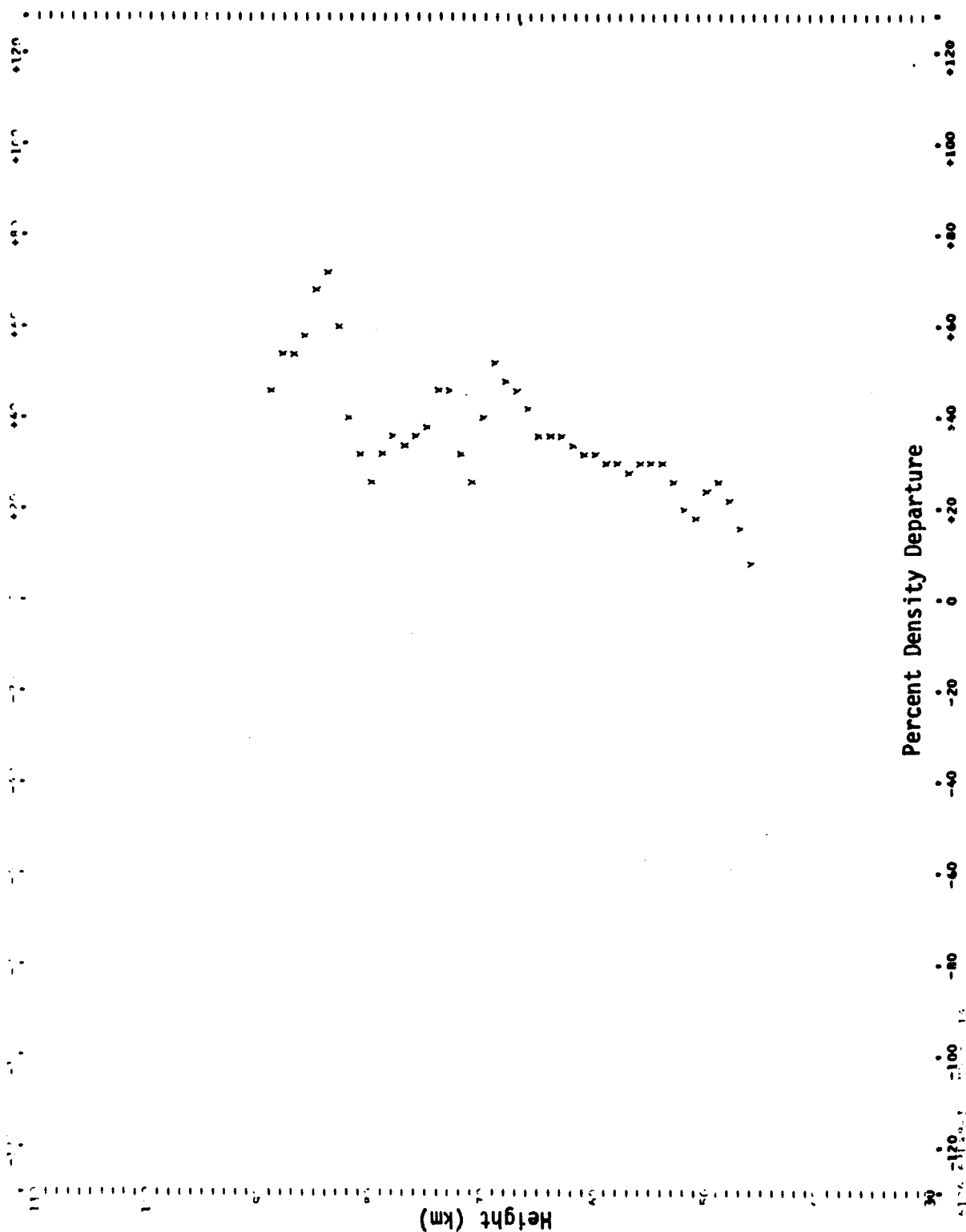


Figure 4. - Single pass of binomial filter on typical falling sphere sounding

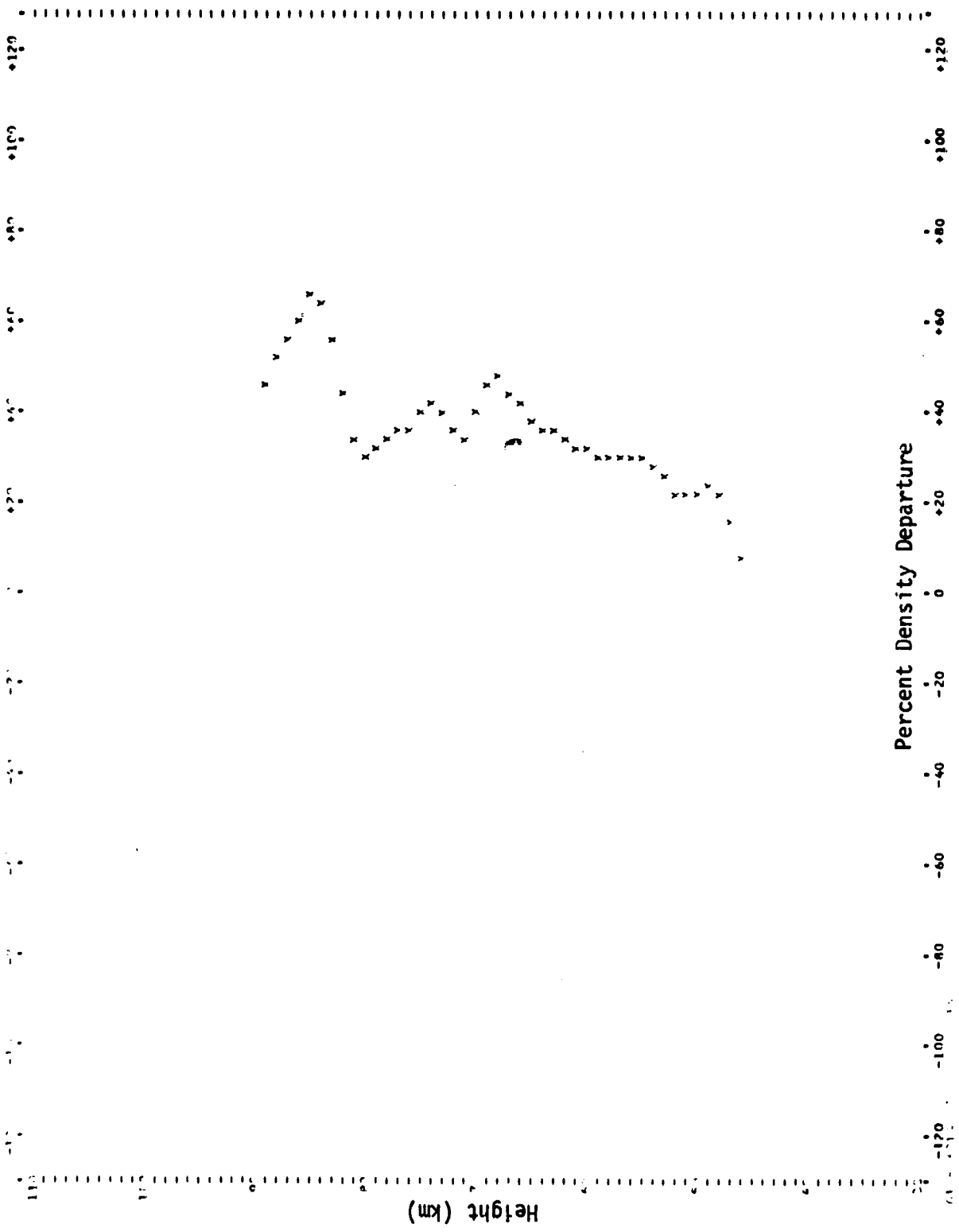


Figure 5 - Triple pass of binomial filter on typical falling sphere sounding

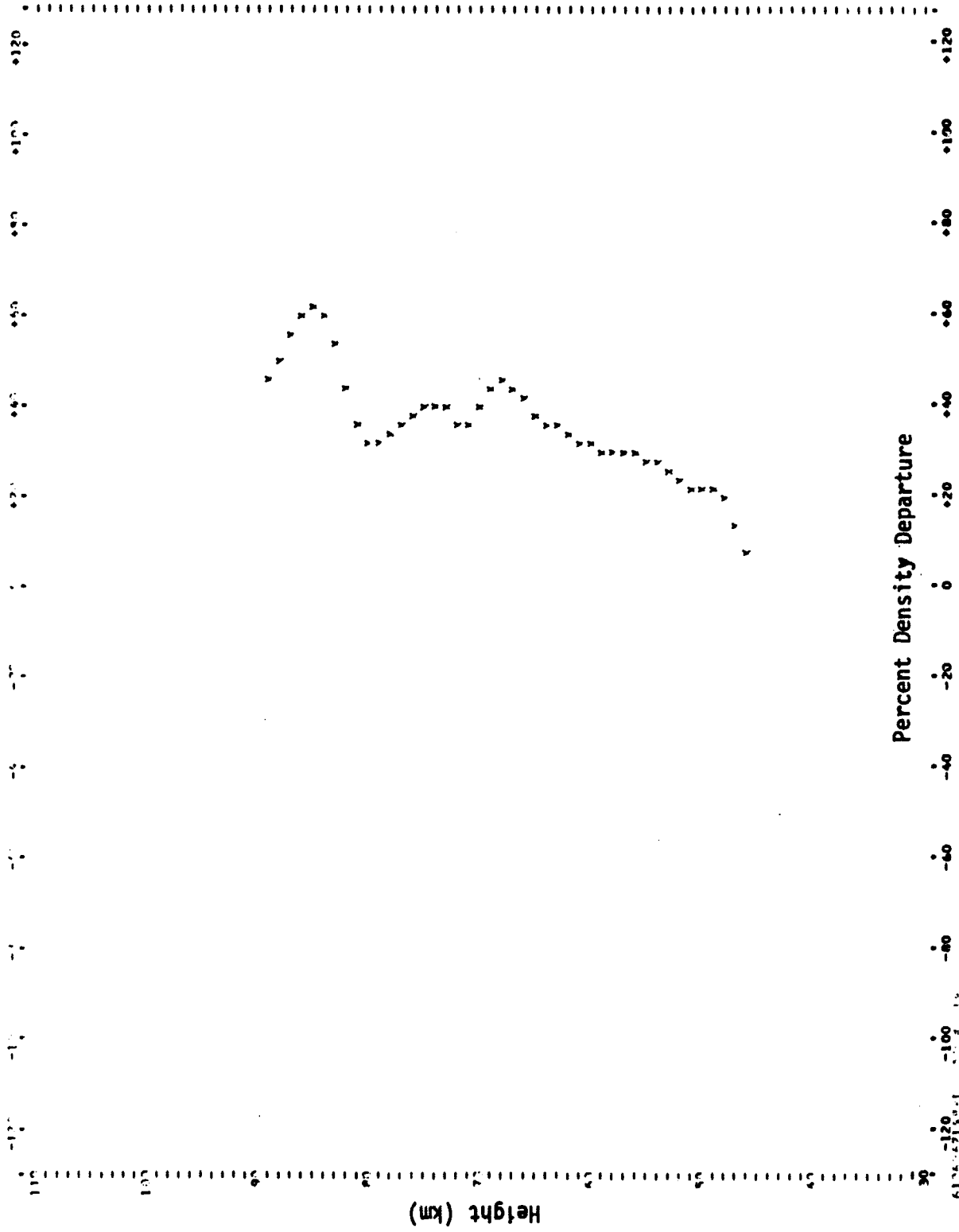


Figure 6 - Quintuple pass of binomial filter on typical falling sphere sounding

were abstracted for the three-hour period, bracketing the launch date and time of the soundings. In addition, the eight previous 3-hour values have been abstracted to permit an investigation of lag relationships. Appendix B provides a listing of these data.* Each sounding is identified by a date-time-site sequence followed by the K_p index starting with the previous 24-hour value and ending with the index observed during the three-hour period bracketing the launch time.

The quasi-logarithmically scaled K_p index may be converted to a linear "equivalent amplitude" scale a_p (in gammas) by means of the conversions given in Table V. K_p values given in Appendix B were converted to values of a_p by means of a computer program and merged with the basic sounding records.

To facilitate the investigation of functional relationships between atmospheric density and time, it is more convenient to express time as a continuous variable rather than as a sum of years, days and months. A conventional way of doing this is to express the date and time of the soundings by their Julian date. The Julian date gives a continuous count of time elapsed since Greenwich mean noon on January 1, 4713 B.C.; for example, the Julian date on January 1, 1952 is 2,437,665.5.

The Julian date in terms of days and fractions of a day was calculated for the Greenwich mean time and the local apparent time of each sounding. These values were added to each record of the data set. In addition, the Julian day number for the first day of the year of each sounding was calculated and added to each record.

The listings given in Appendix B also tabulated the latitude of the launch site. This information was merged with the basic sounding records to permit the investigation for latitudinal dependences on density variations. Southern hemisphere sites were assigned negative latitude values.

Sorting and formatting.- A limited number of the soundings included in the data set were incomplete, primarily due to missing observations of solar flux or geomagnetic index. Since there appeared to be no feasible way to compensate for the missing data in the statistical analysis, and since relatively few soundings were incomplete, the incomplete records were simply eliminated from the data set. This editing resulted in the removal of six soundings from the basic set of 437 soundings. The computer program that was developed to edit the data, and to calculate and insert Julian dates is listed in Appendix C.

The final step in the data preparation was to sort the data records so that they would be listed on the data tape by altitude, the low altitudes first and the high altitudes last. This was done by means of a standard IBM sort program (Ref. 15).

* Planetary geomagnetic index data were not available for the soundings taken in 1947 and 1948.

TABLE V

CONVERSIONS BETWEEN K_p AND a_p

K_p	a_p
0.	0
0+	2
1-	3
1.	4
1+	5
2-	6
2.	7
2+	9
3-	12
3.	15
3+	18
4-	22
4.	27
4+	32
5-	39
5.	48
5+	56
6-	67
6.	80
6+	94
7-	111
7.	132
7	154
8-	179
8.	207
8+	236
9-	300
9.	400

The sorted, edited data tape now contains one logical record for each density observation. The information given within each of these records is listed in Table VI. A detailed description of the record format and data storage parameters for these data will be found in Appendix C.

DIURNAL VARIATIONS IN ATMOSPHERIC DENSITY

Diurnal variations of atmospheric density in the upper atmosphere represent one of the least well documented elements of model atmosphere studies. Because the magnitude of diurnal density changes are generally recognized to be small by comparison to seasonal and latitudinal variations, a large effort is required to obtain sufficient measurements to characterize the diurnal cycle. Quiroz (Ref. 1) has synthesized a tentative model for density variations up to 90 km based on the limited observational evidence which has been collected. His model suggests that the magnitude of the diurnal range increases with height up to about 90 km, where a quasi-isopycnic layer has been observed. In the 30 to 40 km interval, the diurnal range is estimated to be 2 to 5 percent with a minimum during the daytime. In the 45 to 90 km interval, observations indicate a diurnal range of 10 percent with the maximum density occurring in the afternoon. There is a suggestion that a maximum in the diurnal range exists near 65 km, where 25 percent variations have been recorded.

Previously published results by Minzner and Morgenstern (Ref. 2) on the latitudinal dependence of density variations have treated seasonal and diurnal effects independently. That is, seasonal variations have been shown without regard to diurnal factors, and vice versa. The basic calculations which produced these results, however, permit an analysis of the data on the basis of the joint variations due to latitude, season, and time of day. This is feasible because of a system of three-way stratification which was used to classify the data into quasi-homogeneous cells. In spite of the limitations of the stratification method discussed earlier, the availability of a processed set of results appeared to justify the effort required to perform a more detailed analysis. The following sections describe the stratification scheme originally used to classify the data, and discuss the analysis of the results for diurnal variations as a function of season and latitude.

Description of the Stratification Scheme

A detailed description of the method for stratifying the 437 soundings into season, latitude, and time of day has been published with the earlier analyses (Ref. 2). Several permutations of this scheme were tested for its suitability to the given data base; one of these was selected as the best compromise and is briefly described.

TABLE VI
CONTENT OF DATA TAPE RECORDS

<u>SEQUENCE</u>	<u>DATA</u>
1	Date and time (GMT) of sounding
2	Launch site code
3	Measurement technique code
4	Height in geopotential km
5	Density in kg/m ³
6	10.7 cm solar flux for preceding day
7	10.7 cm solar flux for same day
8	Local apparent time
9	Sub-solar angle
10	Shadow height in km
11	Geomagnetic index (-24 hours)
12	" " (-21 hours)
13	" " (-18 hours)
14	" " (-15 hours)
15	" " (-12 hours)
16	" " (- 9 hours)
17	" " (- 6 hours)
18	" " (- 3 hours)
19	" " (current)
20	Latitude of launch site
21	Julian date (GMT)
22	Julian date (local apparent time)
23	Julian date (GMT at beginning of year)

The seasonal classification and coding of the soundings is based on partitioning the data into the four, nearly equal, time intervals as shown in Table VII. The dates defining the limits of these intervals were keyed to the occurrence of the vernal equinox. For leap years, one day is added to the day of the year for the months March through December. Correspondingly, no correction is made for the accumulated quarter-day errors in successive members of the remainder of the four year cycle insofar as the seasonal division is concerned. For southern hemisphere sites the seasons are inverted by subtracting 183 from the number of the day of the year when that number is equal to or greater than 183, or by adding 183 when that number is less than 183.

In addition to the four season classification, two extreme-season periods of about 46 days in duration have been designated which span the middle of the summer and winter seasons.

The classification of launch sites into latitude belts is shown in Table VIII. This division allows for 7 latitude belts in a single hemisphere, each belt being 15 degrees wide with the exception of the tropical and polar belts which are only 7.5 degrees in one hemisphere. Data from a particular latitude belt in the southern hemisphere are combined with the data in the corresponding latitude belt in the northern hemisphere after the southern hemisphere data have had a 183-day phase shift applied prior to the seasonal designation.

The coding of diurnal cycles into a three-division classification is based jointly on the sub-solar angle or zenith angle of the sun, and the height of the earth's shadow during nighttime periods. The limits for these criteria are given in Table IX. The daytime cases are defined as those during which the sub-solar angle is less than 60 degrees; the shadow height must necessarily be zero for these cases. Nighttime cases are defined as those conditions during which the subsolar angle is greater than 60 degrees, and the shadow height is greater than 300 km. All intermediate conditions which do not satisfy either the daytime or nighttime criteria are classified as transition cases.

The seasonal distribution of sample sizes resulting from this classification scheme have been shown earlier in Table II. There are at least four general factors which contribute to the disproportionate distribution of the sample size: these factors involve geographical, sociological, psychological and astronomical considerations. Of these, only the latter can be specifically defined, but some subjective comments appear to be applicable to the others. The more remote areas, and hence the the subarctic arctic belts, have fewer soundings merely because of the logistical problems involved. The first half of the winter period up to mid-January has very few soundings in any latitude belt largely because of the holidays. Arctic and subarctic regions are most uncomfortable during the winter, and field parties tend to avoid discomfort by avoiding extreme conditions. These reasons are largely responsible for the fact that only 37 percent of all extreme-season soundings occurred during the winter-extreme period.

TABLE VII
DEFINING CONDITIONS OF SEASONAL CODING FOR NON-LEAP YEARS

Date	Day of Year	Days in Season	Four-Season Code	Extreme-Season Code
Feb 26	57		---	
		23	S	
Mar 21	80		P	
		23	R	
Apr 13	103		I 1	
		23	N	
May 06	126		G	
		23		
May 29	149		---	
		23	S	---
Jun 21	172		U	S
		23	M	U 8
Jul 14	195		M 2	X
		23	E	---
Aug 06	218		R	
		23		
Aug 29	241		---	
		23	A	
Sep 21	264		U	
		23	T	
Oct 14	287		U 3	
		23	M	
Nov 06	310		N	
		22		
Nov 28	332		---	
		23	W	---
Dec 21	355		I	W
		22	N	I 9
Jan 12	12		T 4	X
		23	E	---
Feb 04	35		R	
		22		
Feb 26	57		---	
		23		
Mar 21	80			
		23		
Apr 13	103			

TABLE VII
(Continued)

For Southern Hemisphere sites the seasons are inverted by subtracting 183 from the number of the day of the year when that number is equal to or greater than 183, or by adding 183 when that number is less than 183.

For leap years, one day is added to the day of the year for months March through December. Correspondingly no correction is made for the accumulated quarter-day errors in successive members of the remainder of the four year cycle, insofar as the seasonal division is concerned.

Abbreviations: SUX - Summer Extreme, WIX - Winter Extreme,

TABLE VIII

LATITUDE CODING

Range of Latitude Increments	Latitude Code	Name of Band of Latitude	Sites Included
Degrees			
0.00 to +07.50	0	Equatorial	SA
0.00 to -07.50	0	Equatorial	
+7.51 to +22.50	1	Tropical	BS,GM,KW
-7.51 to -22.50	1	Tropical	AI
-22.51 to -37.50	2	Subtropical	CA,WO
+22.51 to +37.50	2	Subtropical	AQ,EG,HA,PM,WS
+37.51 to +52.50	3	Midlatitude	KY,SF,WI
-37.51 to -52.50	3	Midlatitude	
+52.51 to +67.50	4	Subarctic	FC,SB,SD,SE,SG,SH
-52.51 to -67.50	4	Subarctic	
+67.51 to +82.50	5	Arctic	HI,SC,TH
-67.51 to -82.50	5	Arctic	MS
+82.51 to +90.00	6	Polar	
-82.51 to -90.00	6	Polar	

Latitudes in the Northern Hemisphere are designated positive.
 Latitudes in the Southern Hemisphere are designated negative.

TABLE IX
 DIURNAL CODING AS RELATED TO RANGES OF
 SUBSOLAR ANGLE AND SHADOW HEIGHT

<u>Shadow Height</u>	<u>Subsolar Angle</u>	<u>Diurnal Classes</u>
≥ 300 km	> 60 Deg	2 Nighttime
- - - - -		- - - - -
		0 Transition
	- - - - -	- - - - -
< 300 km	≤ 60 Deg	1 Daytime
	- - - - -	- - - - -
		0 Transition
- - - - -		- - - - -
≥ 300 km	> 60 Deg	2 Nighttime

Midnight is never designated as 24.00 Hours of the just-ending day.
 Rather it is designated as 00.00 hours of the just-beginning day.

Table X shows that the joint frequency distribution of soundings by latitude belt and with time of day. Nearly half of the launches fall into the transition period between daytime and nighttime conditions. This predominance of transition cases is particularly accentuated with increasing latitude where the transition period constitutes a larger fraction of the diurnal cycle.

In retrospect it is apparent that the defined astronomical conditions for day and night divisions in the study are responsible for a large amount of the disproportionate distribution of sample size, particularly in the subarctic and arctic belts, although these reasons also apply to a lesser degree to the mid-latitude belt. In particular, on the day of the winter solstice no such daytime conditions exist at latitudes greater than 36.56° and even at the summer solstice, the northern boundary of the arctic belt is just within the latitude which satisfies the condition. Similarly, autumn daytime conditions are almost non-existent in the arctic belt with the total number of daytime hours per autumn season gradually increasing as the latitude decreases.

The definition of nighttime required an earth's shadow height of 300 km. It may be shown that this condition is met at local midnight when the sum of the latitude and the declination angle is equal to, or less than 71.43° (atmospheric refraction being considered). Taking the value of the sun's declination angle is equal for those dates which serve as boundaries to the several seasons as defined by us, one may readily estimate the periods when no nighttime conditions exist at the various latitudes. One sees that there is no summer night in the arctic and almost none in the subarctic. Even at the more northerly portions of the mid-latitude belt, summer nighttime as defined by us does not exist from some days around the summer solstice. Spring and autumn nighttimes are severely curtailed in the arctic, and partly curtailed in the subarctic and mid-latitudes by our definition.

Statistical Calculations

The computational procedures used to develop the altitude profiles of density variations used in this analysis have been described in detail by Minzner and Mello (Ref. 16). Briefly, the variations of density at each altitude were determined by comparing the differences between average values of density for a particular latitude-season-diurnal sub-sample and a common reference density value for that altitude. To isolate the effects of diurnal variations (and seasonal variations) from latitudinal variations, the cell average was compared with a reference value consisting of the average density for that latitude belt. This procedure yields 18 profiles for each latitude band, e.g., three diurnal periods for each of six seasonal classifications. In addition to these, the individual cell samples were combined into larger groupings to provide annual averages (for a fixed diurnal period), and similarly differenced with the latitudinal average density for an additional three profiles per latitude belt.

TABLE X
 DISTRIBUTION OF SAMPLE SIZE WITH
 LATITUDE AND DIURNAL CYCLE

	D A Y	N I G H T	T R A N S
ARCTIC	4	7	50
SUBARCTIC	9	11	38
MIDLATITUDE	8	15	40
SUBTROPICAL	51	60	73
TROPICAL	31	23	17
TOTAL	103	126	208

To normalize and linearize the results, the density differences were computed as percent departures from the reference mean. These profiles were then smoothed using a 5-point running mean smoothing procedure.

Plotted Results

Comparisons other than those types described here also made in the original computations, but only the ones contributing to an interpretation of diurnal variations are considered herein. To facilitate extracting the appropriate profiles from this data base, a computer program was developed which compiled the desired set of statistical results. The analysis only considered those statistics based on a minimum sample size of three soundings. This computer program performed additional smoothing of the percent density departures using 20 passes of a 1/4, 1/2, 1/4 binomial filter. Finally, the program generated instructions for plotting these data on a Stromberg-Carlson model 4020 plotter.

The plotted results presented in Figures 7 through 39 compare daytime, nighttime, and diurnal transition profiles for fixed seasonal and latitudinal classifications. The graphs show only those sounding segments which satisfied the minimum sample size requirement; in many cases this eliminated the entire sounding from the graph. An analysis of these graphs indicated the following characteristics:

Tropical latitude belt.- In the height interval 40 to 65 km the largest daytime to nighttime differences were observed during the summer season, and the smallest difference was found for the autumn season. For the summer season, the average daytime density exceeded the average nighttime value by 15 percent at 65 km. Above 65 km, the daytime and nighttime profiles cross at about 95 km, and near 100 km the nighttime exceeds the daytime by 18 percent.

The annual mean shows another reversal in the day-night maximum and minimum near 110 km.

Sub-tropical latitude belt.- In the 40- to 70-km interval, the only systematic day-night difference observed is for the spring season. The daytime exceeds the nighttime by just over 10 percent at 70 km. The summer and autumn data do not show clear patterns, while the winter season possesses insufficient nighttime data.

The large negative departures above 100 km exhibited by the winter and annual mean graphs are unexplained, but are suspected to be related to undetected measurement errors in the original data.

Mid-latitude belt.- The profiles available for characterizing mid-latitude diurnal variations are very limited. This is partly a consequence of the astronomic definitions used to delineate daytime and nighttime conditions and is discussed further in the next section. The summer season is the only one providing a basis for observing systematic daytime-nighttime differences.

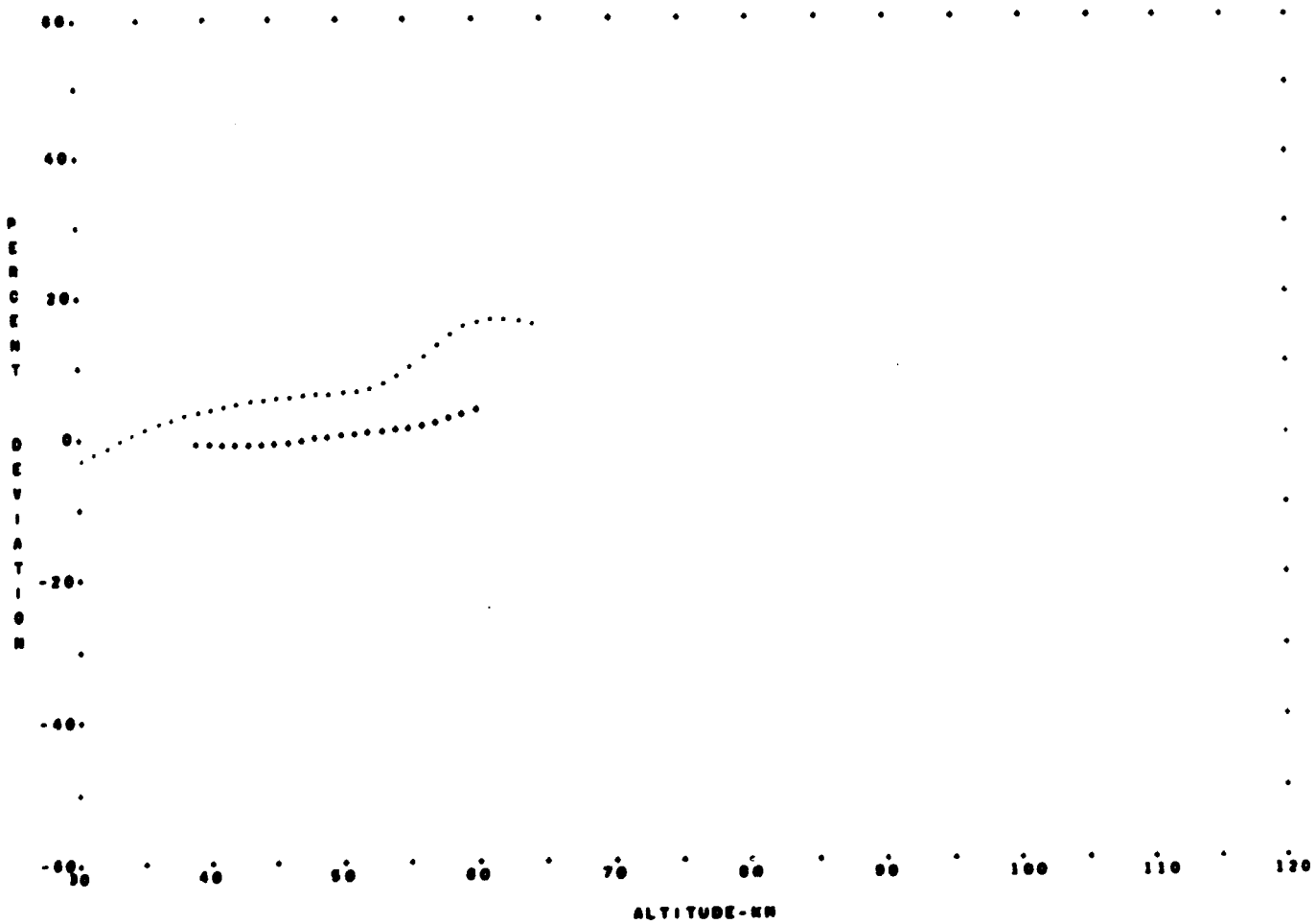


FIGURE 7 - COMPARISON OF DIURNAL VARIATIONS FOR THE SPRING.
 ... DIURNAL TRANSITION
 ... DAYTIME

TROPICAL STRATIFICATION

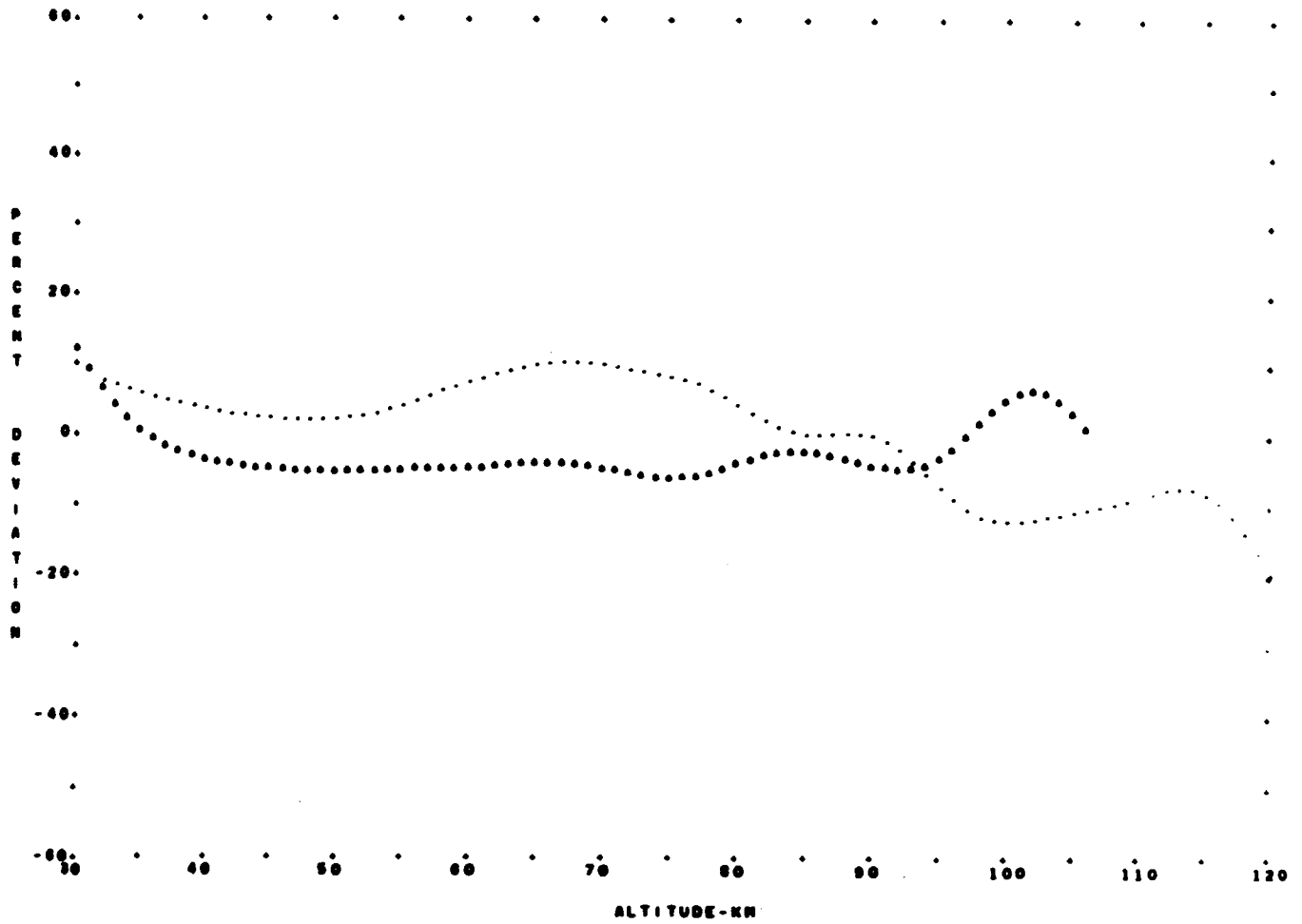


FIGURE 8 - COMPARISON OF DIURNAL VARIATIONS FOR THE SUMMER.
 ... DAYTIME
 ... NIGHTTIME

TROPICAL STRATIFICATION

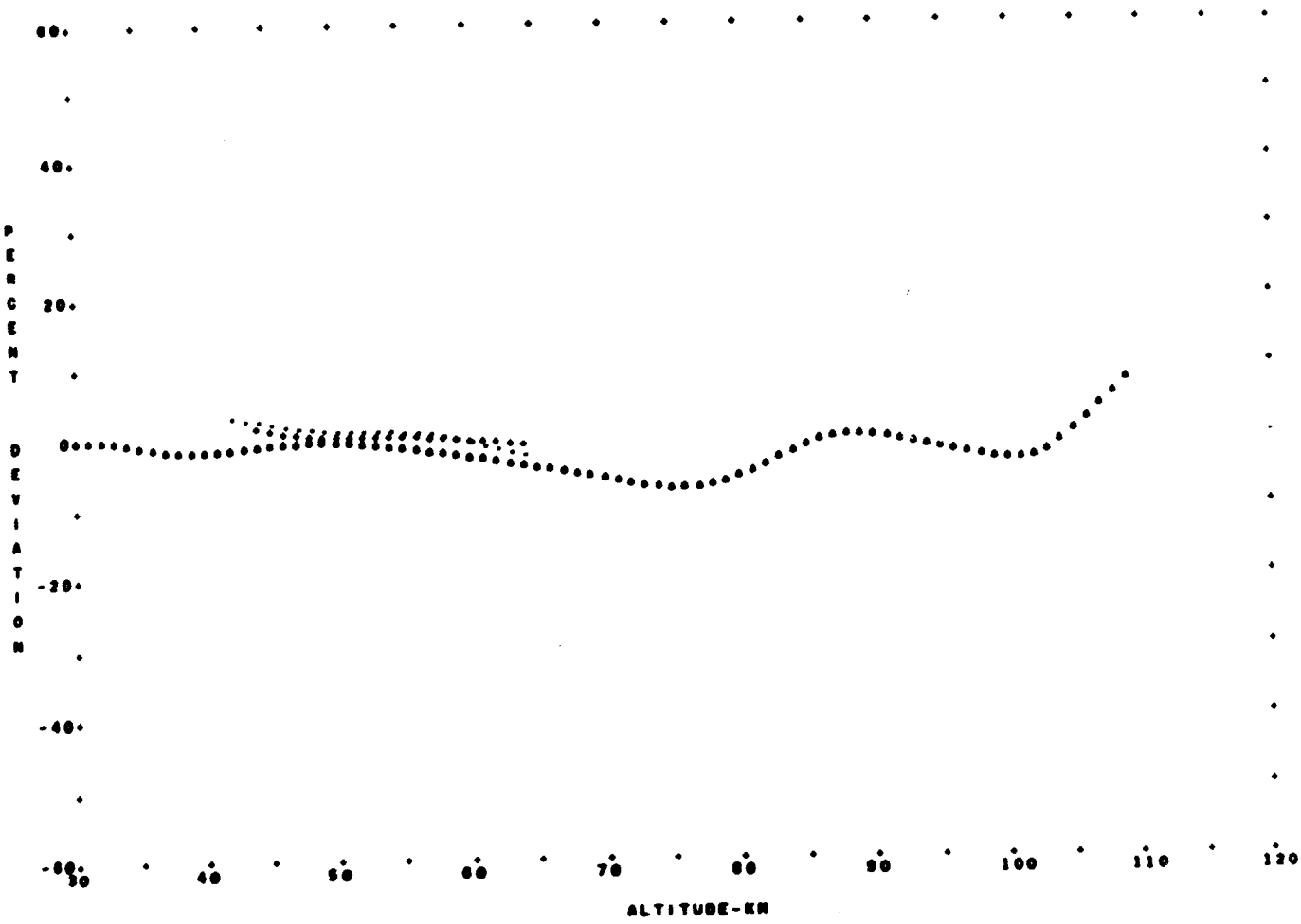


FIGURE 9 - COMPARISON OF DIURNAL VARIATIONS FOR THE AUTUMN.
 ... DIURNAL TRANSITION
 ... DAYTIME
 ... NIGHTTIME

TROPICAL STRATIFICATION

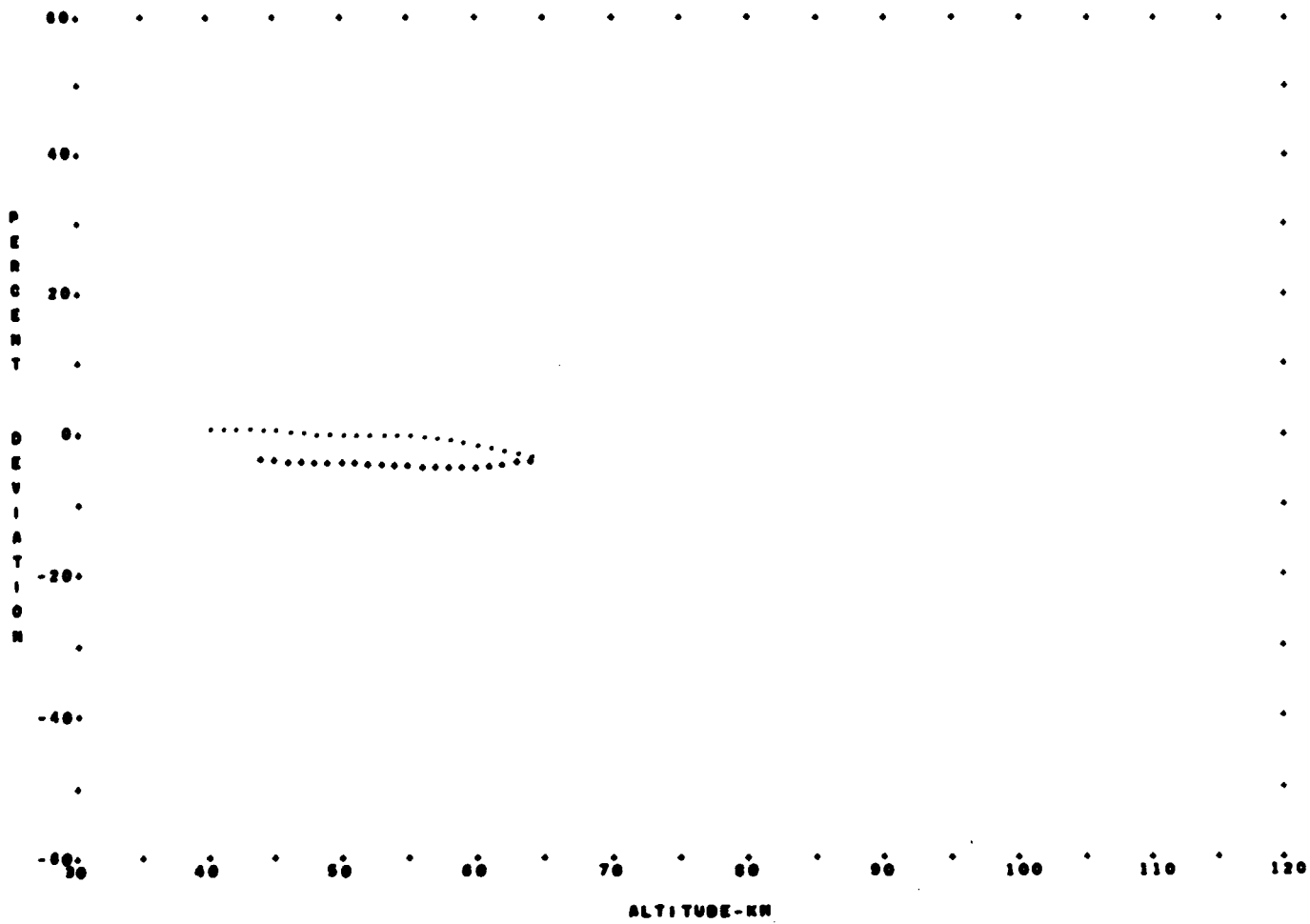


FIGURE 10 - COMPARISON OF DIURNAL VARIATIONS FOR THE WINTER,
 ... DIURNAL TRANSITION
 ... DAYTIME

TROPICAL STRATIFICATION

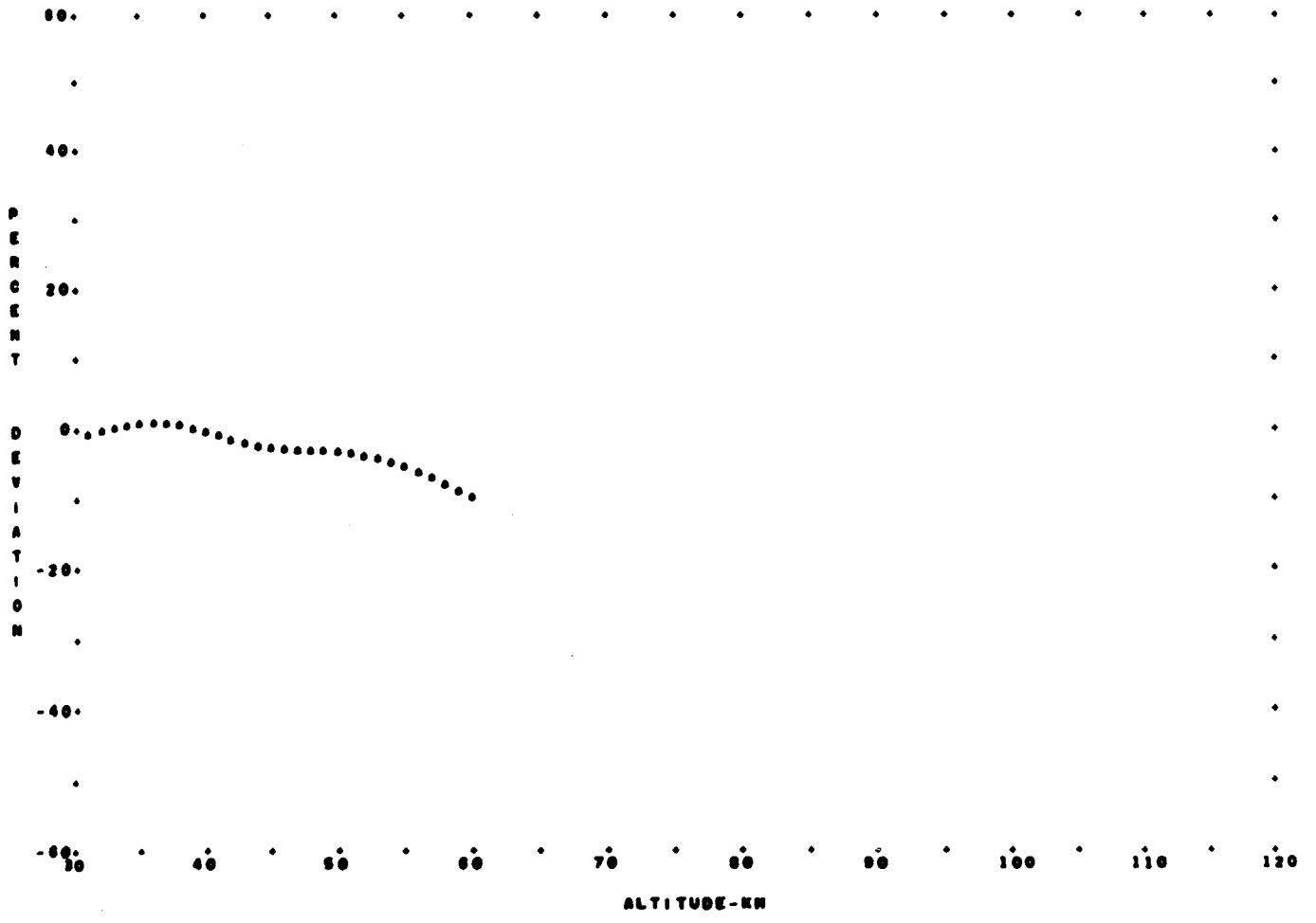


FIGURE 11 - COMPARISON OF DIURNAL VARIATIONS FOR THE SUMMER EXTREME, TROPICAL STRATIFICATION
 ... NIGHTTIME

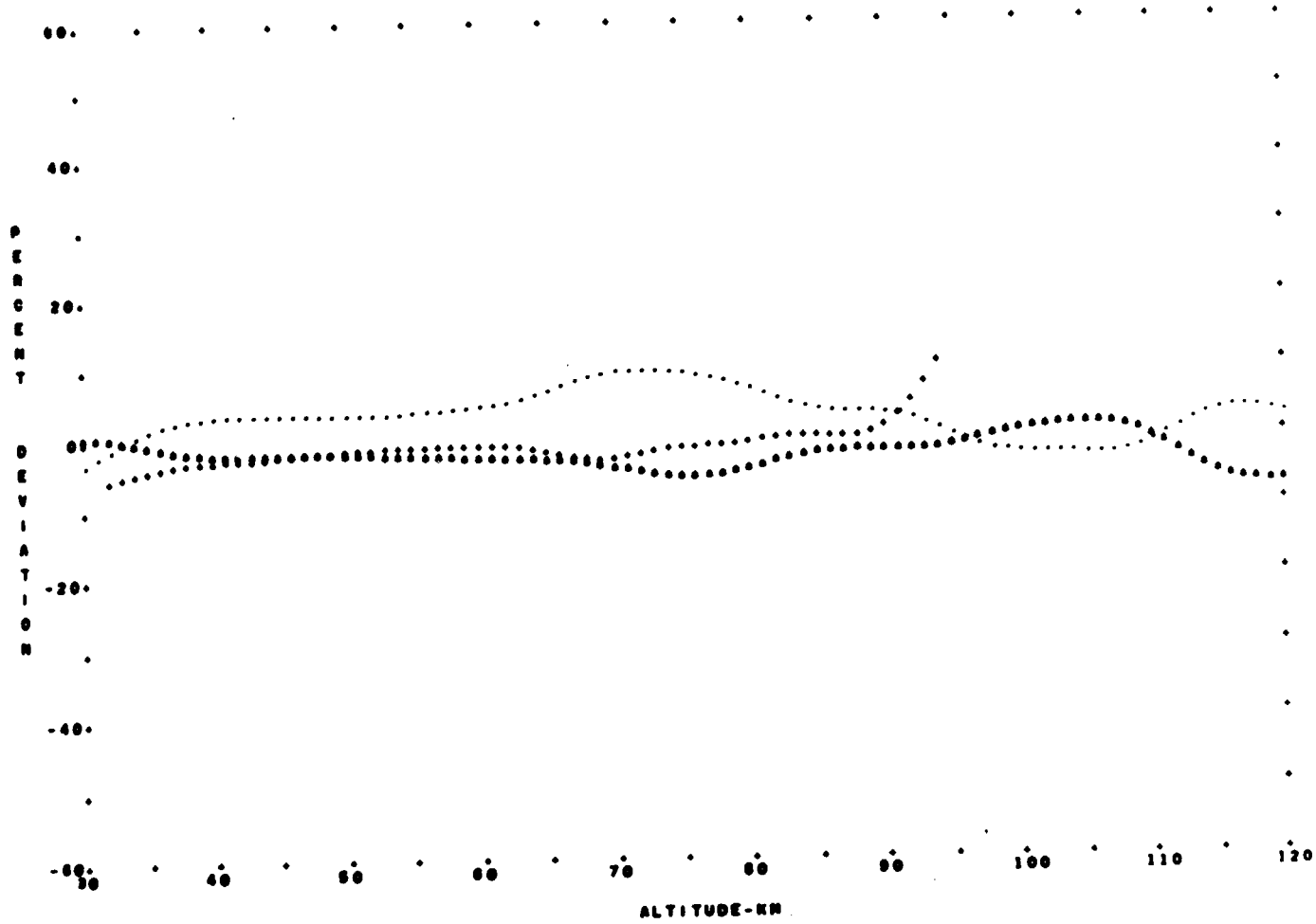


FIGURE 12 - COMPARISON OF DIURNAL VARIATIONS FOR THE ANNUAL MEAN.
 ... DIURNAL TRANSITION
 ... DAYTIME
 ... NIGHTTIME

TROPICAL STRATIFICATION

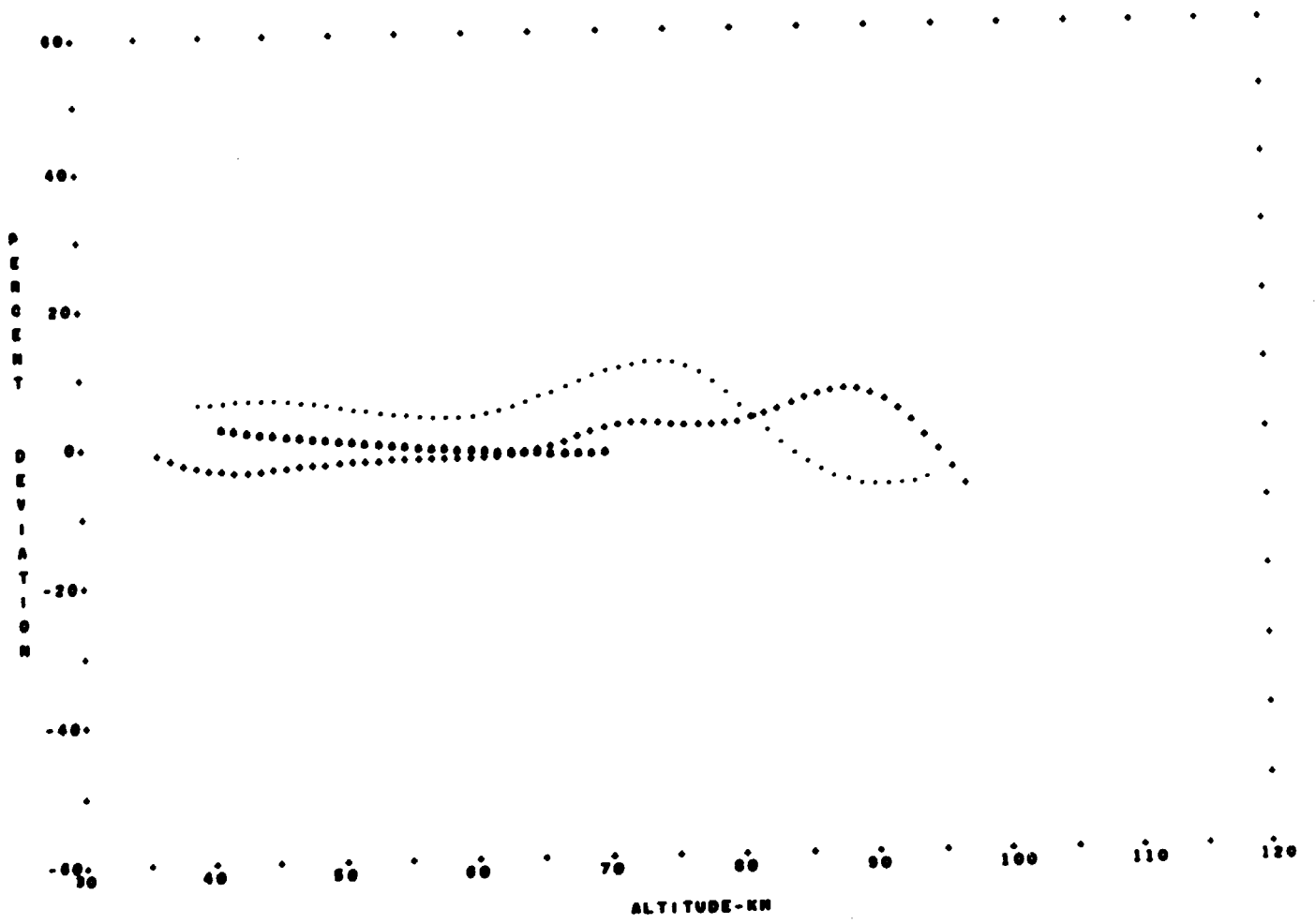


FIGURE 13 - COMPARISON OF DIURNAL VARIATIONS FOR THE SPRING.
 ... DIURNAL TRANSITION
 ... DAYTIME
 ... NIGHTTIME

SUBTROPICAL STRATIFICATION

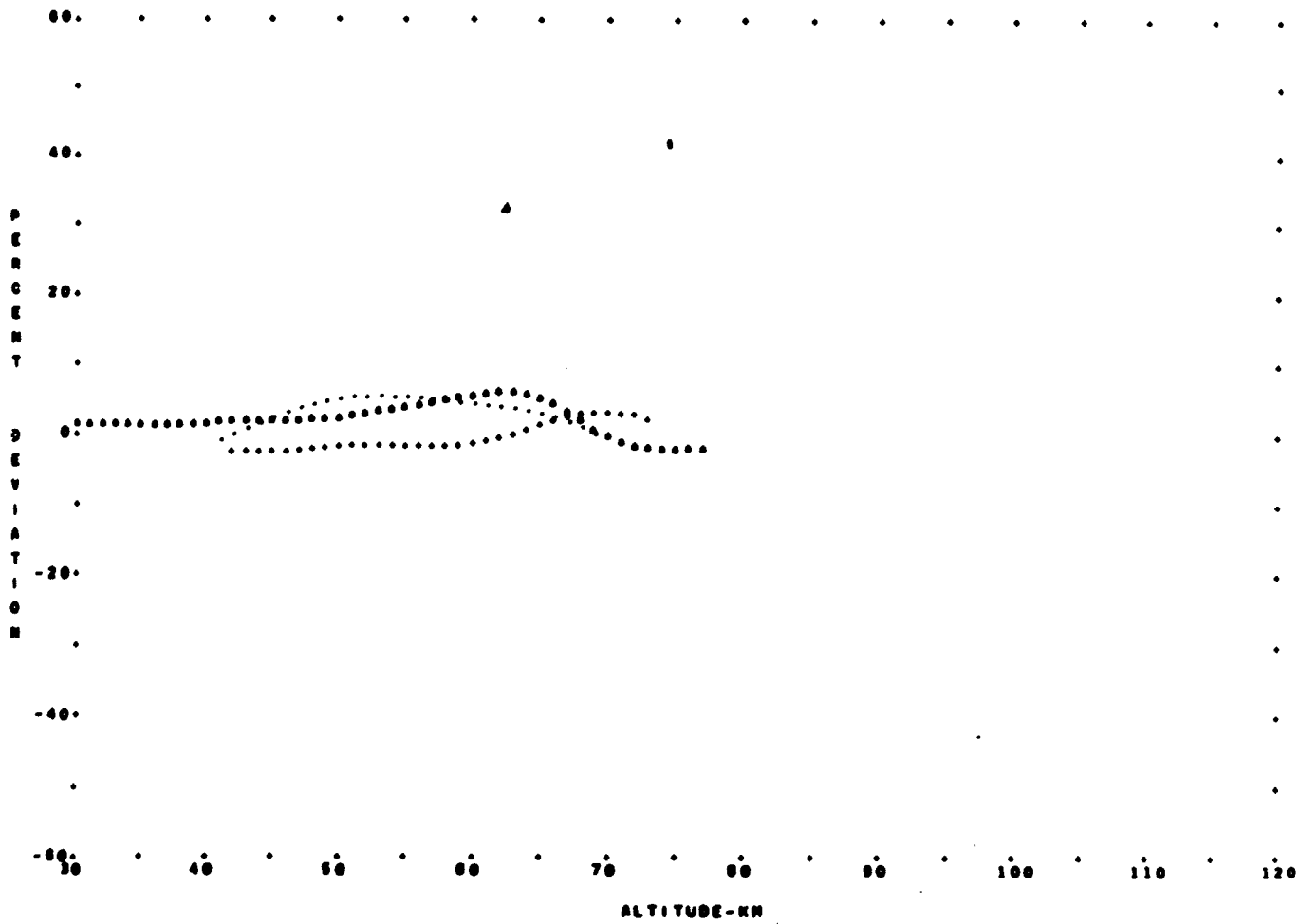


FIGURE 14 - COMPARISON OF DIURNAL VARIATIONS FOR THE SUMMER, SUBTROPICAL STRATIFICATION
 ... DIURNAL TRANSITION
 ... DAYTIME
 ... NIGHTTIME

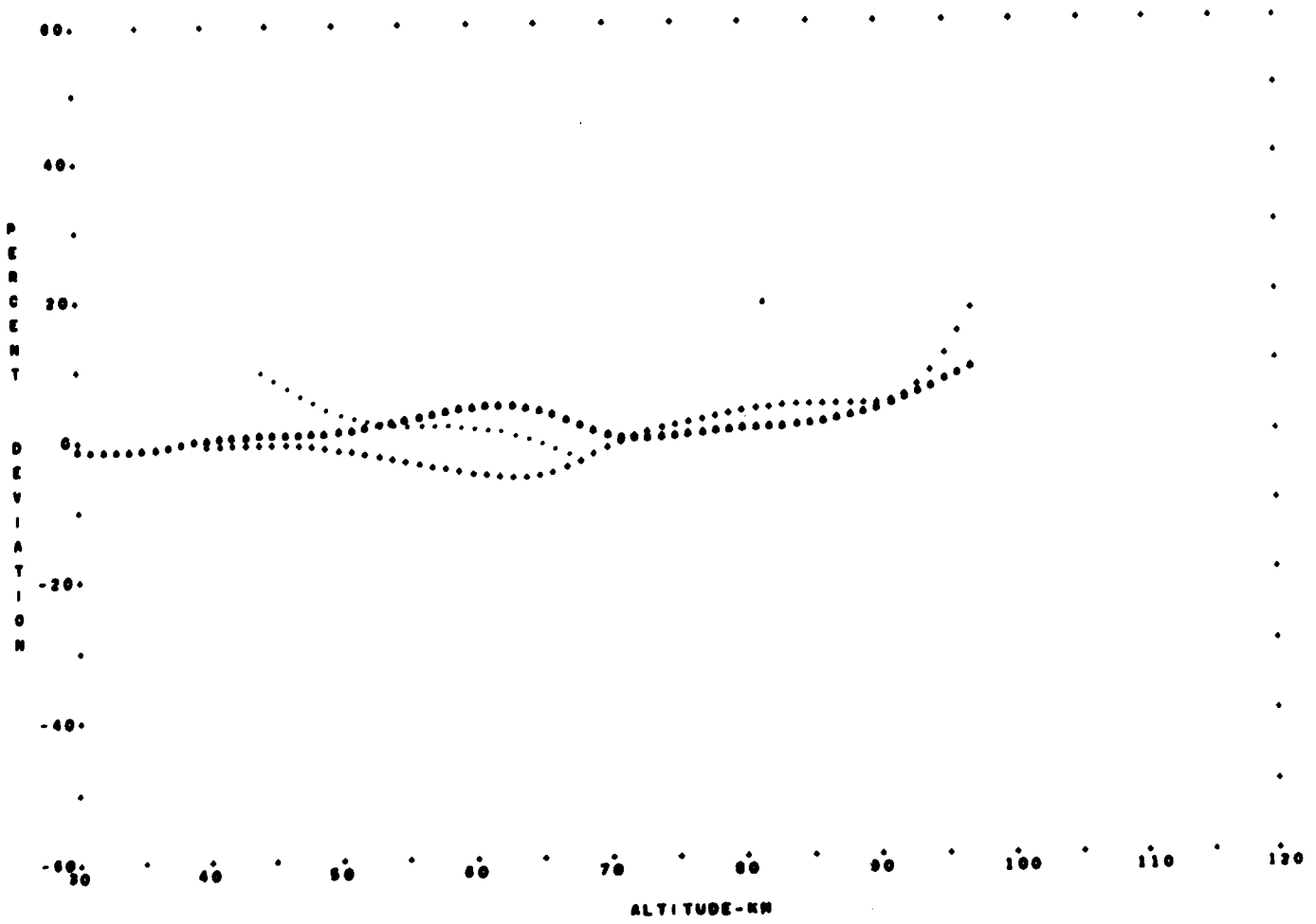


FIGURE 15 - COMPARISON OF DIURNAL VARIATIONS FOR THE AUTUMN.
 ... DIURNAL TRANSITION
 ... DAYTIME
 ... NIGHTTIME

SUBTROPICAL STRATIFICATION

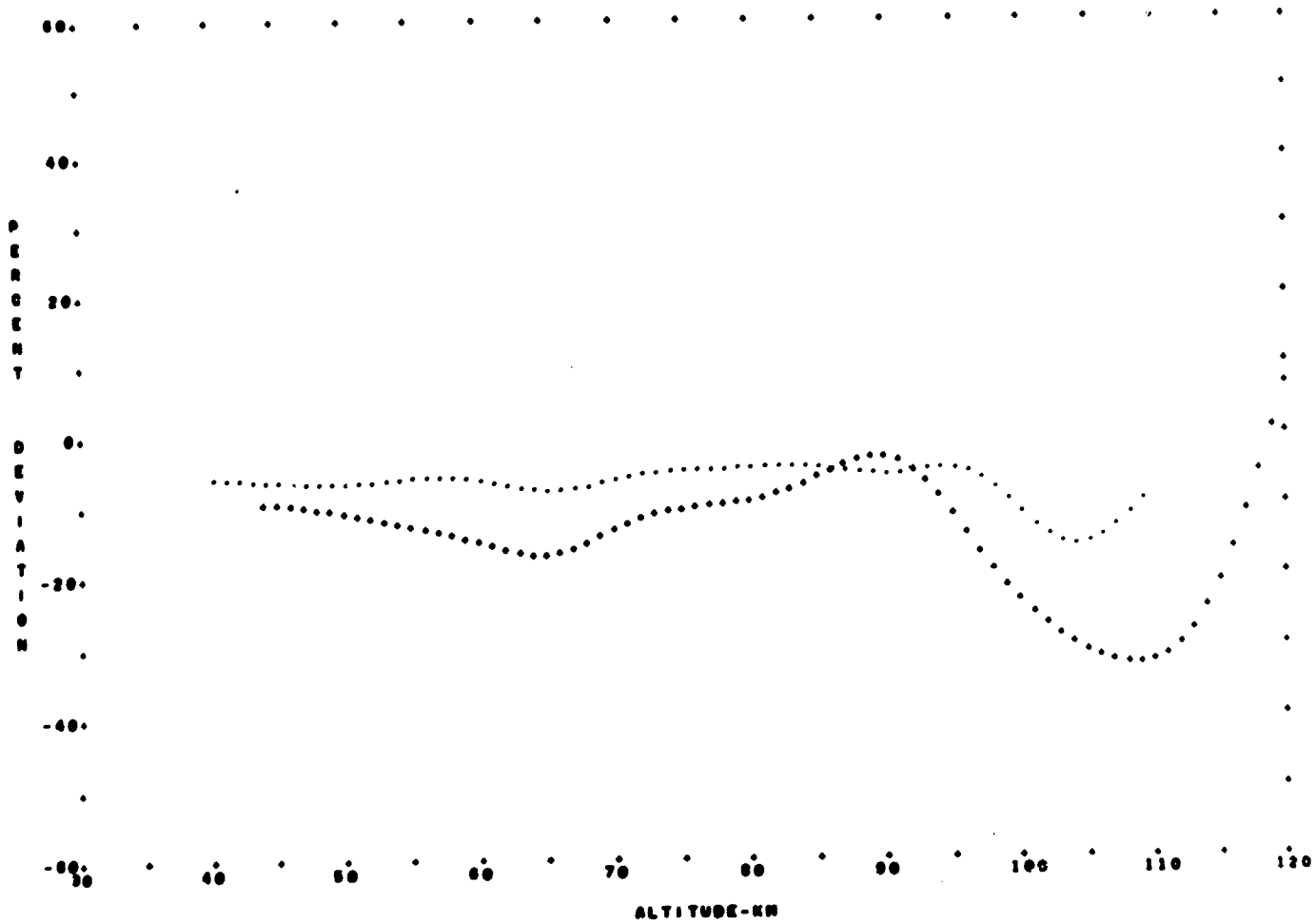


FIGURE 16 - COMPARISON OF DIURNAL VARIATIONS FOR THE WINTER.
 ... DIURNAL TRANSITION
 ... DAYTIME

SUBTROPICAL STRATIFICATION

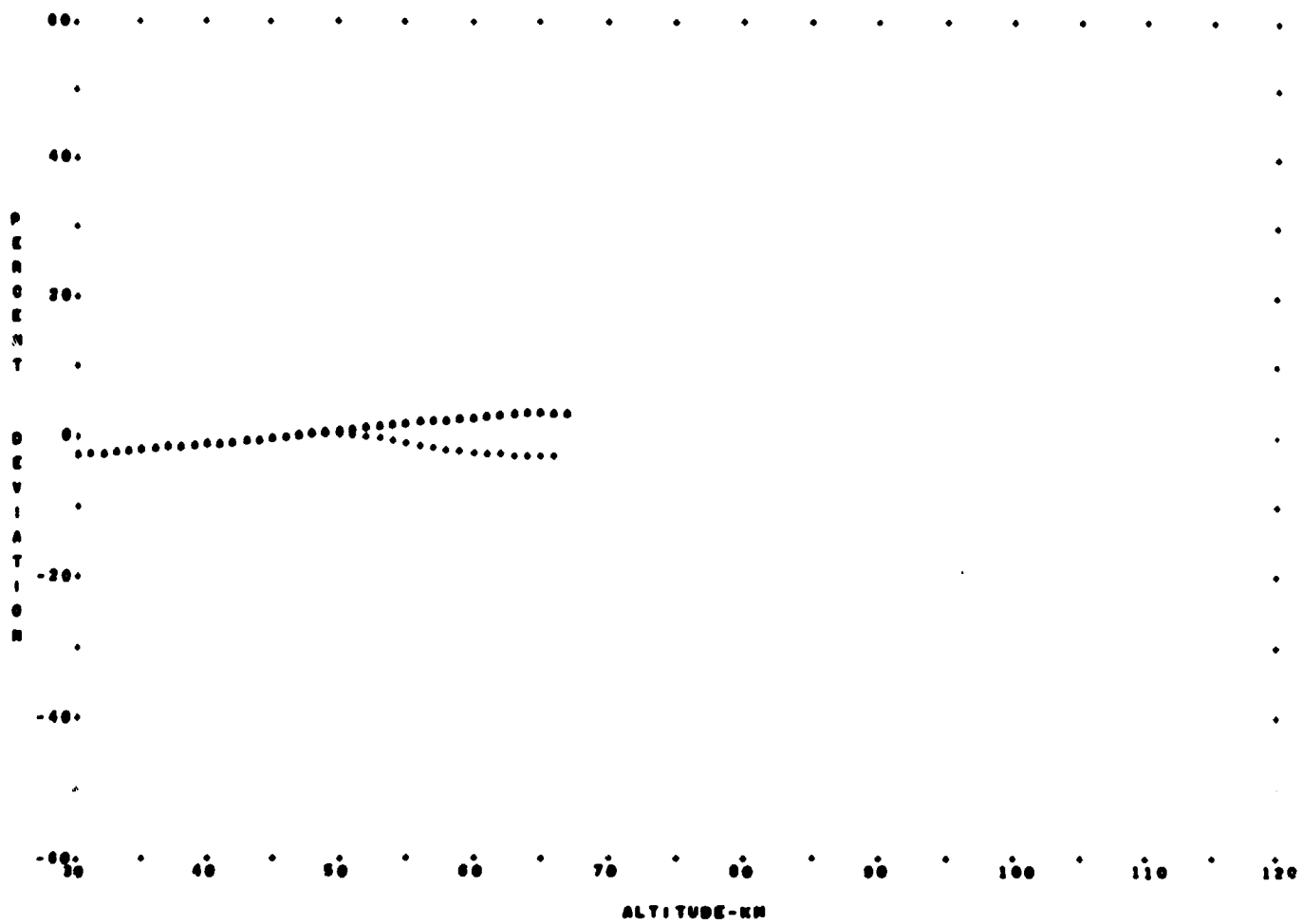


FIGURE 17 - COMPARISON OF DIURNAL VARIATIONS FOR THE SUMMER EXTREME, SUBTROPICAL STRATIFICATION
 *** DIURNAL TRANSITION
 *** NIGHTTIME

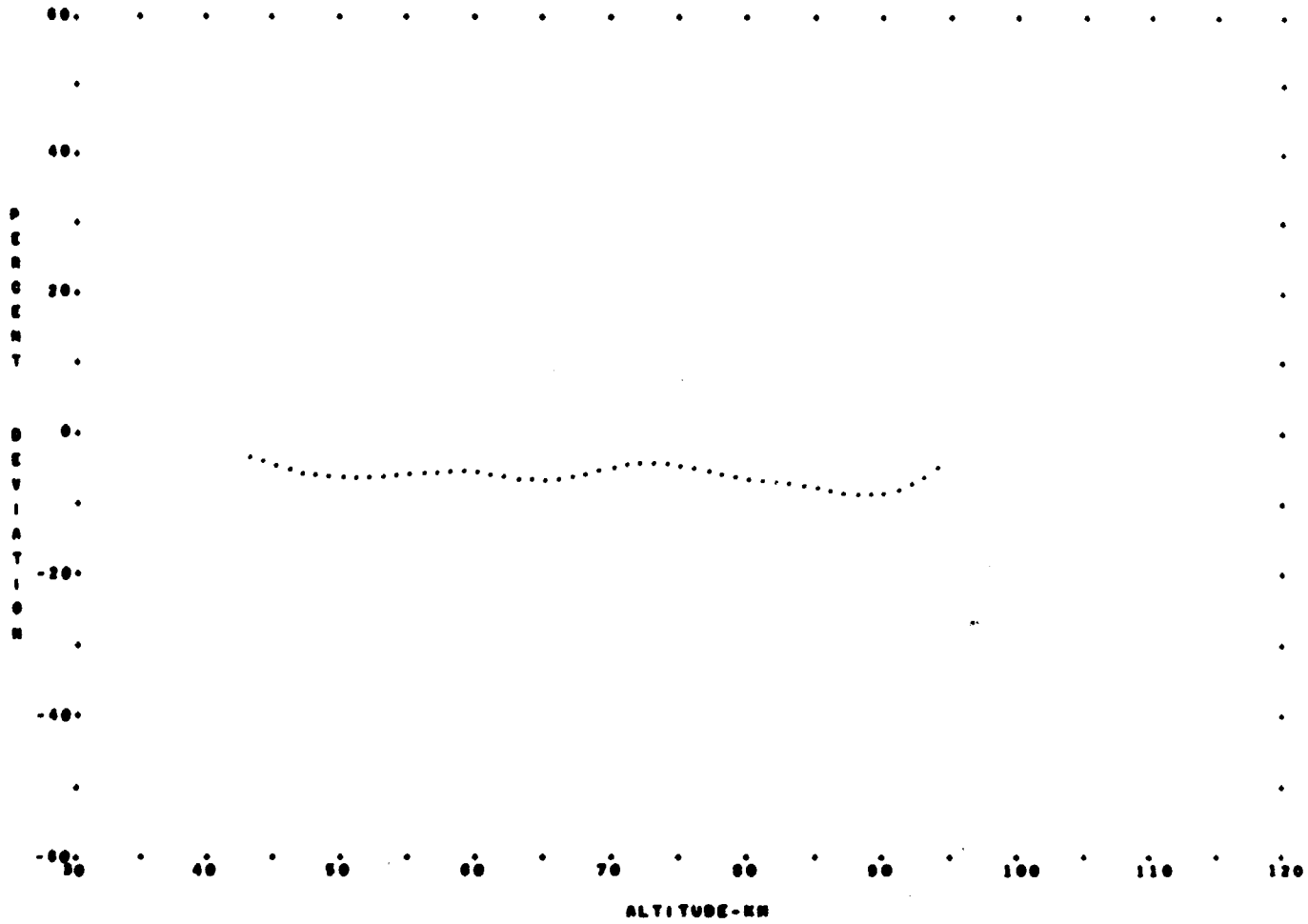


FIGURE 18 - COMPARISON OF DIURNAL VARIATIONS FOR THE WINTER EXTREME, SUBTROPICAL STRATIFICATION
 ... DAYTIME

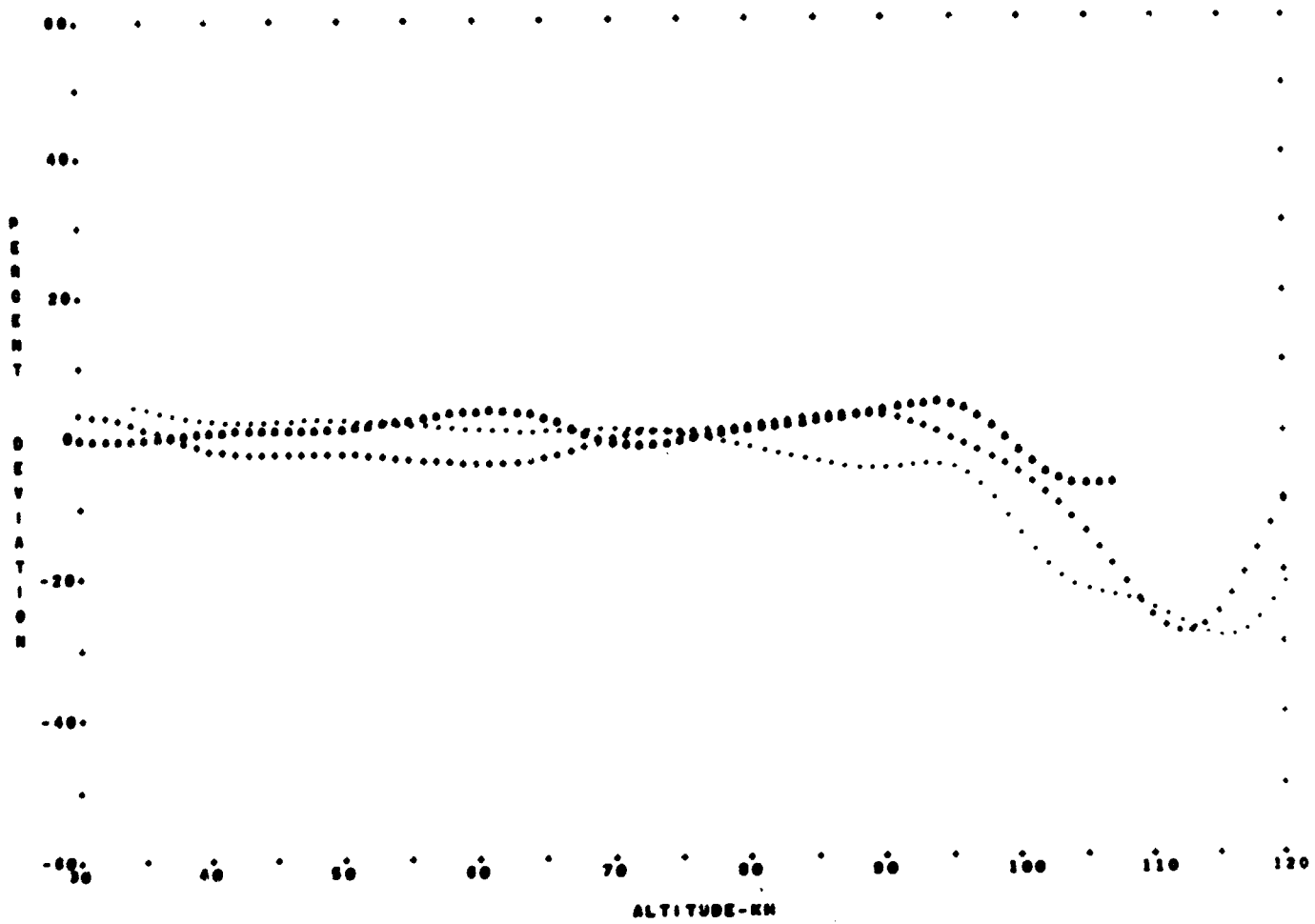


FIGURE 19- COMPARISON OF DIURNAL VARIATIONS FOR THE ANNUAL MEAN, SUBTROPICAL STRATIFICATION
 ... DIURNAL TRANSITION
 ... DAYTIME
 ... NIGHTTIME

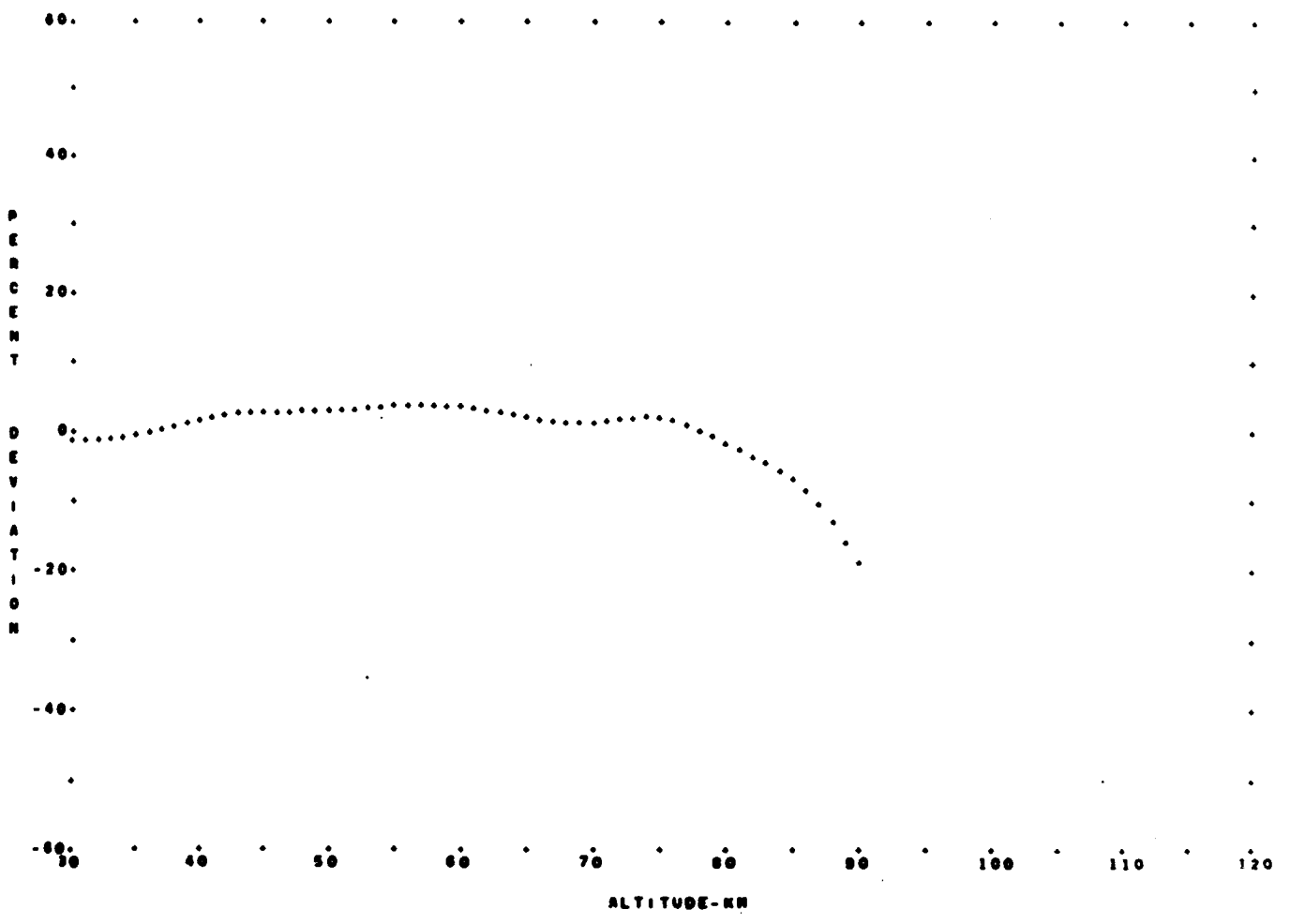


FIGURE 20 - COMPARISON OF DIURNAL VARIATIONS FOR THE SPRING, MIDLATITUDE STRATIFICATION
 ... DIURNAL TRANSITION

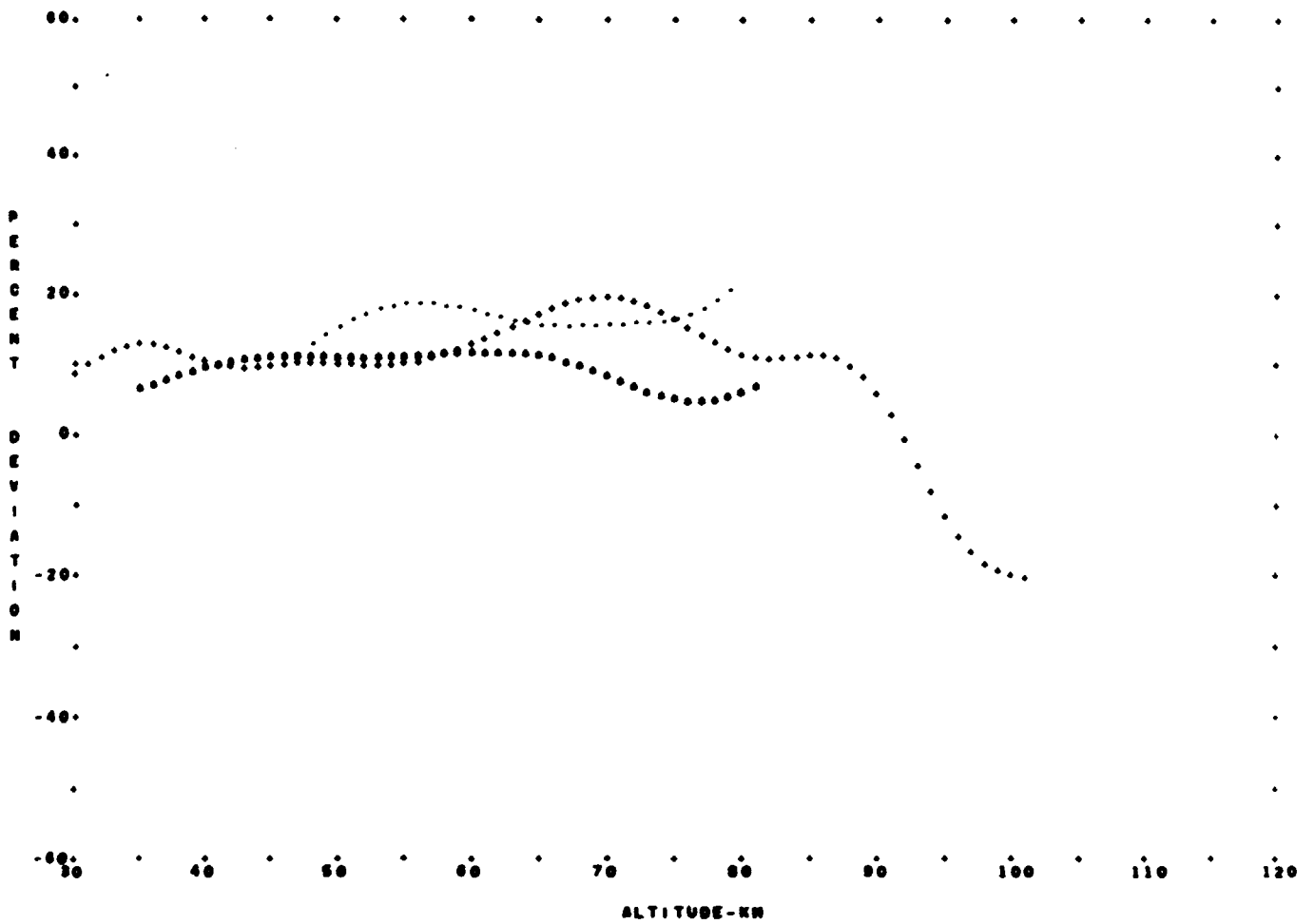


FIGURE 21 - COMPARISON OF DIURNAL VARIATIONS FOR THE SUNNER,
 ... DIURNAL TRANSITION
 ... DAYTIME
 ... NIGHTTIME

MIDLATITUDE STRATIFICATION

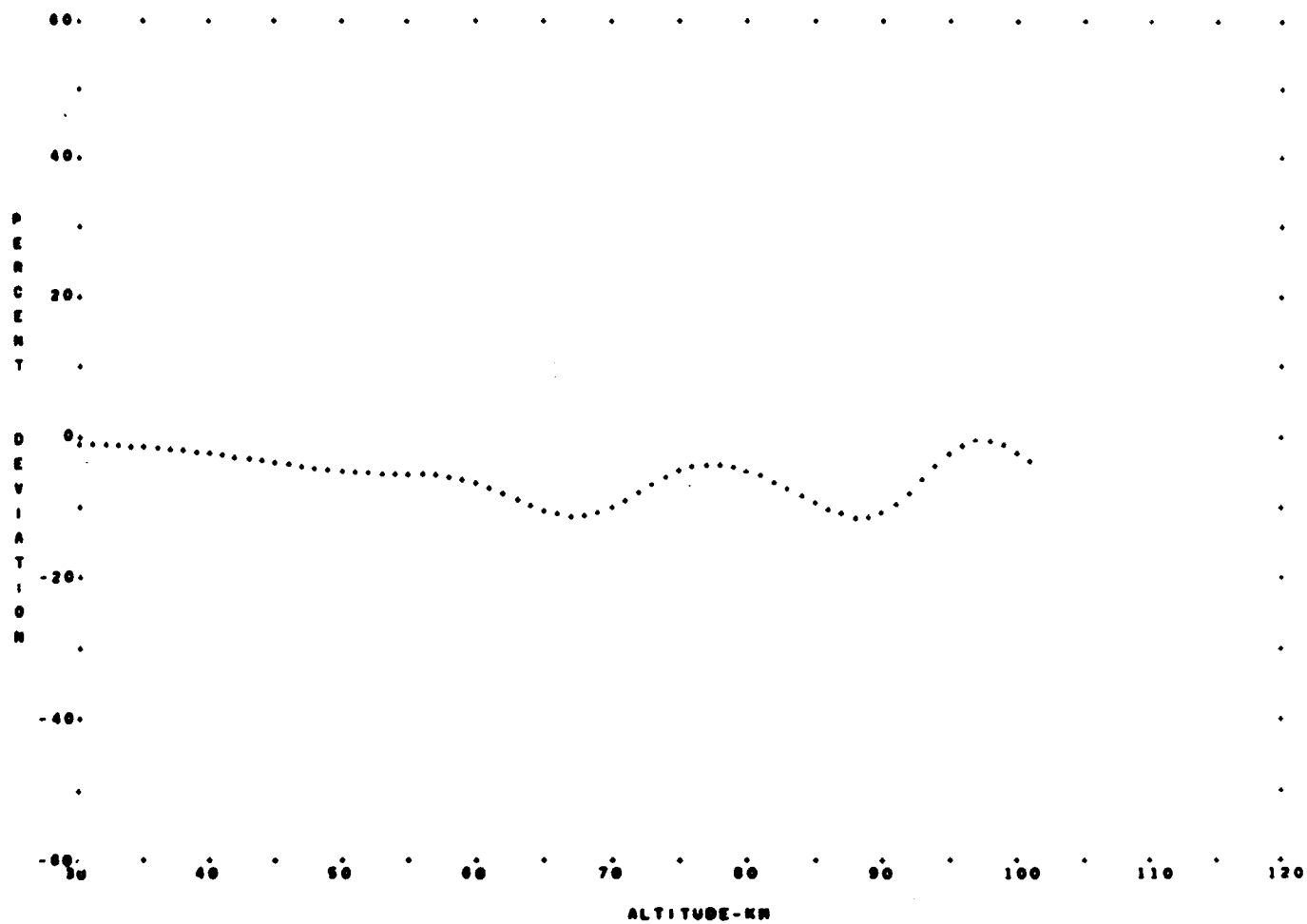


FIGURE 22 - COMPARISON OF DIURNAL VARIATIONS FOR THE AUTUMN,
... DIURNAL TRANSITION

MIDLATITUDE STRATIFICATION

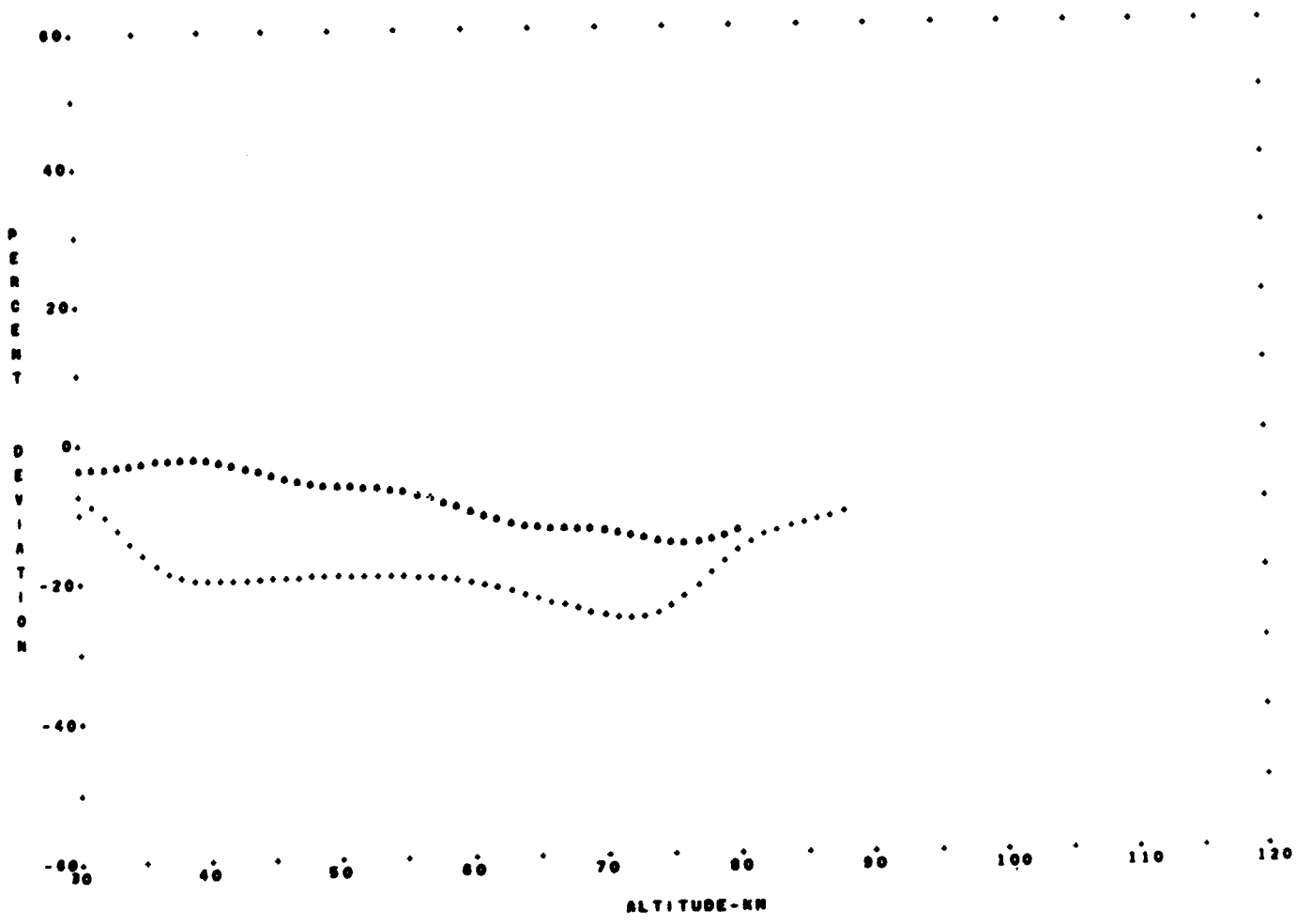


FIGURE 23 - COMPARISON OF DIURNAL VARIATIONS FOR THE WINTER.
 ... DIURNAL TRANSITION
 ... NIGHTTIME

MIDLATITUDE STRATIFICATION

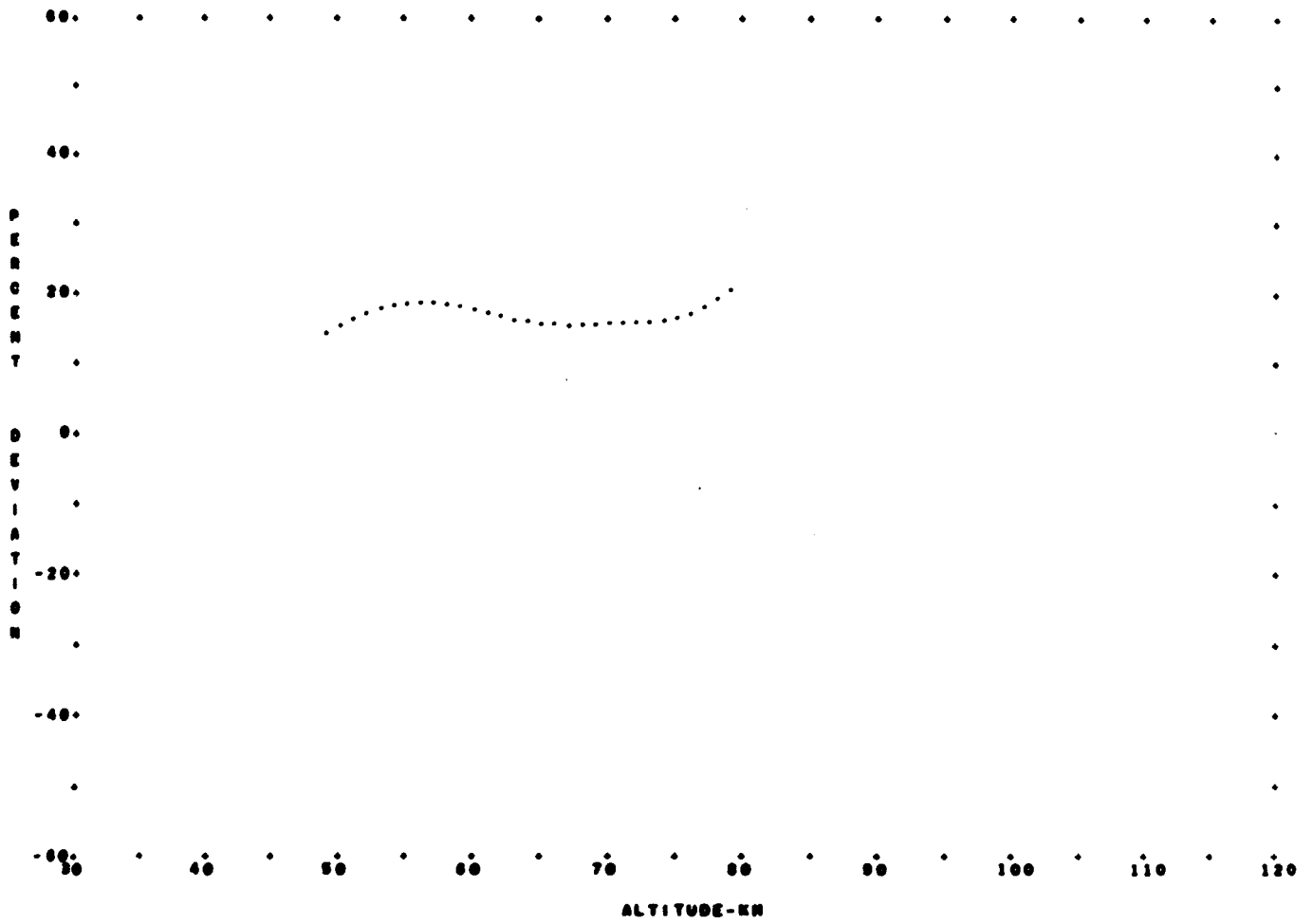


FIGURE 24 - COMPARISON OF DIURNAL VARIATIONS FOR THE SUMMER EXTREME, MIDLATITUDE STRATIFICATION ... DAYTIME

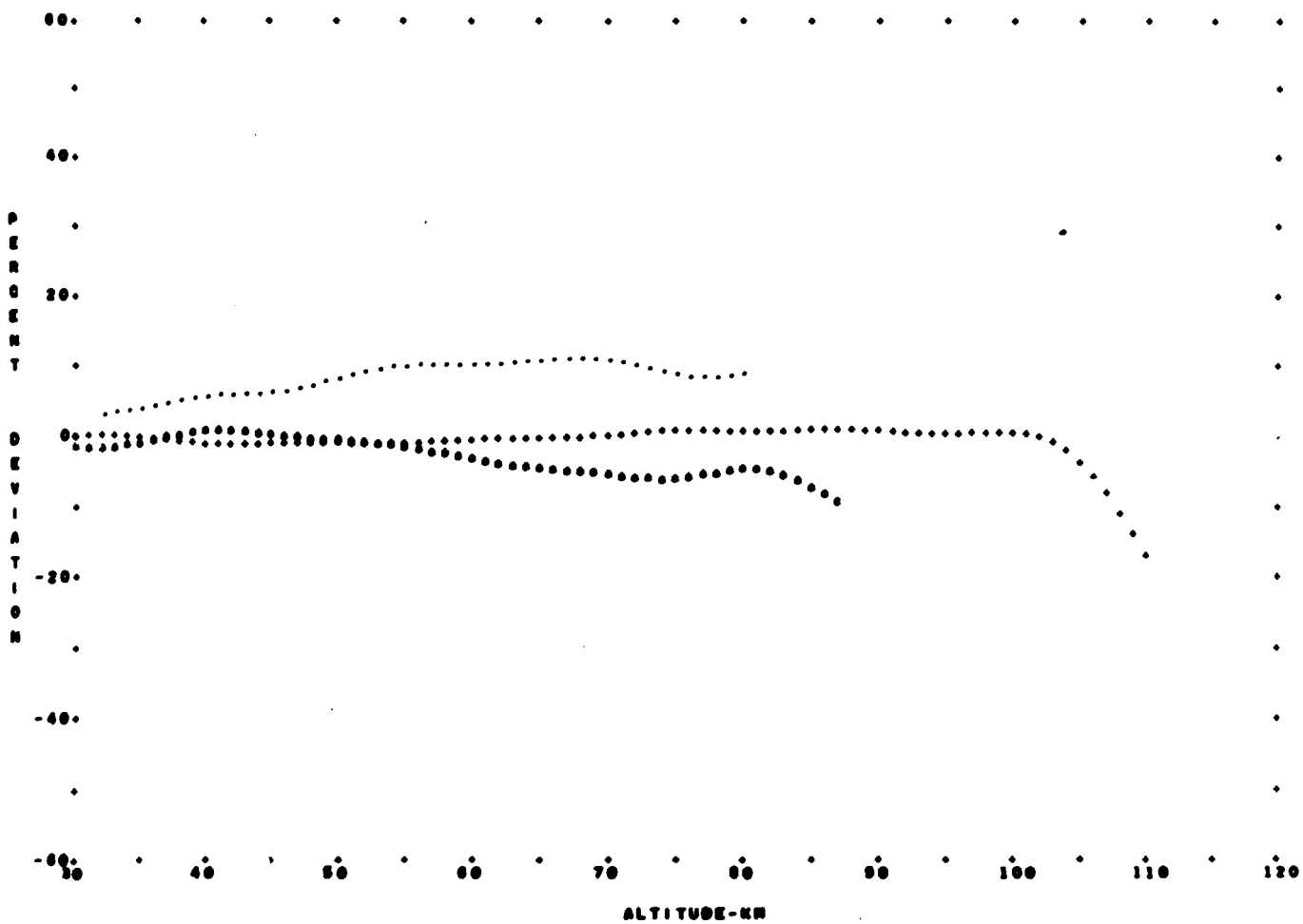


FIGURE 25 - COMPARISON OF DIURNAL VARIATIONS FOR THE ANNUAL MEAN, MIDLATITUDE STRATIFICATION
 *** DIURNAL TRANSITION
 *** DAYTIME
 *** NIGHTTIME

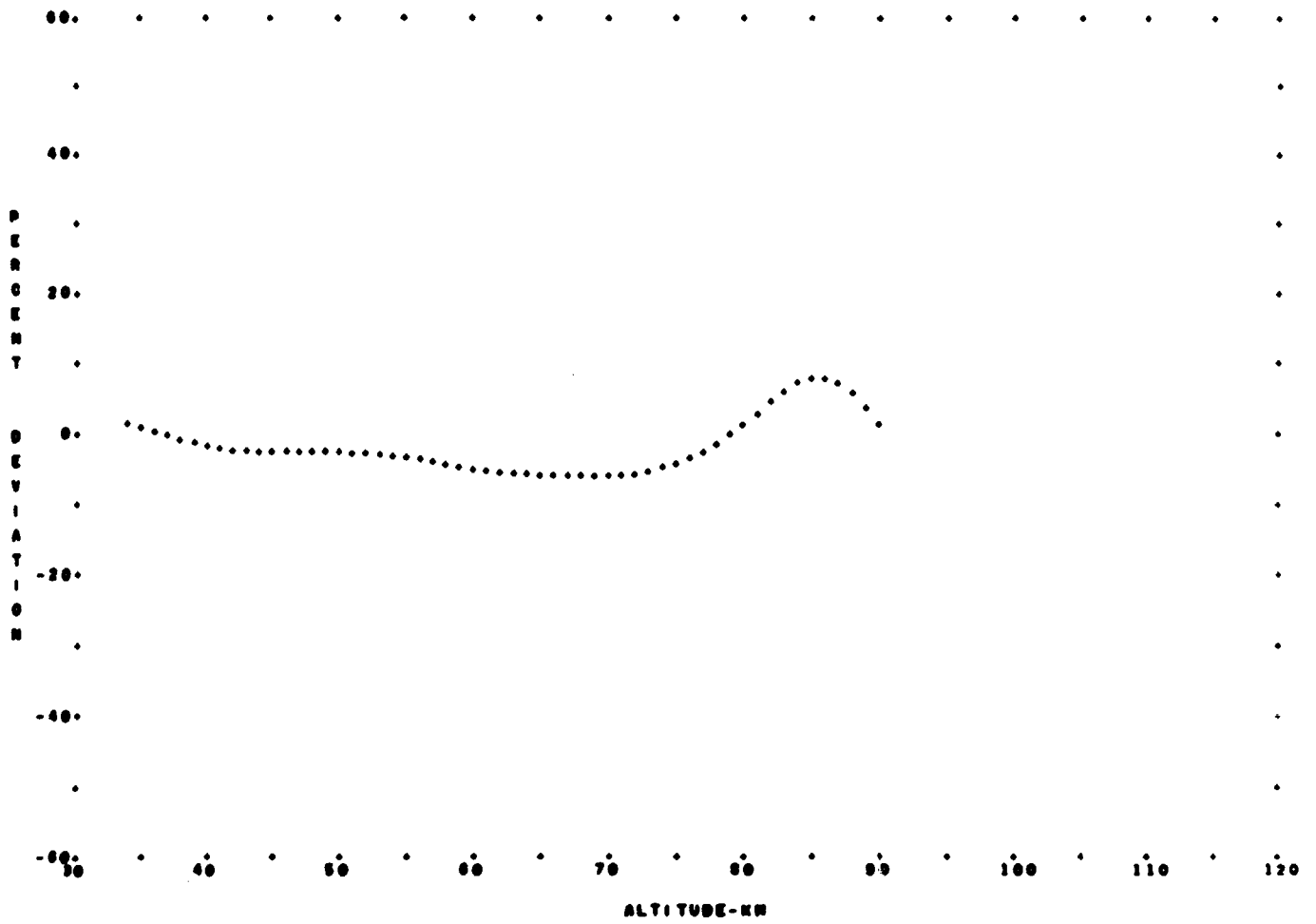


FIGURE 26 - COMPARISON OF DIURNAL VARIATIONS FOR THE SPRING, SUBARCTIC STRATIFICATION
 ... DIURNAL TRANSITION

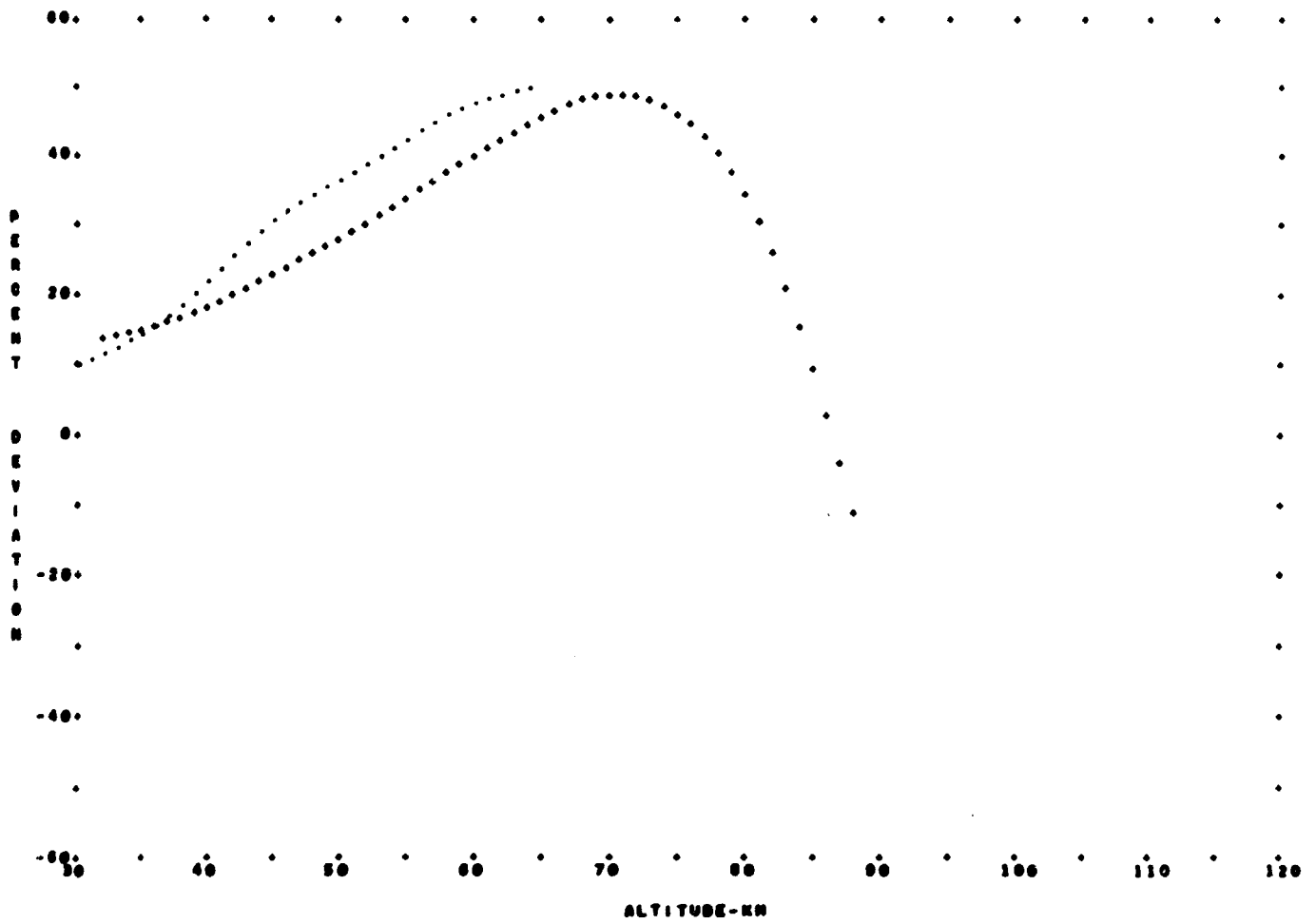


FIGURE 27 - COMPARISON OF DIURNAL VARIATIONS FOR THE SUMMER,
 ... DIURNAL TRANSITION
 ... DAYTIME

SUBARCTIC STRATIFICATION

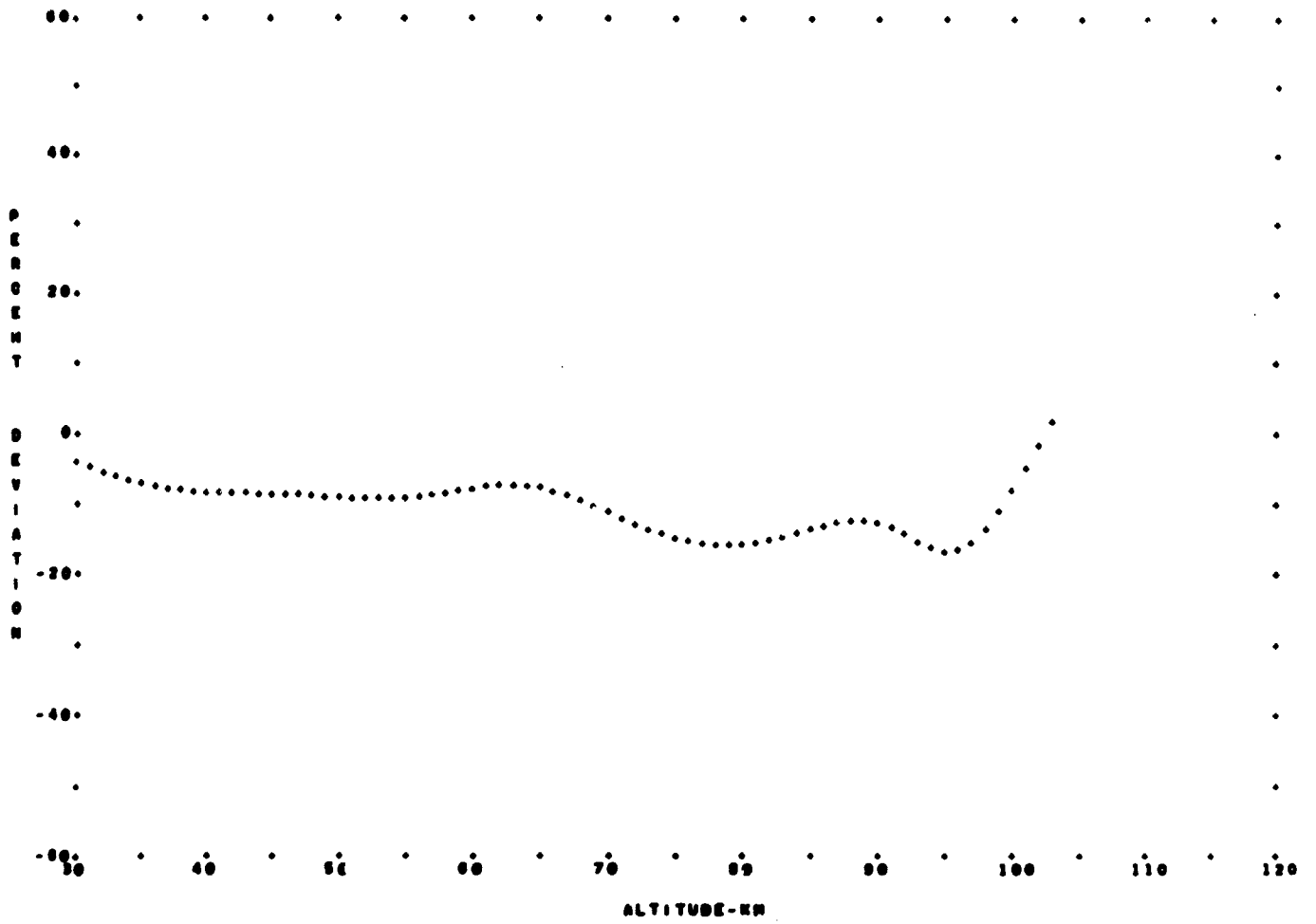


FIGURE 28 - COMPARISON OF DIURNAL VARIATIONS FOR THE AUTUMN.
 ... DIURNAL TRANSITION

SUBARCTIC STRATIFICATION

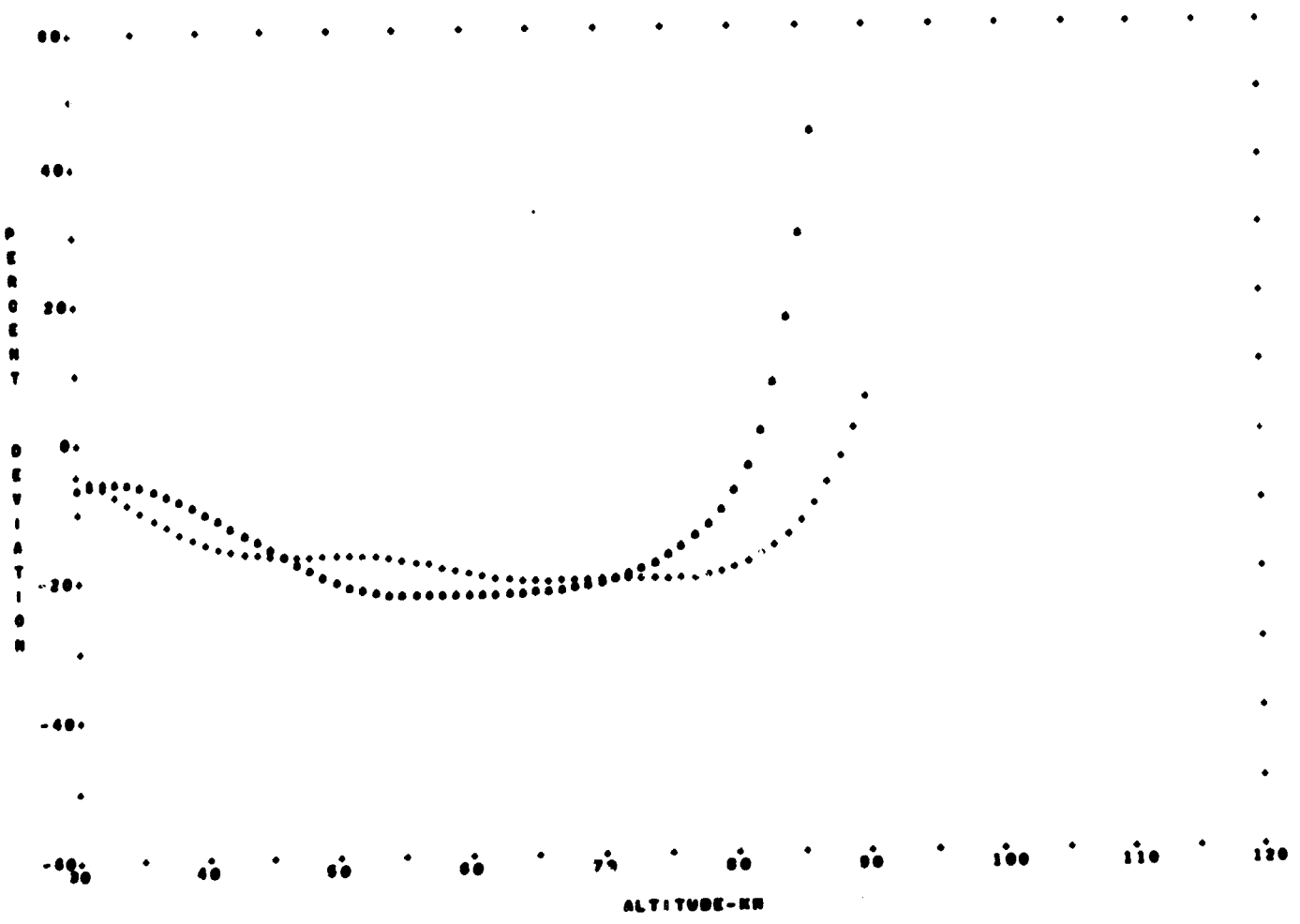


FIGURE 29 - COMPARISON OF DIURNAL VARIATIONS FOR THE WINTER,
 ... DIURNAL TRANSITION
 ... NIGHTTIME

SUBARCTIC STRATIFICATION

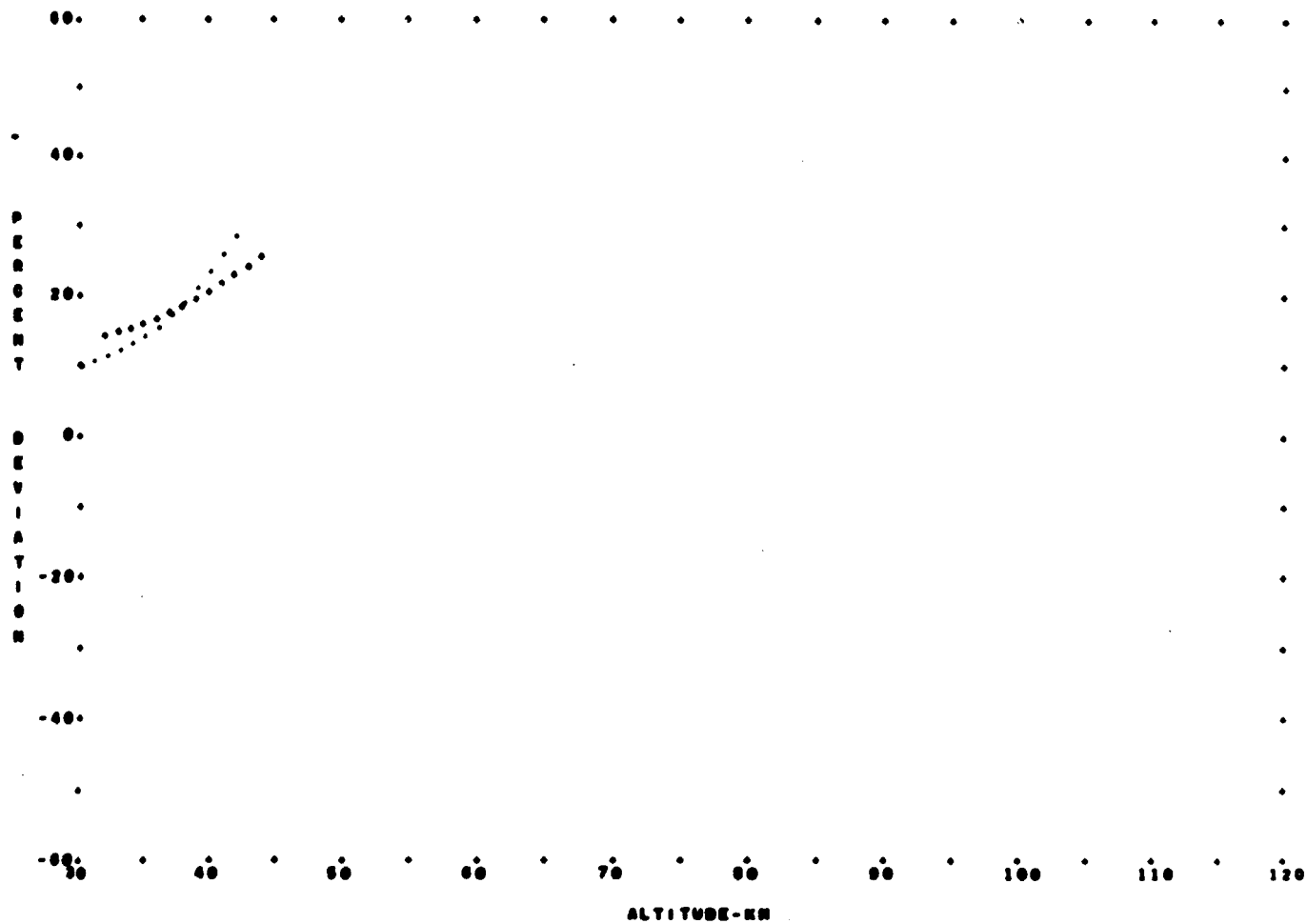


FIGURE 30 - COMPARISON OF DIURNAL VARIATIONS FOR THE SUMMER EXTREME, SUBARCTIC STRATIFICATION
 ... DIURNAL TRANSITION
 ... DAYTIME

ANOM

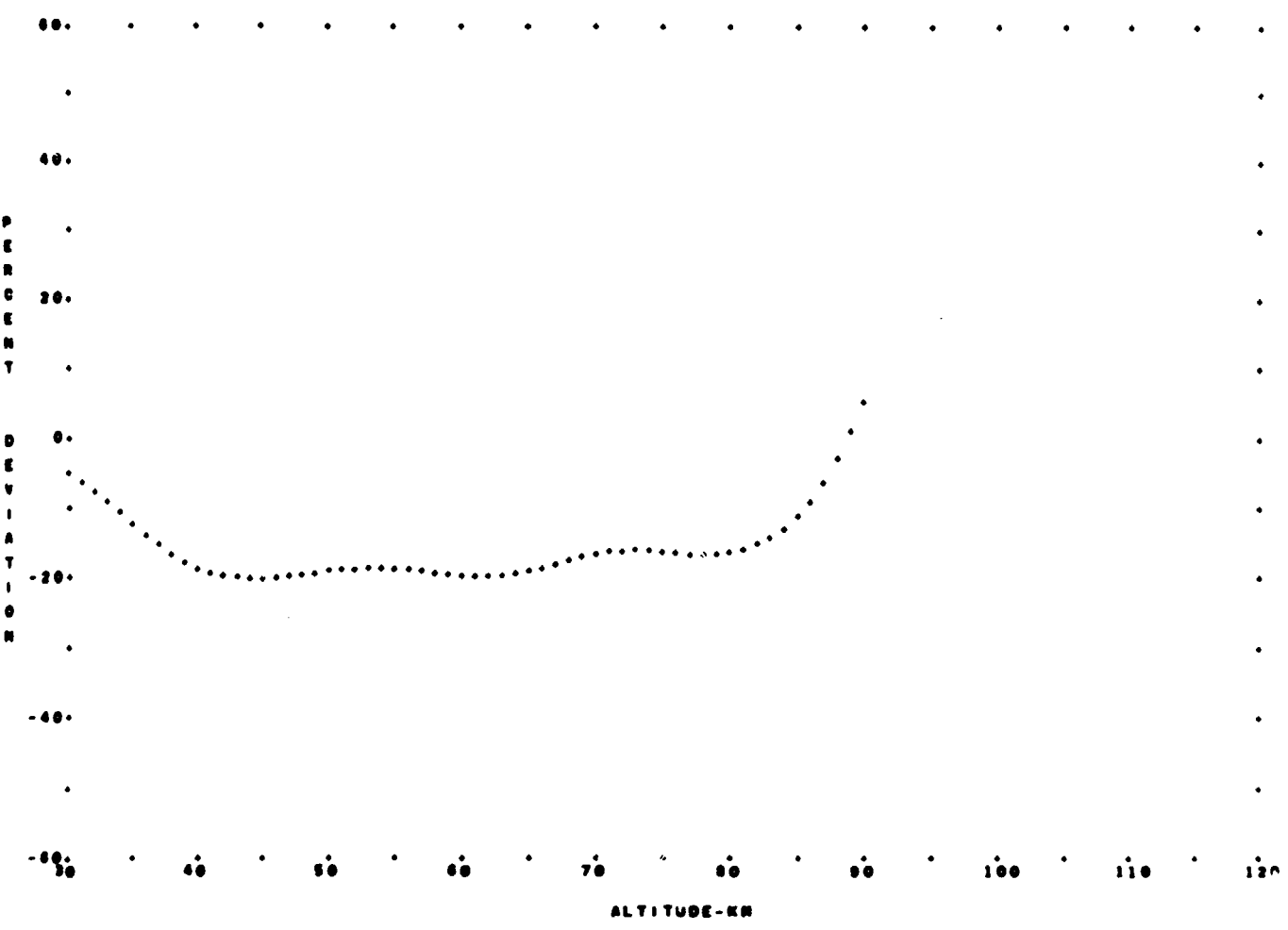


FIGURE 31 - COMPARISON OF DIURNAL VARIATIONS FOR THE WINTER EXTREME, SUBARCTIC STRATIFICATION
... DIURNAL TRANSITION

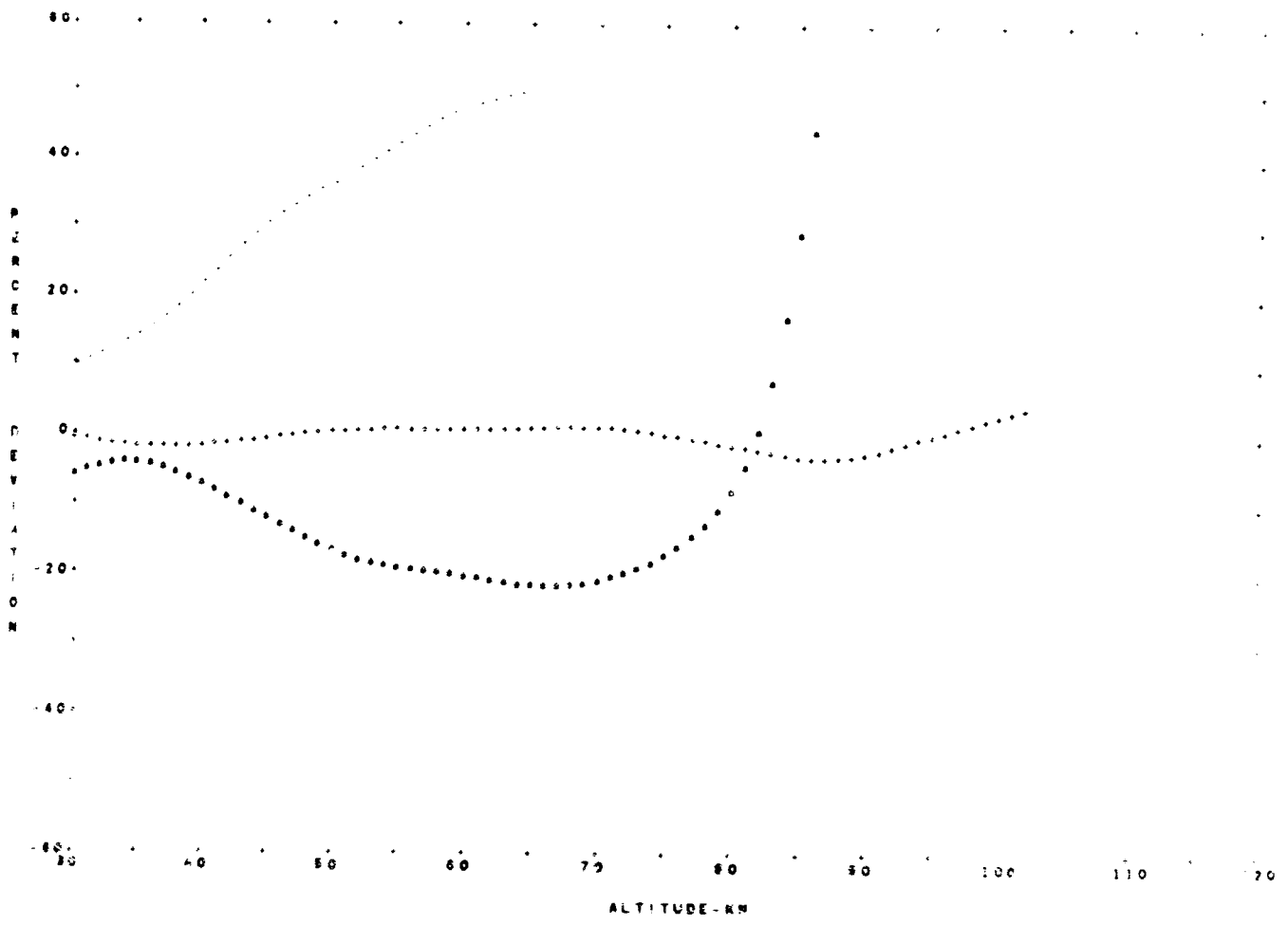


FIGURE 11 - COMPARISON OF DIURNAL VARIATIONS FOR CUMULATIVE MEAN, SUBARCTIC STRATIFICATION, DIURNAL TRANSITION, DAYTIME AND NIGHTTIME

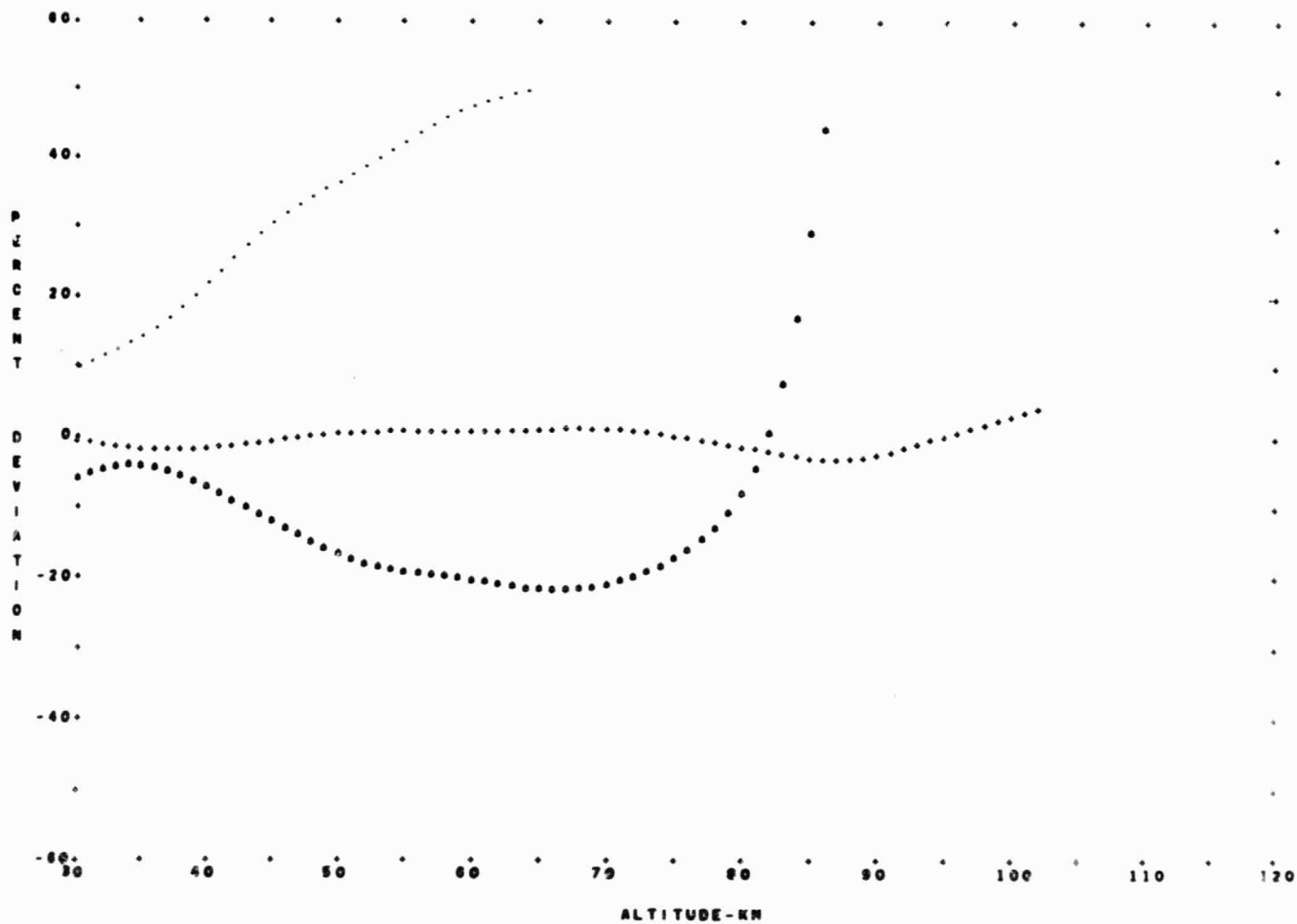


FIGURE 32 - COMPARISON OF DIURNAL VARIATIONS FOR THE ANNUAL MEAN, SUBARCTIC STRATIFICATION
 ... DIURNAL TRANSITION
 ... DAYTIME
 ... NIGHTTIME



ARCTIC STRATIFICATION

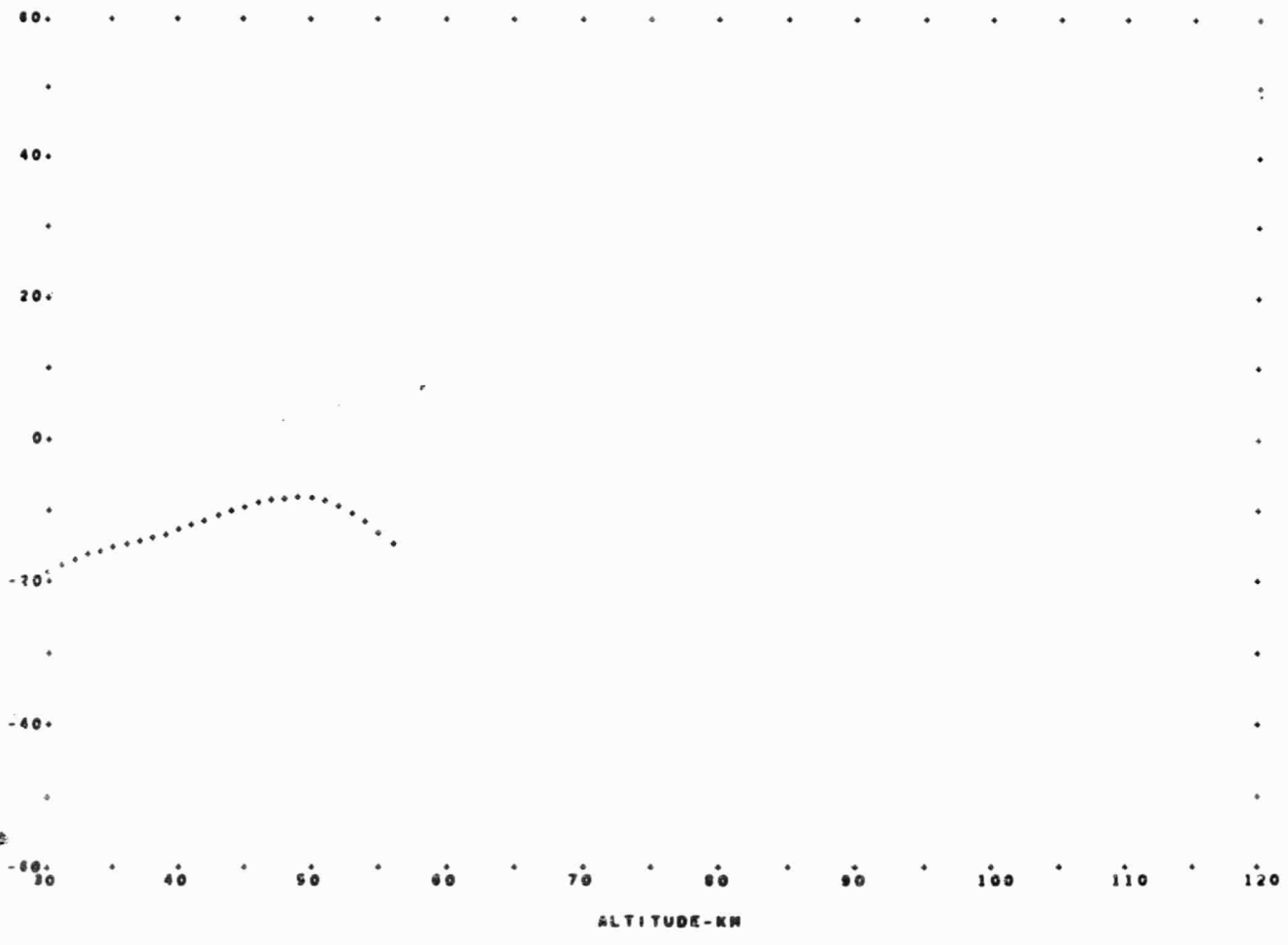


FIGURE 33 - COMPARISON OF DIURNAL VARIATIONS FOR THE SPRING,
... DIURNAL TRANSITION

ARCTIC STRATIFICATION

1999

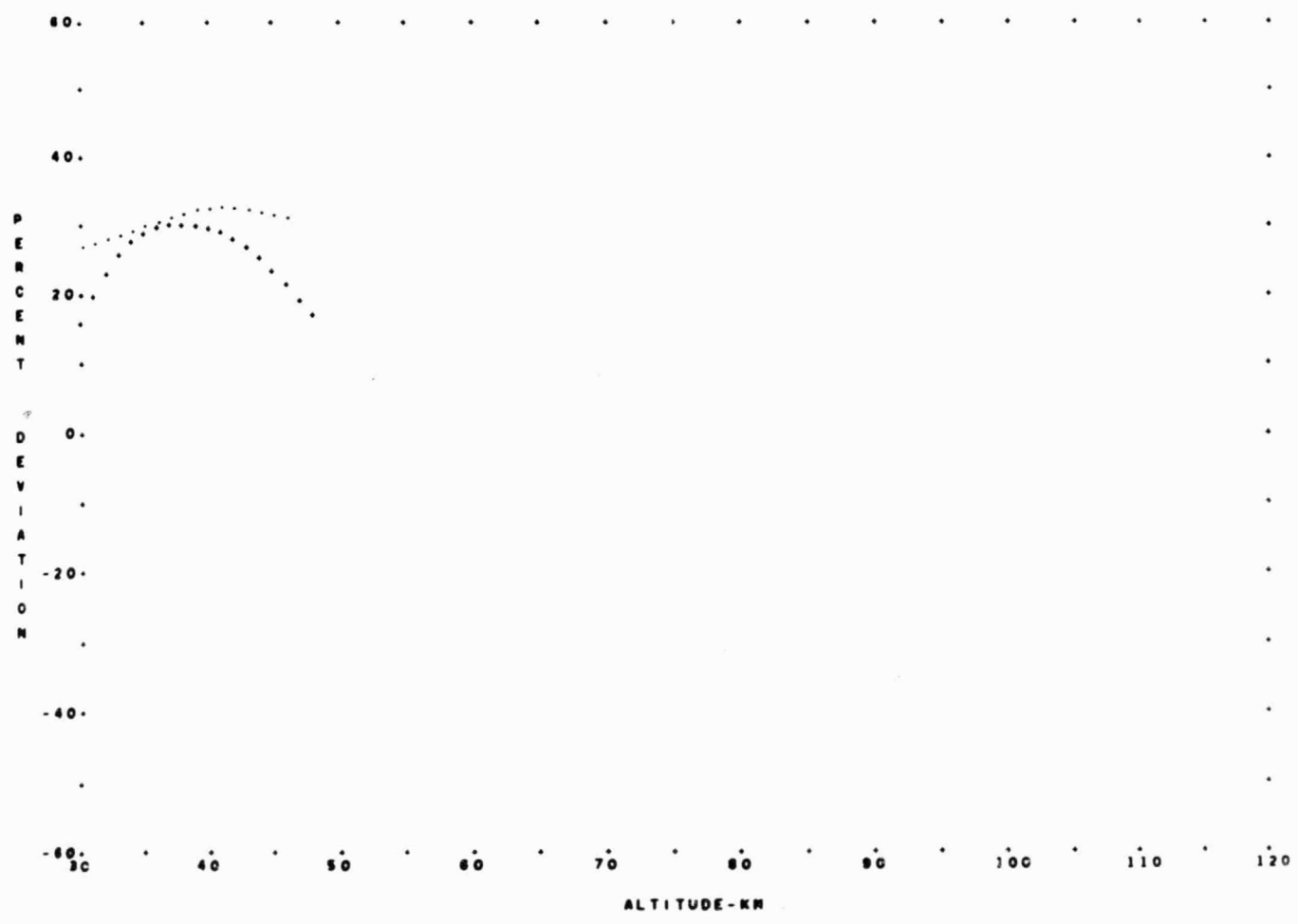


FIGURE 34 - COMPARISON OF DIURNAL VARIATIONS FOR THE SUMMER. ARCTIC STRATIFICATION
... DIURNAL TRANSITION
... DAYTIME

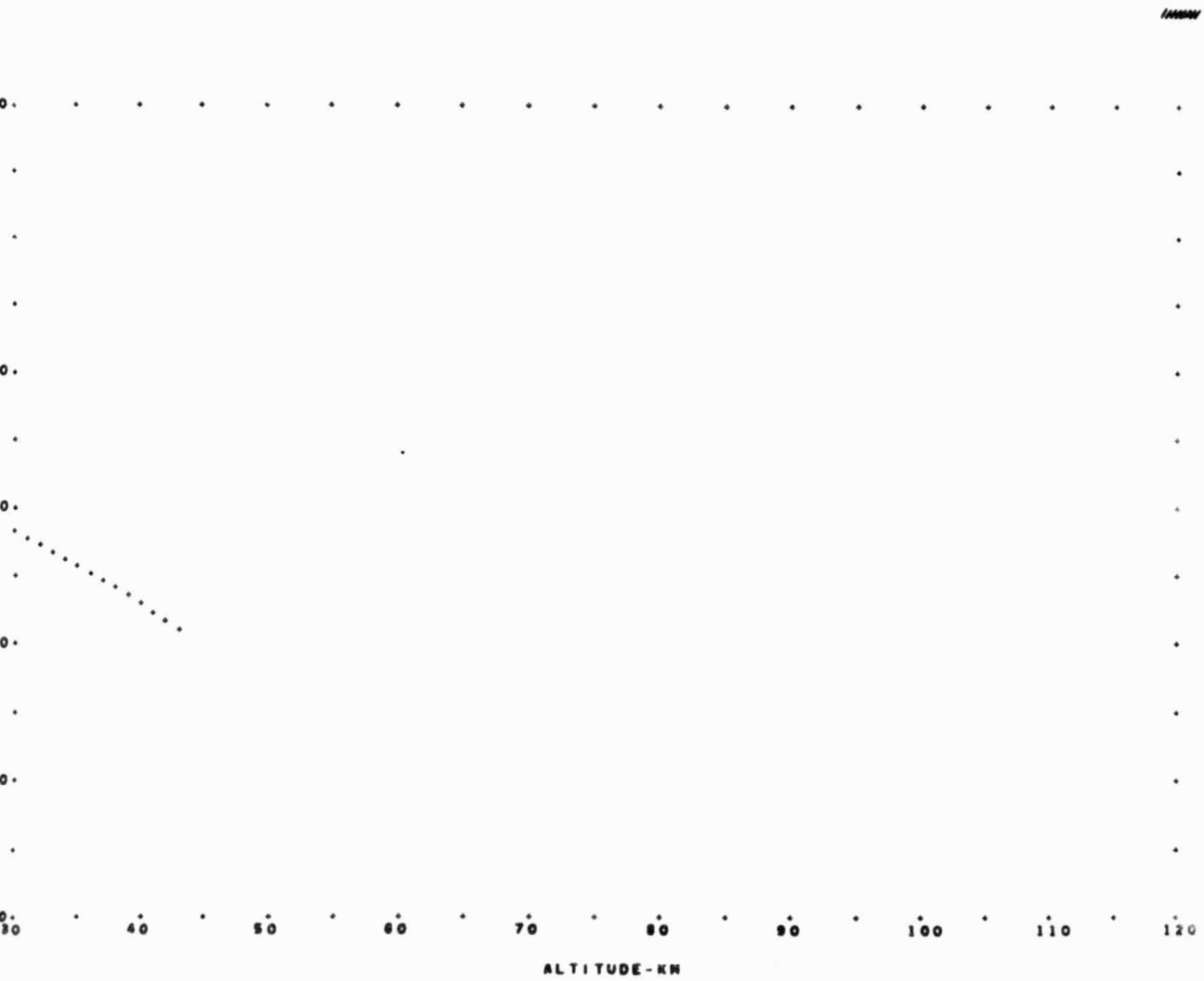


FIGURE 35 - COMPARISON OF DIURNAL VARIATIONS FOR THE AUTUMN,
 ... DIURNAL TRANSITION

ARCTIC STRATIFICATION

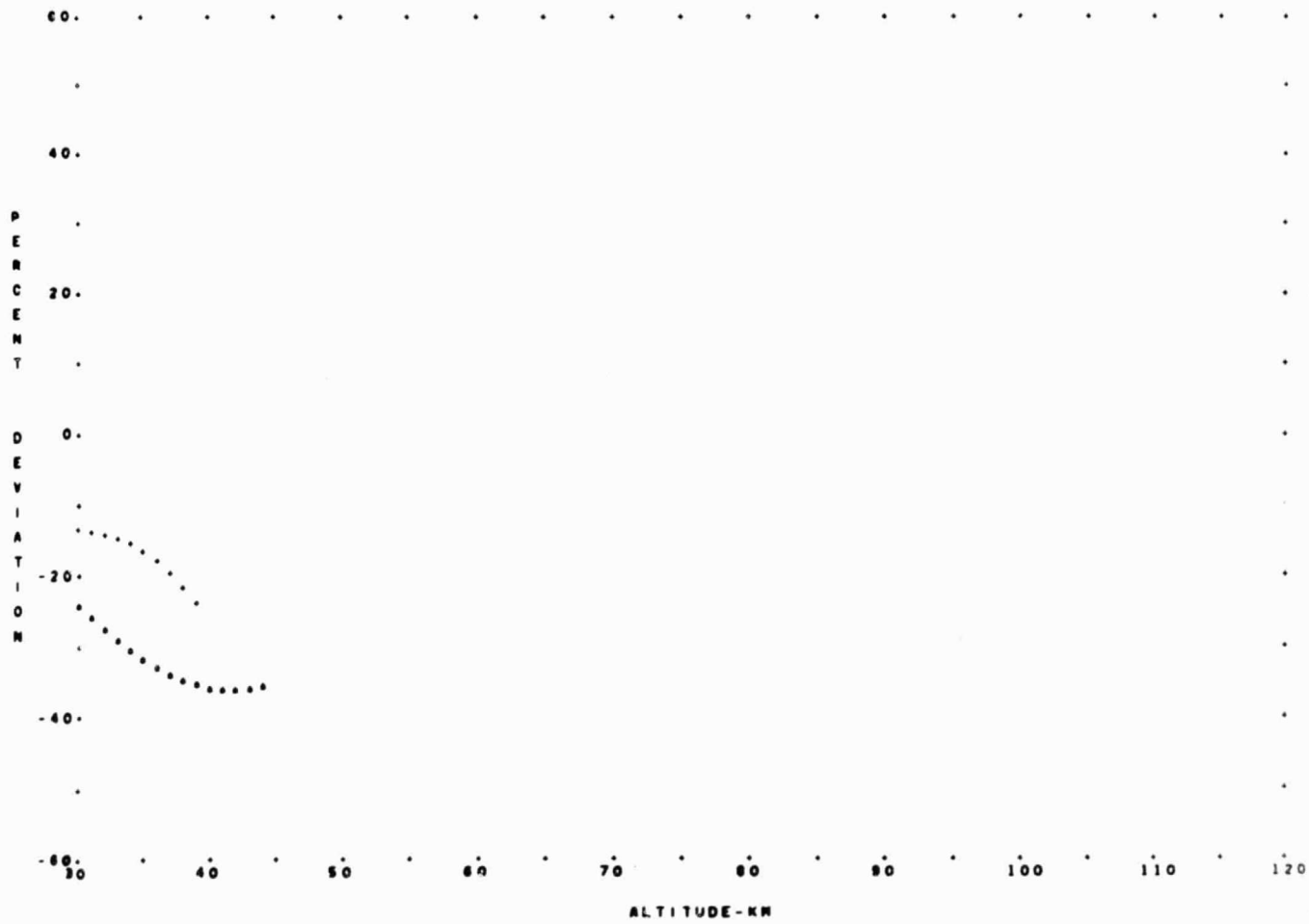


FIGURE 36 - COMPARISON OF DIURNAL VARIATIONS FOR THE WINTER,
 ... DIURNAL TRANSITION
 ... NIGHTTIME

ARCTIC STRATIFICATION

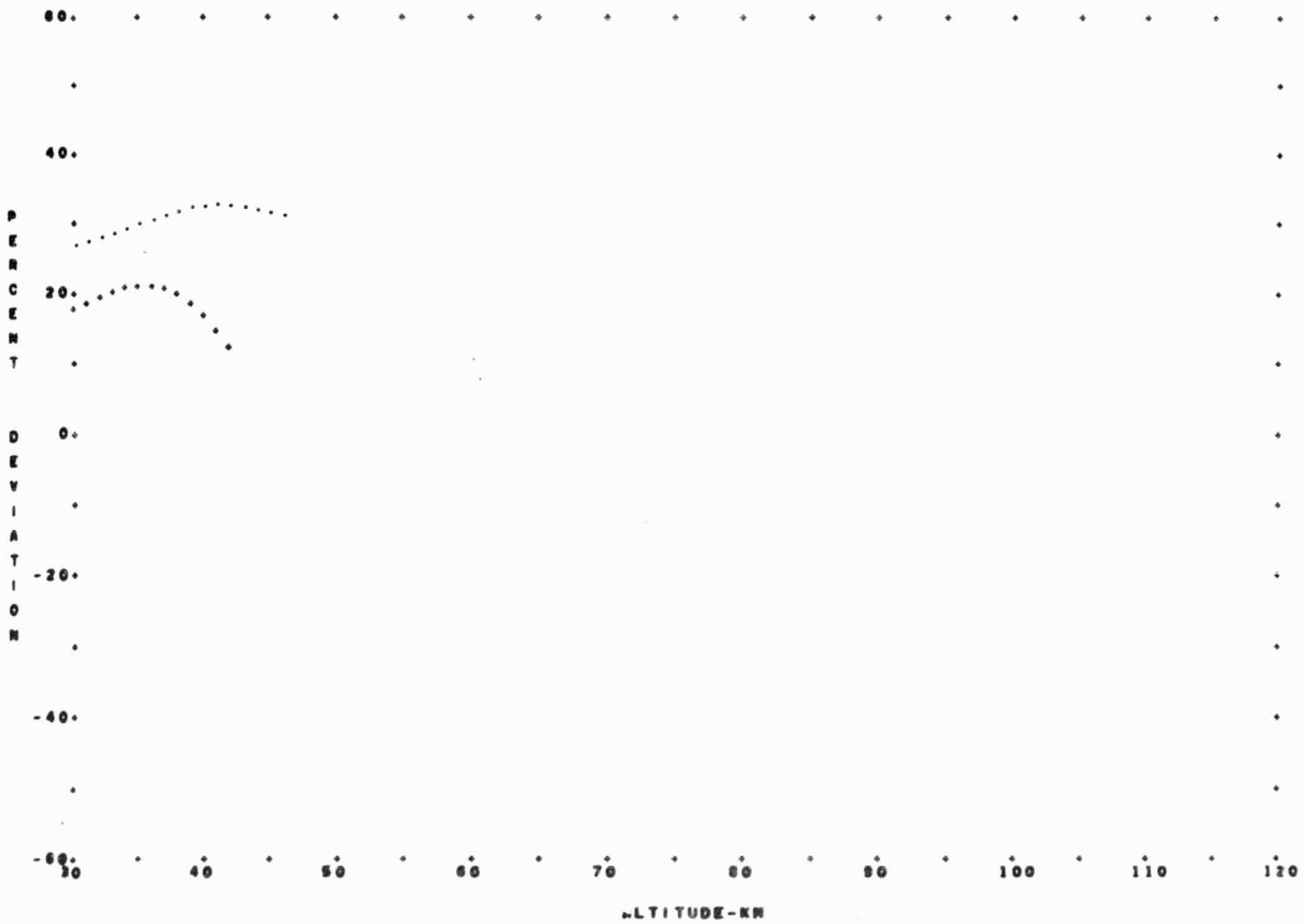


FIGURE 37- COMPARISON OF DIURNAL VARIATIONS FOR THE SUMMER EXTREME, ARCTIC STRATIFICATION
 ... DIURNAL TRANSITION
 ... DAYTIME

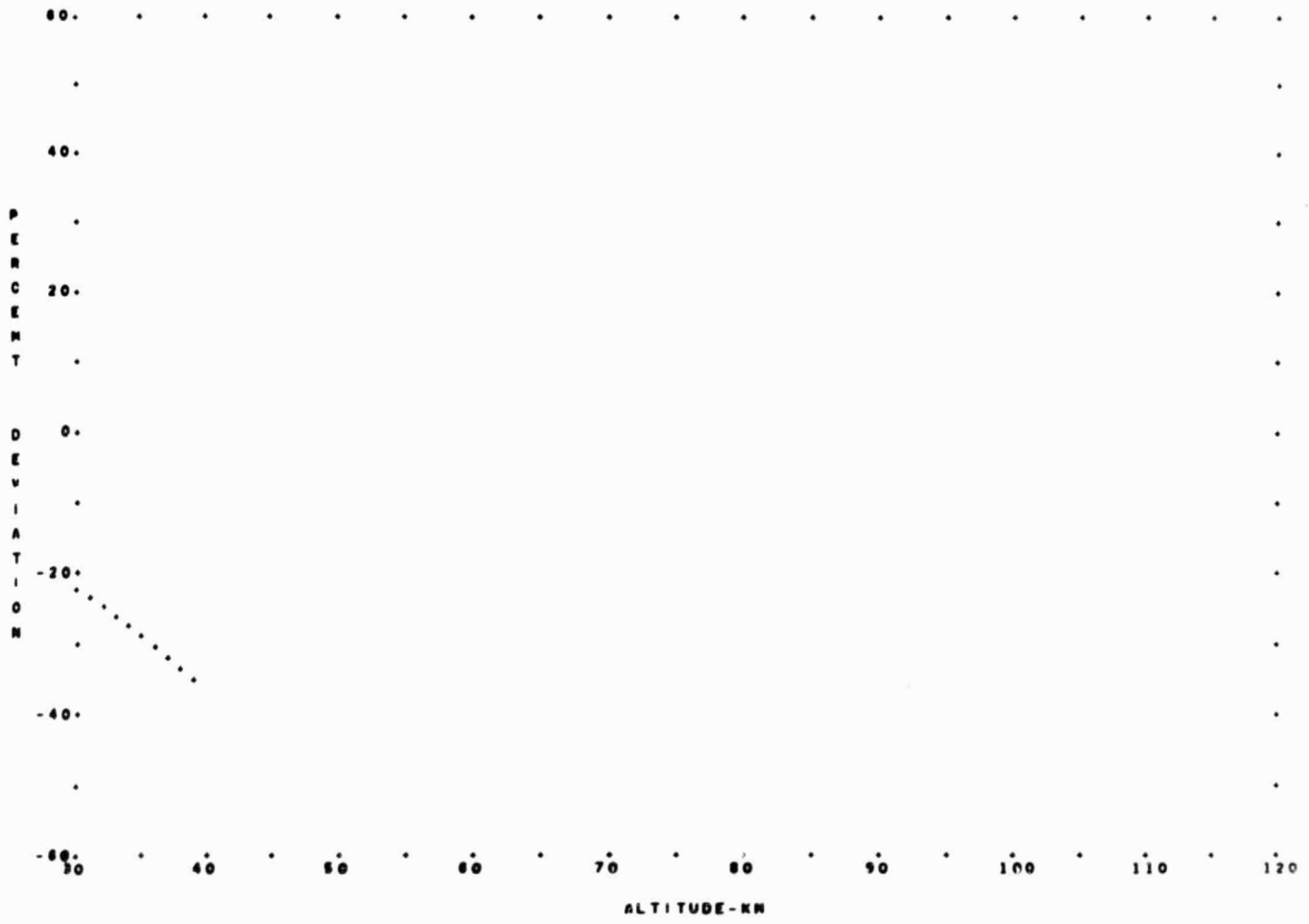


FIGURE 38- COMPARISON OF DIURNAL VARIATIONS FOR THE WINTER EXTREME, ARCTIC STRATIFICATION
 ... DIURNAL TRANSITION

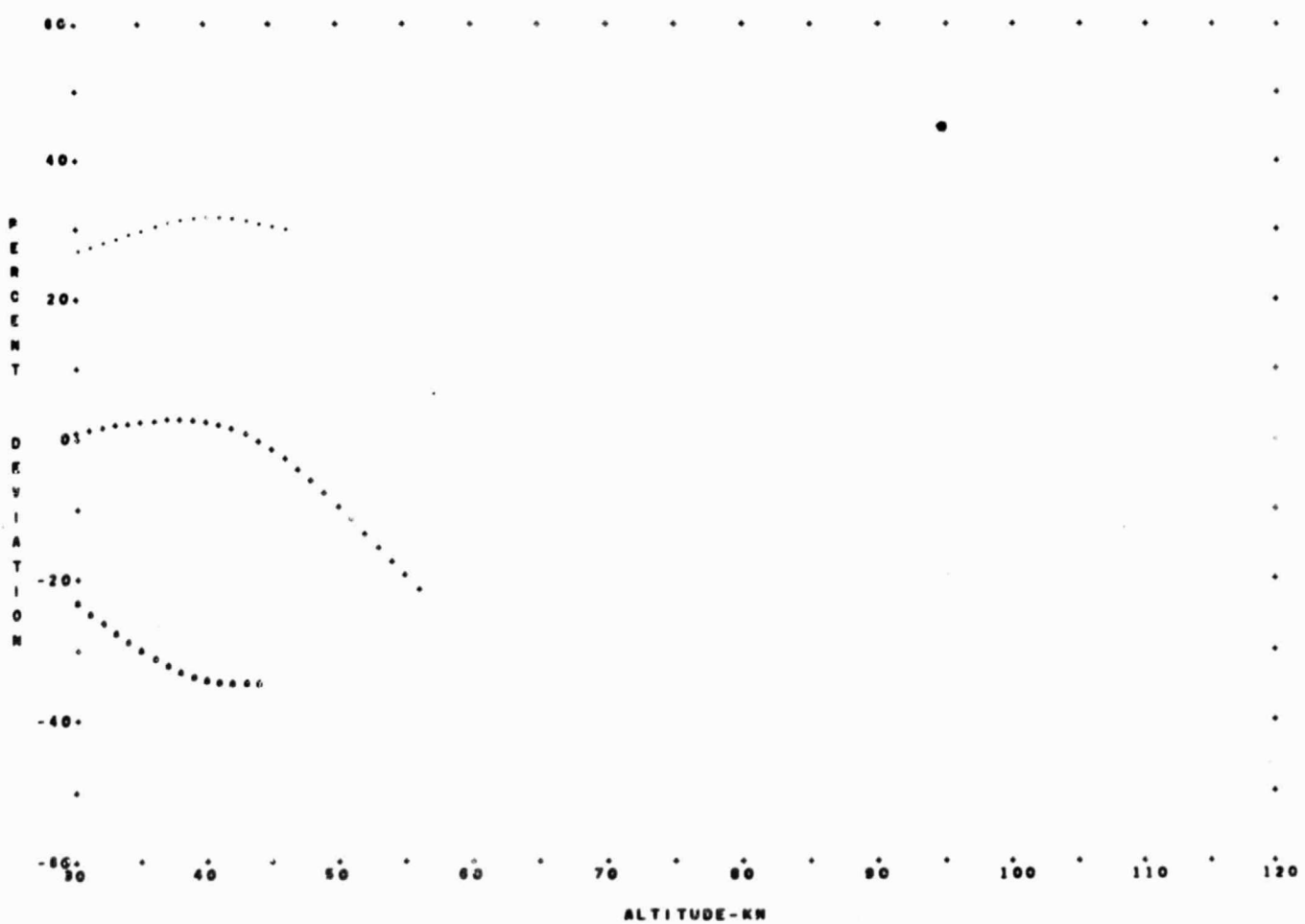


FIGURE 39 - COMPARISON OF DIURNAL VARIATIONS FOR THE ANNUAL MEAN.
 ... DIURNAL TRANSITION
 ... DAYTIME
 ... NIGHTTIME

ARCTIC STRATIFICATION

In the 35 to 80 km height region, the summer season shows a general increase in the diurnal change to a maximum observed value of about 15 percent at 80 km.

The annual mean profiles show a similar increase in the divergence of the daytime and nighttime curves with increasing height. The difference shows a maximum of 18 percent between 65 and 70 km. Part of the diurnal difference may only be an apparent one, and is actually seasonal in origin as a consequence of the disproportionate distribution of the data into the various classification cells.

Sub-arctic and arctic latitude belts.- The profiles available for analysis in the sub-arctic and arctic belts do not provide for a direct comparison of day-night density variations. The reason for this lies in the definitions of the astronomical conditions which were used to classify the data as discussed earlier.

The consequence of these limitations in the classification scheme are that the summer season graphs show only diurnal transition and daytime curves, while the winter season graphs show only diurnal transition and nighttime curves. The spring and autumn seasons, however, show only diurnal transition cases. Furthermore, the large daytime to nighttime differences shown in the annual mean graphs are largely a reflection of seasonal, i.e., summer to winter variations rather than diurnal variations.

METHOD OF ANALYSIS

The stratification procedures described above were not extended to the present study. Instead the current investigation emphasized a statistical analysis of the data based on stepwise multiple regression methods. This type of analysis has significant advantages in studies where cause and effect relationships are poorly understood, necessitating numerical experimentation with a large number of independent variables. The number of independent variables is limited by the sample size, but the method permits testing of both linear and non-linear functional relationships between these variables. The major advantages of stepwise multiple regression for the present study are:

1. It provides a procedure for selecting from a large number of potential predictors, those variables that contain most of the information about the dependent variable, and provide the "best fit" to the data. The chosen variables are presented in the order of their significance as predictors.

2. It provides an empirical functional relationship between the dependent variable (atmospheric density) and the independent variables (periodic and geophysical parameters).

There are, however, several limitations that may be encountered in the application of this technique. These include the definition of variables, i.e., functional relations, and the testing of the statistical significance of the derived regression equation. A major problem stems from the requirement that the variables to be included in the regression model and their functional relationships must be defined a priori. In the present application, the variables tested were selected on the basis of our current knowledge of upper atmospheric behavior, while the selection of functional relationships has generally been approached by including a number of functional transformations for each variable, and relying on the screening procedure to select which one or combination of transformations best fits the data.

One of the requirements in testing for the statistical significance of the regression model is that the error term in the regression equation follows a normal distribution, and is independent of the other variables. This is not necessarily true in the case of atmospheric variables. A second standard assumption for testing the fit of a regression model to a given set of data is that the independent variables be chosen at random from the set defined for the model. The stepwise multiple regression procedure does not select predictors at random, but instead chooses them in the order of their significance in explaining the variability in the data. For this reason the standard F-test for significance has to be modified prior to its application to the stepwise regression results.

Multiple Regression

For the purpose of describing this procedure, let the dependent variable Y represent atmospheric density and the independent variables X_1, X_2, \dots, X_k represent the periodic and geophysical predictors. We also will assume that there are n sets of random observations of the Y and X_i variables. Multiple regression analysis attempts to fit to this data an equation of the form:

$$Y = a_0 + a_1X_1 + a_2X_2 + \dots + a_kX_k \quad (4)$$

where a_0, a_1, \dots, a_k are constants to be determined. These constants are chosen by the regression analysis so as to provide a best fit to the data in the least squares sense.

Geometrically, the procedure can be understood by considering the observations to be represented by n points in $(k + 1)$ dimensional space. The equation then represents a plane, or hyperplane that provides the closest fit to these data points, i. e., it minimizes the sum of the squares of the distances from the points to the plane.

For the application to the present study, the regression equation in the above form is not entirely suitable, since it assumes a linear relationship to

exist between each of the geophysical predictors and the atmospheric density variable. It appears, in fact, that most predictors do not follow a linear relationship with density, and it is necessary therefore to use non-linear transformations for most variables in the study. These may be in the form of functions of the basic variable and/or cross-product terms.

The regression model may take the form

$$Y = a_0 + a_1 f_1(X_1) + a_2 f_2(X_2) + a_3 f_3(X_1, X_2) + \dots \quad (5)$$

This equation can be linearized and written in the standard form by the following substitutions:

$$\begin{aligned} x_1 &= f_1(X_1) \\ x_2 &= f_2(X_2) \\ x_3 &= f_3(X_1, X_2) \\ &\vdots \end{aligned} \quad (6)$$

The procedure for solving the simple linear model for the a_i is well known, and may be found for example in Ostle (Ref. 17).

Analysis of variance in multiple regression. - The total variance in Y (atmospheric density) about the mean value for the data sample is measured by computing the sum of the squares of deviations

$$SS_T = \sum_{i=1}^n (Y_i - \bar{Y})^2 \quad (7)$$

where SS_T is the total sum of squares, and \bar{Y} is the mean value of Y for the sample.

The residual variance in Y is a measure of the deviations of the observed values of the dependent variable from the values predicted (\hat{Y}_i) by the regression equation. This variance is measured by computing the sum of squares of the deviations of the observed Y_i from the \hat{Y}_i .

$$SS_R = \sum_{i=1}^n (Y_i - \hat{Y}_i)^2 \quad (8)$$

where SS_R is the residual sum of squares and \hat{Y}_i is the value predicted from the i th set of (x_1, x_2, \dots, x_k) observations.

The explained sum of squares is equal to the difference between the total SS_T and the residual SS_R ,

$$SS_{ex} = SS_T - SS_R \quad (9)$$

and indicates how well the chosen regression model fits the given data. A more common measure of the fit of the model to the data is provided by the multiple correlation coefficient, defined as the square root of the ratio of the explained SS_{ex} to the total SS_T ,

$$R = \sqrt{SS_{ex}/SS_T} \quad (10)$$

where the positive root is customarily chosen. Hence, the square of the multiple correlation coefficient, in fact, represents the proportion of the total variance in Y explained by the assumed regression model.

Stepwise regression.- In the present study a stepwise procedure was followed in order to select the most significant variables from the total set of those defined. The procedure consists of adding one variable at each step and computing the multiple correlation coefficient, and the residual sum of squares. At each step of the procedure the variable selected from the list of unused variables is the one that, when added to the equation of the previous step, provides the greatest reduction in the residual sum of squares. That is, the variable that provides the most additional information about the dependent variable Y . Thus, at some step in the procedure, a variable that is highly correlated with Y may not be chosen in favor of one that has a lower correlation with Y . This will occur if the highly correlated variable simply duplicates information provided by a previously chosen variable.

In the present study this masking of significant variables has occurred, for example, in the case of two variables that were used to measure seasonal variations in density. One variable indicates the time of year, the other measures the angular distance from the point of observation to the sub-solar point. Although both variables were highly correlated with atmospheric density, generally when one was selected at an early step in the procedure, the other was dropped until a much later step. This was due to the fact that both variables contained almost equivalent information on seasonal variations in density.

Significance Testing . - In order to test that the variance explained by a given regression model is not merely a random occurrence, it is necessary to determine the statistical significance of the fit provided by the model. For this purpose, an F-ratio test has been used at each step of the multiple regression procedure to determine whether the reduction in the residual sum of squares due to the added variable is statistically significant. The F-score for a given step was obtained from the ratio (See Ref.18),

$$F_p = \frac{SS_{R, p-1} - SS_{R, p}}{SS_{R, p}} (n-k-1) \quad (11)$$

where F_p is the F-score for testing the significance of the variable added at the pth step.

$SS_{R, p}$ and $SS_{R, p-1}$ are the residual sum of squares for pth and (p-1)st step, respectively,

n is the sample size, and

k is the number of variables included in the pth step.

To determine the significance of the added variable, F_p must be compared with the critical value determined from an F distribution with (1, n-k-1) degrees of freedom. In general, the critical F value has been taken at the 0.95 confidence level so that there is a 5 percent chance of accepting a variable as significant when it actually is not.

An important underlying assumption in application of the F-test is that the added variable whose significance is being tested has been randomly chosen from the total group defined. In the case of the stepwise regression analysis, however, this choice is not random. In fact, at each step the most significant of the remaining variables has been selected and, therefore, the F-test is likely to over estimate the significance of the added variable. To compensate for this, an adjustment to the F value has been proposed by Miller (Ref. 19). According to his hypotheses, the adjusted 0.95 critical value to be used with the stepwise procedure is:

$$F_{0.95}^* = F_{\left(1 - \frac{1}{20n}\right)} \quad (12)$$

In general, this adjustment has been made in the current study when testing for the significance of added variables. The consequence of this adjustment is that the larger the number of variables included in the set of potential predictors for a given analysis, the more stringent becomes the requirements for accepting each additional variable to the regression equation. Thus, when large sets of potential variables are considered simultaneously, this test cannot be given a precise interpretation. However, it does provide guidelines for deciding which variables to include in the final regression equations.

Computer Programming

A number of standard computer programs are available for stepwise regression analysis. For our purpose, however, the most suitable appeared to be an IBM type III FORTRAN program prepared for the IBM System 360 data processing system. This program has the advantage that it permits various types of mathematical transformations to be applied to the independent variables. For the purpose of this study, some additional modifications were made to the basic IBM program. These modifications were to provide a data input procedure that would suit the format of the prepared data and to include various data transformation procedures that were not included in the original program. A complete listing of the modified program is presented in Appendix C.

SELECTION OF BASIC VARIABLES

As a guide to the search for periodic and geophysical variables which may be related to variations in atmospheric density in the current study, it is useful to review briefly similar studies conducted at higher altitudes using density data derived from satellite drag measurements. In particular, Jacchia (Ref. 20) has described four types of atmospheric variations at heights greater than 200 km, namely:

1. A variation with solar activity
2. A semi-annual variation
3. A diurnal variation, and
4. A variation with geomagnetic activity.

Each of these variations has been found to be related to one or more observable parameters and Jacchia has developed empirical formulas to compute the predicted model atmosphere when the values for these parameters are known.

In the case of variations with solar activity, Jacchia has found that the 10.7-cm solar flux monitored by the National Research Council

in Ottawa provides a convenient parameter for characterizing solar activity. This parameter exhibits both long and short period oscillations. The first major time scale of possible interest is variations in solar activity during the slowly changing eleven-year cycle in which case seasonal averages of solar flux may suffice. Superimposed on this are shorter period day-to-day changes which are observed within one 27-day solar rotation and for which daily mean flux values are a suitable parameter. These daily values of the 10.7-cm solar flux are available on a continuous basis for periods extending back at least as far as the period for which upper atmospheric density data are available (approximately early 1947) (Ref.21).

The diurnal variation or so-called "diurnal bulge" of upper atmospheric density has been observed to peak at about 2 p.m. local solar time. The morning minimum occurs around 4 a.m. so that the decay in density from the center of the bulge at 2 p.m. is somewhat steeper on the morning side than on the evening side. Some more recent results by Jacchia and Slowey (Ref. 22) suggest that above the F₂ layer the center of the bulge does not migrate north and south of the equator following the migrations of the sub-solar point, rather the center remains stationary over the equator. This stationarity may only be an apparent one produced by the method of averaging used to reduce the data. At lower altitudes, the coincidence of the bulge center and the subsolar point still appears to be correct. Hence, at the altitudes of the rocket density data, the sub-solar point (or declination angle of the sun) may serve as a convenient diurnal variation parameter.

A very stable semi-annual density variation has been found in eight years of upper atmospheric density data (Ref. 22). These changes show a deep minimum in July, followed by a high maximum in October to November with a secondary minimum in January and a secondary maximum in April. Although the period of these oscillations can be related to the number of days elapsed during each year, the amplitude seems to be a function of the solar cycle and as such can be related to the seasonally averaged 10.7-cm solar flux.

The current study also has considered the earth's shadow height at the time of the sounding as a potentially significant diurnal variable. The shadow height is taken to be zero during daylight conditions at the earth's surface. An existing computer program for calculation of the shadow height was adapted for execution on the IBM System 360/75 during the course of the current study.

Finally, Jacchia (Ref. 13) has shown that temperature and density of the upper atmosphere increase during magnetic storms. During these storms the temperature variations seem to be related in a near-linear fashion with the 3-hourly planetary geomagnetic index

while during quieter periods the relation is nearly linear with the logarithm of this index. Later investigation by Jacchia, Slowey and Verniani (Ref. 23) revealed a lag in the atmospheric perturbation behind the geomagnetic perturbations by several hours. At the satellite altitudes of these results (250 to 550 km), and for latitudes below 55° , the time lag turns out to be between 6 and 7 hours. The time lag is slightly shorter at latitudes greater than 55° varying between 5 and 6 hours.

Although the mechanism through which the atmosphere is heated during geomagnetic disturbances is not known, the existence of such heating and the large day-to-day temperature variations that accompany the most minute changes of the geomagnetic field show that the presence of ions in the earth's magnetic field is an important controlling factor of the upper air temperature. The semi-annual temperature variation also lacks a good explanation, and its coincidence with the height variation of the F_2 layer suggests that the magnetic field of the earth may have a larger effect on controlling the temperature of the upper atmosphere than was pre-supposed heretofore. Possibly the most that can be stated at this time is that this controlling influence may extend down to altitudes below those of the satellite drag measurements.

DISCUSSION OF RESULTS

In all, four complete sets of regression analyses were carried out, each with a modified set of independent variables. The choice of variables for the initial calculation was based on the considerations discussed in the previous section. For subsequent calculations, the variable selection was based on an analysis of the results of all the previous calculations. New variable transformations were added at succeeding runs as a result of hypotheses suggested by the interpretation of previous runs. The complete set of variables included in the study is presented in Tables XI through XIII.

The regressions were performed for each of a series of altitudes. Initially the choice of the altitudes was limited to three selected heights. In order to gain further information on the variation of the regression coefficients with height, however, subsequent runs included analyses at each 5 km of height from 30 to 110 km. The altitude region above 110 km was considered to contain too few samples to yield reliable results.

Initial Analysis

The initial set of calculations was carried out for altitudes of 40, 65, and 100 km. These altitudes were selected on the basis of expected maximum annual, diurnal, and radiation effects, respectively. The list of variables included in the initial run is presented in Table XI.

TABLE XI
LIST OF VARIABLES AND TRANSFORMATIONS
INITIAL RUN

<u>VARIABLE NAME</u>	<u>TRANSFORMATION</u>
Annual period (sin)	$\sin (2\pi \cdot \frac{d}{365})$
Diurnal period (sin)	$\sin (2\pi \cdot \frac{h}{24})$
Latitude difference (cos)	$\cos (SL-L)$
Shadow height	= 1 for observation in earth's shadow = 0 otherwise
Sub-solar angle (cos)	$\cos (SA)$
Log geomagnetic index (n hours lag)	$\text{Log}_e (GI_n)$
Solar flux reciprocal (m days lag)	$1/SF_m$

where

- d is the number of days elapsed since the spring equinox (i.e., vernal equinox in the northern hemisphere, autumnal equinox in the southern) in days and fractions of a day,
- h is the local apparent time of the observation in hours and fractions of an hour,
- SL is the latitude of the sub-solar point at the time of the observation,
- L is the latitude of the location of the observation,
- SA is sub-solar angle of the observation point at the time of the observation,

TABLE XI (continued)

GI_n is the equivalent scale geomagnetic index n hours before the time of the observation. The data gives values of GI_n for $n = 0$ to 24 in steps of 3 hours,

SF_m is the 10.7-cm solar flux radiation m days before the day of the observation. The data gives values of SF_m for $m = 0$ and 1.

One of the problems encountered at this point resulted from the fact that the equivalent geomagnetic index was zero for many observations and, therefore, the log-transformation was not defined. To circumvent this problem, the regressions excluded those observations with zero as a value for this variable. Although this approach had the undesirable effect of reducing the total number of observations for each altitude, it appeared to be the only feasible way to complete the analysis using a log-transformation.

The results from the initial analysis were incomplete because a number of computer problems were encountered in the early stages of the computations. These early results did, however, show the predominance of the annual variation in atmospheric density.

Second Analysis

The second set of calculations also was carried out at altitudes of 40, 65, and 100 km, but with several modifications to the list of variables. The equivalent geomagnetic index was treated as a linear variable rather than changed through a logarithmic transformation, because our analysis of scatter diagrams did not reveal a strong logarithmic relation. This change avoided the requirement to eliminate data records for undefined values.

It also was recognized that a time lag may exist in the annual and diurnal variations. A suitable relationship to describe the annual variation in density can be of the form

$$Y = A \sin \left(2\pi \frac{d-B}{365} \right) \quad (13)$$

where A is the amplitude coefficient to be determined, and

B is the lag coefficient to be determined.

This can be expanded into the form

$$Y = a_1 \sin \left(2\pi \frac{d}{365} \right) - a_2 \cos \left(2\pi \frac{d}{365} \right) \quad (14)$$

where

$$a_1 = A \cos \left(2\pi \frac{B}{365} \right)$$

$$a_2 = A \sin \left(2\pi \frac{B}{365} \right)$$

The coefficients a_1 and a_2 can be determined by including both the sine and cosine of the annual period in the regression equation; then the lag coefficient is determined by means of the relationship

$$B = -\left(\frac{365}{2\pi}\right) \tan^{-1} \left(\frac{a_2}{a_1}\right) \quad (15)$$

A similar procedure can be followed in the case of the diurnal density variation by the inclusion of both a sine and cosine transformation of the diurnal variable to permit estimation of the time lag.

In the case of the other trigonometric transformations (cosine of latitude difference and cosine of sub-solar angle) a time lag interpretation cannot be made so easily. Nevertheless, both sine and cosine terms were included for these variables in order that an orthogonal component of the transformation could be estimated.

Finally, two variables related by DeVries (Ref. 24) to high altitude density variations were also included. These two periodic variations were a semi-annual variation (183 day period), and a 25 day cycle related to the 27 day synodic period of the sun. Both of these variables were included with sine and cosine transformations. The complete list of variables for the second run is presented in Table XII.

The results of the analysis are listed in Table D-1 of Appendix D. For each altitude, the variables listed are given in the order of their selection by the regression analysis. Variables have been excluded from the calculation if their F-scores for additional variance explained are well below the critical F-values. For those variables considered significant, the regression coefficients (a_j) have been listed. These are the coefficients for all the significant variables in the regression step. The constant term is the a_0 coefficient. Also listed are the F-scores for the explained variance due to each of the variables and the critical F-scores ($F_{0.95}$ and $F^*_{0.95}$ as described in an earlier section) for each step of the regression analysis. In general when deciding which variables should be considered significant, the $F_{0.95}$ critical value was considered too lenient because of the non-random selection of variables, while the $F^*_{0.95}$ value was too severe because of the large number variables considered. The basis for setting the cutoff point for excluding variables, thus, was somewhat arbitrary. It was based on our interpretation of the regression model as well as on the $F_{0.95}$ and $F^*_{0.95}$ values.

The 40 km region - The regression equation derived from the second run for the 40 km region is given below:

$$Y = 0.317 \times 10^{-2} + 0.879 \times 10^{-3} \cos(SL-L-10.2^\circ) + 0.285 \times 10^{-3} \sin\left(2\pi \cdot \frac{d-39.6}{365}\right) - 0.125 \times 10^{-3} \sin\left(4\pi \cdot \frac{d}{365}\right) - 0.178 \times 10^{-3} I \quad (16)$$

TABLE XII
LIST OF VARIABLES AND TRANSFORMATIONS
ADDED OR CHANGED FOR THE SECOND RUN

<u>VARIABLE NAME</u>	<u>TRANSFORMATION</u>
Annual period (cos)	$\cos \left(2\pi \cdot \frac{d}{365} \right)$
Diurnal period (cos)	$\cos \left(2\pi \cdot \frac{h}{24} \right)$
Latitude difference (sin)	$\sin (SL-L)$
Sub-solar angle (sin)	$\sin (SA)$
Geomagnetic index (n hrs)	GI_n
Semi-annual period (sin)	$\sin \left(4\pi \cdot \frac{d}{365} \right)$
Semi-annual period (cos)	$\cos \left(4\pi \cdot \frac{d}{365} \right)$
25 day period (sin)	$\sin \left(2\pi \cdot \frac{d'}{25} \right)$
25 day period (cos)	$\cos \left(2\pi \cdot \frac{d'}{25} \right)$

where d' is the Julian date of the observation less the Julian date at the beginning of the year 1940.

where

SL is the latitude of the sub-solar point,

L is the latitude of the point of observation, and

I is equal to 0 when the earth's shadow height is less than 40 km, and 1 otherwise.

The multiple correlation coefficient derived for this regression model from our data sample is 0.732.

Some of the implications of this model should be noted. In this equation the annual (sin) and annual (cos) terms have been combined to give an annual periodic variation with a phase lag. The indicated phase lag is 39.6 days. This means that the maximum density appears to occur in mid-summer (July in the north, January in the south) with the peak value following the time of the summer solstice by about 40 days.

The latitude difference (cos) term also indicated that a maximum density occurs where the difference between the latitude of the solar point and the latitude of the observation point is at a minimum (i.e., mid-summer). The semi-annual variation appears to follow a pattern similar to that first suggested by Paetzold and Zschorner (Ref. 25) reaching maximum densities in early May and early November and reaching minimum densities early February and early August. The effect of the earth's shadow appears to be such that the densities are lower when the observation point is within the earth's shadow. There appears to be no other significant diurnal variable at this altitude. Correlations of density with geomagnetic index and solar flux also appear to be insignificant.

There is one other important point to note. Although the semi-annual term and the shadow height term were chosen by the regression analysis later than the cosine term of the annual period, both show a higher significance level than the annual (cos) variable. This apparently inconsistent result can occur if the combined effect of two variables explain considerably more variance than the individual effects of the same two variables. In this case it indicates that the annual and semi-annual periodicities in combination explain more of the variation in atmospheric density than they do individually - probably because the density variation follows some complex function that is best expressed as a summation of harmonics. Similarly the effect of the earth's shadow height on density is apparently influenced by the annual periodicity.

The 65-km region - The regression equation derived for the 65-km region is

$$Y = 0.105 \times 10^{-3} + 0.596 \times 10^{-4} \cos(SL-L) + 0.480 \times 10^{-4} \cos(SA) + 0.315 \times 10^{-4} \cos\left(2\pi \cdot \frac{h}{24}\right) \quad (17)$$

where

SA is the sub-solar angle at the time of the observation, and

h is the hour of the day (local apparent time) at the time of the observation.

The multiple correlation coefficient for this model was 0.822. The improvement in the fit of the model at this altitude when compared to that at 40 km (indicated by the higher correlation coefficient) resulted primarily from the fact that the latitude difference (cos) term explained a greater percentage of the total variance.

In the 65 km region the diurnal variability appears to play a more important role. Both the diurnal (cos) term and the sub-solar angle (cos) term, which is related to the time of day, appear in the regression equation.

The diurnal (cos) term has a positive coefficient indicating that maximum atmospheric density occurs at midnight. The sub-solar angle (cos) term, on the other hand, indicated that maximum atmospheric density occurs when the sub-solar angle is minimized - i.e., at midday. Some further study was made of this apparent contradiction. Although the sub-solar angle term had a correlation with density of 0.28, the diurnal term was almost uncorrelated with density (0.16). Evidently the diurnal term alone could not explain much variability. In combination with the sub-solar angle, however, it was able to explain a significant amount of the density variation. In fact, its F-score, when chosen by the regression analysis after the sub-solar angle had been included, was well above the critical F-values. This indicated that the sub-solar angle (cos) term had the effect of providing a type of weighting factor to the diurnal variation. A consideration of the change of sub-solar angle with time of day shows that the effect of the weighting is to cause a maximum diurnal variation to occur at high latitudes, and almost no diurnal variation to occur in the equatorial region. At the high latitudes, densities reach a maximum near midnight and a minimum near midday. To illustrate this weighting, consider the following two extreme cases. First consider an observation point to be near a pole and the sub-solar point to be at the equator. The sub-solar angle for this observation point will show little change with the time of day hence, the sub-solar angle (cos) term will remain constant and all diurnal variation will be accounted for by the diurnal (cos) term alone (showing maximum density at night). Next consider both the observation point and the sub-solar point to be on the equator. In this case the sub-solar angle will vary from 0° at noon to 180° at midnight and the sub-solar angle (cos) term will, therefore,

follow a sinusoidal variation that is directly out of phase with the diurnal (cos) variable. Since the regression coefficients for these two terms are almost equal the resulting effect will be to cancel out most of the diurnal density variations.

The 100-km region - The only significant influence on density variations in this region was the latitude difference (cos) variable. The equation derived was:

$$Y = 0.677 \times 10^{-6} - 0.322 \times 10^{-6} \cos(SL-L) \quad (18)$$

The correlation coefficient derived for this model is 0.474. The sample size available at the 100-km region was small (41 soundings) when compared to that available at 40 and 65 km. This may explain the low correlation coefficient, and probably accounts for the fact that only one variable was found to be significant.

It should be noted that the sign of the regression coefficient for latitude difference is negative in this region indicating that maximum densities are occurring during the winter months rather than the summer months as indicated at lower altitudes. This sign reversal is consistent with our expectation for the regions above and below the isopycnic layer at 90 km. There was no evidence of a time lag between the peaking of the density variation and the winter solstice.

Third Analysis

The third set of calculations were done for the altitudes of 30 km, 40 km, 60 km, 65 km, 75 km, 100 km and 110 km. The only significant change made for these calculations was the addition to the list of variables of a linear form for the solar flux variable (see Table XII). Since the reciprocal relationship with the solar flux term had not appeared significant in the previous runs, it was desirable to try this model. The prime purpose of this third run was to see if the linear relationship with the solar flux term would be selected before the reciprocal, and to see if either would be significant. It also appeared desirable to study a wider range of altitudes.

The results of this calculation are presented in Table D-2 of Appendix D.

The results of the third calculation suggest splitting the area of study into three altitudes regions. Below 65 km, seasonal effects account for almost all significant density variations. There is a mid-region at about 65 km where diurnal as well as seasonal effects explain most of the variation, and at the high altitude region above 75 km, extra-terrestrial effects appear to become more important.

Low altitudes - In the low altitude region the model developed from the third run is essentially similar to that developed from the second run. The same set of variables enter into the regression equation with the exceptions that the semi-annual variation does not appear in the 60 km regression equation, and the earth shadow height does not appear in the 40 or 60 km regressions. The fact that the shadow height variable does not appear consistently in the low altitude equations suggests that its apparent significance at the 40 km level may be a chance occurrence. Assuming this to be so the regression equation for the 40-km region should be

$$Y = 0.311 \times 10^{-2} + 0.846 \times 10^{-3} \cos(SL-L-11.1^{\circ}) + 0.304 \times 10^{-3} \sin\left(2\pi \frac{d-32}{365}\right) - 0.133 \times 10^{-3} \sin\left(4\pi \frac{d}{365}\right) \quad (19)$$

The multiple correlatic coefficient for this model is calculated as 0.717. This form of the regression model has been assumed in the tabular presentation for the third run in Appendix D.

It should be noted that the seasonal lag in this equation (number of days by which the atmospheric density peak follows the summer solstice) is about 32 days. In the regression results derived from the 30-km data, the equivalent lag is about 51 days. This result indicates that the seasonal lag is greatest near the earth's surface and decreased with height. At a height of 65 km there is no evidence of a seasonal lag.

Middle Altitudes - In the third run the regression equation developed for the 65-km altitude is very similar to that developed from the second run. Of major interest is the fact that diurnal variations appear to be quite significant at this level. It should also be noted that in the third run the linear solar flux (-1 day) term was selected by the screening procedure immediately after the diurnal terms. Although this solar flux variable does not appear to be significant at this point, it does provide a link between the middle altitude and the high altitude region where extra-terrestrial effects seem to be quite important.

The regression equation developed for the 65 km altitude by the third run is the same as that resulting from the second run.

High altitudes - At the altitudes above 75 km (up to 110 km) the results of the analyses were generally inconclusive since the available data samples were small. As a result, correlation coefficients were low and only one or two variables proved to be significant at each altitude. Nevertheless, it is of interest to note which variables were nearly significant, and the order in which they were selected by the screening procedure.

In general, only the seasonal variations proved to be significant and, hence, the derived regression equations are either in the form developed by the second run for the 100-km sample or in the form,

$$Y = 0.180 \times 10^{-3} + 0.136 \times 10^{-3} \cos(SL-L) - 0.985 \times 10^{-5} \sin\left(2\pi \frac{d}{365}\right) \quad (20)$$

This is the equation derived from the 75-km data. The multiple correlation coefficient estimated for this model is 0.703.

The major point to be noted at these altitudes is the observation that the extra-terrestrial variables have become very nearly significant. In fact, we wonder if slightly larger data samples would have allowed their inclusion in the regression equations. At this point, unfortunately, no quantitative results can be stated about these variables. However, their increasing importance at the higher altitudes is not unexpected since the extra-terrestrial variables are known to be significant at altitudes above 200 km.

Fourth Analysis

The fourth run was carried out for every 5 km of altitude from 30 km to 110 km, and was conducted with the addition of a larger number of additional transformations and variables as described below.

Since the seasonal variables were found to account for the major portion of the atmospheric density variations, it was decided that additional seasonal transformations should be included. A weighting of the seasonal variables by the latitude of the observation point, for example, would provide for greater seasonal changes in the periodic parameters at high latitudes. This weighting can be included in the seasonal transformation by including a cross-product term that multiplies the seasonal variable by some function of latitude of the observation point. A linear function of latitude would weight each observation point directly by its distance from the equator while a sine function of latitude would weight all high latitude observation points more or less equally. Both functions were included in the list of variables for the fourth run and both were in cross product terms with the annual (sin) as well as the annual (cos) term.

The sine and cosine transformation of the latitude difference term are both related to seasonal variations and, hence, were usually chosen early in the regression analysis procedure. The latitude difference (cos) term is in fact very closely related to the cross product of the annual (sin) and the latitude. The latitude difference (sin) term had been included in an earlier run to provide some measure of an orthogonal component of the latitude difference. Unfortunately, due to the fact that northern latitudes are positively signed in the data set, and southern latitudes negatively signed, the latitude difference (sin) term turns out not to be symmetrical about the equator. Since seasonal effects on

atmospheric density are expected to be the same in both hemispheres, a symmetric transformation of the latitude difference (sin) term was expected to provide a better fit to the data. Hence, both the absolute value and the square of the latitude difference (sin) term were included as additional variables in the analysis.

Next we considered the possibility that an annual or semi-annual periodic variation in density may exist that is not related to season, i.e., periodic variations that have the same effects in both hemispheres rather than reversed effects in the north and south. To observe this type of variation, both annual and semi-annual terms, unadjusted for hemisphere, were included with sine and cosine transformations.

Finally, a variation in atmospheric density with latitude may also be expected. To search for such a relationship, three transformations of the latitude of the observation point were included. In order to maintain symmetry about the equator, the transformations used were the absolute value of latitude, the absolute value of the sine of latitude, and the cosine of latitude. A complete list of variables used in this analysis is presented in Table XIII.

The results of the fourth run are presented in Table D-3 of Appendix D. A review of these results re-emphasizes the division of the study into three altitude regions. In the lower region, seasonal effects predominate. At about 65 km, diurnal as well as seasonal effects become significant, while at the high altitudes, seasonal effects and extra-terrestrial variables are important. The isopycnic layer (90 km) is included in the high altitude region. At this altitude there is no evidence of either diurnal or seasonal effects, and geomagnetic index shows the best correlation with density.

Low altitudes (30 to 50 km)- In the low altitude region, the seasonal variations predominate, and account for almost all the explained density variation. In general, the transformation that gives the best fit to the data is a seasonal variation weighted by latitude. This cross product term is almost equivalent to the latitude difference (cos) term and, hence, is highly correlated with that variable. As a result, either the latitude difference (cos) term, or the cross product of the latitude and annual (sin) terms is always selected early in the analysis. The term that is selected first, however, tends to mask the other since they both contain almost equivalent information. Hence, both terms do not usually appear together in the regression equation.

The regression equation derived for the 35-km altitude was selected as typical for the low altitude region:

TABLE XIII

LIST OF VARIABLES AND TRANSFORMATIONS
ADDED OR CHANGED FOR THE FOURTH RUN

<u>VARIABLE NAME</u>	<u>TRANSFORMATION</u>
Solar flux linear (m days lag)	SF_m
Sin lat X annual (sin)	$\sin(L) \sin\left(\frac{d}{365} \cdot 2\pi\right)$
Sin lat X annual (cos)	$\sin(L) \cos\left(\frac{d}{365} \cdot 2\pi\right)$
Lat X annual (sin)	$L \sin\left(\frac{d}{365} \cdot 2\pi\right)$
Lat X annual (cos)	$L \cos\left(\frac{d}{365} \cdot 2\pi\right)$
Latitude difference (sin)	$ \sin(SL-L) $
Latitude difference (sin ²)	$\sin^2(SL-L)$
Annual (sin) not adjusted for hemisphere	$\sin\left(\frac{d''}{365} \cdot 2\pi\right)$
Annual (cos) not adjusted for hemisphere	$\cos\left(\frac{d''}{365} \cdot 2\pi\right)$
Semi-annual (sin) not adjusted for hemisphere	$\sin\left(\frac{d''}{365} \cdot 2\pi\right)$
Semi-annual (cos) not adjusted for hemisphere	$\cos\left(\frac{d''}{365} \cdot 2\pi\right)$
Latitude (abs)	$ L $
Latitude (sin)	$ \sin(L) $
Latitude (cos)	$\cos(L)$

where d'' is the number of days of the year elapsed since the vernal equinox in days and fractions of a day.

$$Y = 0.817 \times 10^{-2} - 0.122 \times 10^{-4} |L| + [0.776 \times 10^{-4} L - 0.417 \times 10^{-2} \sin(L)] \sin\left(\frac{d-40}{365} 2\pi\right) + 0.389 \times 10^{-3} \sin(SL-L) - 0.288 \times 10^{-3} \sin\left(4\pi \frac{d}{365}\right) \quad (21)$$

This equation includes a linear function of the latitude of the observation point. It indicates that the mean atmospheric density decreased with distance from the equator. It also includes the semi-annual variation that was discovered in the earlier calculations. As before, this variation reaches a maximum density in May and November.

The coefficient of the annual variation term has assumed a complex form in this equation since both the cross product with latitude and sine latitude have been included. In Fig. 40 the value of this coefficient has been plotted as a function of latitude. It shows that in weighting the seasonal variation the high latitudes should be stressed.

The time lag indicated in this equation (the number of days by which the density peak follows the summer solstice) is about 40 days. This lag is characteristic for 35-km altitude. At higher altitudes the lag decreases and is estimated as about 4 days at 45 km.

Middle altitudes (55 to 65 km)- In the 55-to 65-km region, the seasonal terms are evident with the addition of diurnal variations and, as in previous calculations, there is evidence of a latitudinal dependence in the amplitude of the diurnal change. The regression equation for 65 km is representative of this region, namely,

$$Y = 0.237 \times 10^{-3} - 0.761 \times 10^{-4} |\sin(L)| - 0.562 \times 10^{-4} \cos(SL-L) + [0.408 \times 10^{-5} L - 0.204 \times 10^{-3} \sin(L)] \sin\left(2\pi \frac{d}{365}\right) + 0.333 \times 10^{-4} \cos(SA) + 0.202 \times 10^{-4} \cos\left(2\pi \frac{h}{24}\right) \quad (22)$$

The latitude variation in this relationship, i.e., $|\sin(L)|$ indicates that the mean density decreases with distance from the equator. Both the sub-solar angle and the diurnal (cos) terms are in the regression model, which is equivalent to weighting the diurnal variation by the latitude of the observation point as was discussed in the second analysis.

In the high latitudes density variations apparently reach their peak around midnight. This effect is reversed in the low latitudes since the term involving sub-solar angle, with its larger coefficient, predominates resulting in a density maximum around noon.

High altitudes - At the high altitudes, seasonal effects weighted by latitude are dominant. The regression equation for 80 km was selected as typical for this region,

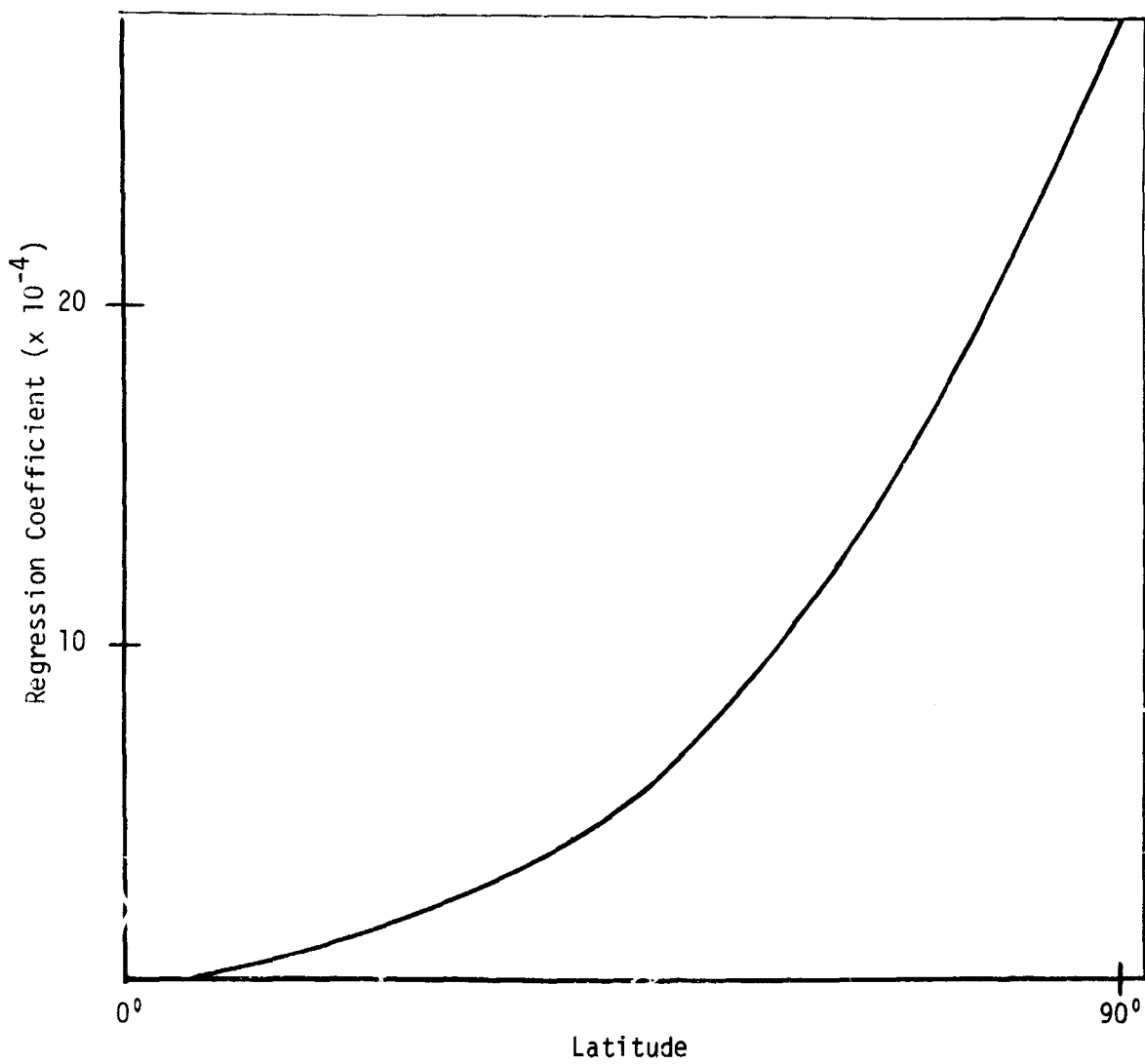


Fig. 40. Weighting of Seasonal Variation by Latitude

$$Y = 0.161 \times 10^{-4} + [0.519 \times 10^{-6} L - 0.291 \times 10^{-4} \sin(L)] \sin(2\pi \frac{d}{365}) \quad (23)$$

Again the problem of small sample sizes limited the analysis. Although they were not significant, extra-terrestrial effects appeared to be next most significant following the annual variation.

The isopycnic layer near 90 km is included in the high altitude region. At this height, annual variations appeared to be insignificant and, while the equivalent geomagnetic indices explained some of the density variation, the unexplained variation remained large. The multiple correlation coefficient calculated for the model at 90 km was 0.278.

At altitudes above the isopycnic region, only annual variations were significant. The sign of the regression coefficients were reversed so that above 90 km, maximum densities were predicted for mid-winter while below this altitude maximum densities were predicted for mid-summer.

CONCLUSIONS

The limitations of the data base used in this investigation did not permit a statistical analysis of the entire 30 to 200 km height interval. The size of this sample did, however, provide sufficient data to study empirical models for characterizing atmospheric density up to altitudes of about 110 km. The results from the multivariate analyses of this height interval substantiated our original concept of three statistically quasi-homogeneous regions. The lowest region extends from 30 km to 50 km, the middle region extends from 55 km to 65 km, and the highest region extends from 70 km to the 110 km. Imbedded in the higher region between 90 and 95 km is the well-known isopycnic layer which exhibits a unique statistical behavior.

The seasonal variations in atmospheric density (or annual period) weighted by a complex latitudinal dependence are dominant over the entire 30 to 110 km height interval. The density maximum occurs during the hemisphere mid-summer near 30 km, but comes progressively earlier with increasing altitude. At 65 km the density maximum occurs in the early spring, close to the hemisphere spring equinox. This cycle is reversed at altitudes above 90 km where the peak density occurs near the hemisphere autumnal equinox. These results are not unexpected in view of our current knowledge of upper atmosphere characteristics. The more interesting results, however, are the secondary effects which are detected by the analysis:

1. The 30-to 50-km region is characterized by a semi-annual variation showing maximum densities in early May and November, and minimum densities in early February and August.

2. The 55- to 65-km region shows a diurnal variability which is dependent upon latitude. Peak densities are observed near midnight at high latitudes, whereas peak densities occur at midday in low latitudes. In the tropical latitude belt, the average daytime density exceeded the average nighttime density by about 15 percent during the summer season. In the sub-tropical belt, the day-night difference was just over 10 percent during the spring season.

3. The influence of extra-terrestrial effects can be observed just below the statistical rejection level in the 70 to 110 km region. The 90-km region in particular acts as a "window", and shows significant relationships with the geomagnetic index at 6 hour lag.

RECOMMENDATIONS

The results of the current investigation are distinctly encouraging as evidenced by the multiple correlation coefficients obtained. These show that the models have explained at least 50 percent of the variability in atmospheric density in the interval 30 to 75 km. Most of this is due to the seasonal terms, but a detectable part is due to other periodic and solar effects. It is these secondary effects which add to our understanding of upper atmospheric processes.

It is our recommendation that this type of investigation be continued. We suggest that future work be conducted with a larger data base by adding to the current one, which is limited in time to early 1965. The number of rocket soundings which have been conducted in the interim period could easily double the data base. With such an expanded data base it should be feasible to:

1. Increase the altitude range of the study above the present maximum height.

2. Develop more efficient, and possibly simpler empirical relationships.

3. Validate the models by testing the predictions against an independent set of measured values.

4. Include synoptic effects by considering time lags in the dependent variable.

REFERENCES

1. U.S. Standard Atmosphere Supplement 1966, Environmental Science Service Administration, National Aeronautics and Space Administration, and U.S. Air Force, U.S. Government Printing Office, Washington, D.C.
2. Minzner, R.A., and Morgenstern, P.: Structure and Variability of Earth's Atmosphere. Final Report, GCA-TR-68-1-N (NASW-1463), GCA Corp., Bedford, Mass., 1968.
3. Minzner, R.A., and Morgenstern, P.: Range and Structure of Ambient Density from 30 to 120 km Altitude. Final Report, GCA-TR-68-15-N (NAS8-20098), GCA Corp., Bedford, Mass., 1968.
4. DeVries, L.L., Friday, E.W., and Jones, L.C.,: Analysis of Density Data Deduced from Low-Altitude, High Resolution Satellite Tracking Data. Presented at COSPAR 7th International Space Science Symposium, Vienna, 1966.
5. Minzner, R.A., Morgenstern, P., and Mello, S.: Tabulation of Atmospheric Density, Temperature, and Pressure for 437 Rocket and Optical-Probe Soundings During the Period 1947 to Early 1965. GCA-TR-67-10-N (NASW-1463 and NASW-1225), GCA Corp., Bedford, Mass., 1967.
6. Meteorological Rocket Network Committee, Editors, 1962-1966: Data Report of the Meteorological Rocket Network Firings. Document 109-62.
7. Handbook of Geophysics. Revised Edition, USAF/Geophysics Research Directorate, The MacMillan Co., New York, 1951.
8. Schultz, E.D.: Research Directed Toward Defining the Variability of the Atmosphere Between 30 and 200 km. GCA-TR-69-11-N under Contract NAS12-617 (Sept. 1969).
9. Minzner, R.A., and Sauermaun, G.O.: Temperature Determination of Planetary Atmospheres-Optimum Boundary Conditions for Both Low and High Solar Activity-Equation Analysis and Error Analysis. GCA-TR-65-6-N (NASW-1225), GCA Corp., Bedford, Mass., 1966.
10. U.S. Standard Atmosphere, 1962, National Aeronautics and Space Administration, U.S. Air Force, and U.S. Weather Bureau, Government Printing Office, Washington, D.C.

11. Elterman, L.: The Measurement of Stratospheric Density Distribution with the Searchlight Technique. *J. Geo. Res.* Vol. 56 (4) pp. 509-520, also AFCRC, Geophys. Res. Papers No. 10, Bedford, Mass., Dec. 1951.
12. Brooks, C.E.P. and Carruthers, N.: Handbook of Statistical Methods in Meteorology. Her Majesty's Stationery Office, London, 1953.
13. Jacchia, L.G.: Corpuscular Radiation and the Acceleration of Artificial Satellites. Nature, 183, pp. 1662-1663, 1959.
14. Bartels, J.: Zahlenwerte und Funktionen aus Physik, Chemie, Astronomie, Geophysik. Landolt-Bornstein, Berlin, 1952. *Terr. Mag.*, 44: 411, 1939 and *Terr. Mag.*, 46:301, 1941.
15. IBM System/360 Operating System Utilities, IBM Systems Reference Library, Form C28-6586-9, Tenth Ed., IBM Corp., Nov. 1968.
16. Minzner, R.A., and Mello, S.: Range and Structure of Ambient Density from 0 to 120 km Altitude. GCA-TR-67-16-N (NAS8-20098), GCA Corp., Bedford, Mass., 1967.
17. Ostle, B.: Statistics in Research. 2nd Ed., Iowa State U. Press, Ames, Iowa, 1963.
18. Mood, A.M. and Graybill, F.A.: Introduction to the Theory of Statistics. 2nd Ed., McGraw-Hill, New York, 1963.
19. Miller, R.G.: Statistical Prediction by Discriminant Analysis. *Meteorol. Monographs* Vol. 4, No. 25, Amer. Meteorol. Soc., Boston, Mass., 1962.
20. Jacchia, L.G.: The Atmospheric Models above 120 km: Derivation, Systematic Variations, Sources, Errors, Limitations. Smithsonian Astrophysical Observatory, Cambridge, Mass., 1966.
21. Smithsonian Astrophys. Observatory, Listing of 10.7 cm Solar Flux.
22. Jacchia, L.G. and Slowey, J.: The Shape and Location of the Diurnal Bulge in the Upper Atmosphere. Special Report Number 207, Smithsonian Astrophysical Observatory, Cambridge, Mass., 1966.
23. Jacchia, L.G., Slowey, J., and Verniani, F.: Geomagnetic Perturbations and Upper Atmosphere Heating. Special Report Number 218, Smithsonian Astrophysical Observatory, Cambridge, Mass., 1966.
24. DeVries, L.L.: An Investigation of Atmospheric Density Between Altitudes of 180 km and 300 km. TR-190, Air Weather Service, USAF, Nov. 1966.

25. Paetzold, H.K., and Zschorner, H.: Bearings of Sputnik III and the Variable Acceleration of Satellites. Space Research I, Proceedings of the First International Space Symposium, Nice, France, January 11-16, 1960.

APPENDIX A

Table A-1

DATE-TIME-SITE		TECHNIQUE	EDITING	
6104051257	WI	S	Truncate sounding above	68 km
6107201030	WI	S	" " "	75 km & below 53 km
6203021115	WI	S	" " "	77 km
6203232345	WI	S	" " "	75 km
6203280004	WI	S	" " "	82 km
6204170928	WI	S	" " "	84 km
6212012125	WI	S	" " "	78 km
6212060532	WI	S	" " "	78 km
6302202347	WI	S	" " "	62 km
6302282211	WI	S	" " "	68 km
6312071311	WI-1	S	Multiply density values	by 10
6402040146	WI	S	Change 34 km density to	0.8554E-02
5210221421	HA	G	Change 48 km density to	0.1085E-02, and
			change 47 km density to	0.1225E-02
6303290257	KW-2	D	Truncate sounding below	63 km
6105101110	EG	D	Truncate sounding above	67 km
5801291906	FC-2	D	" " "	70 km
5803041930	FC-2	D	" " "	70 km
5009080700	AQ	L	" " "	60 km
5009100700	AQ	L	" " "	"
5009130700	AQ	L	" " "	"
5009140700	AQ	L	" " "	"
5010120700	AQ	L	" " "	"
5010140700	AQ	L	" " "	"
5011160700	AQ	L	" " "	"
5205290822	AQ	L	" " "	"
5206140542	AQ	L	" " "	"
5206160645	AQ	L	" " "	"
5206220600	AQ	L	" " "	"
5206230600	AQ	L	" " "	"
5208031017	AQ	L	" " "	"
5209100432	AQ	L	" " "	"
5209190647	AQ	L	" " "	"
5209250607	AQ	L	" " "	"
5209260635	AQ	L	" " "	"
5209270735	AQ	L	" " "	"
5210110335	AQ	L	" " "	"
5210120300	AQ	L	" " "	"
5210170430	AQ	L	" " "	"
5210190340	AQ	L	" " "	"
5210220955	AQ	L	" " "	"
5210230530	AQ	L	" " "	"
5210240535	AQ	L	" " "	"
6411010530	BS-2	D	Truncate sounding below	36 km
6506180805	BS-2	D	Eliminate lowest (30 km) density value	
6506220600	BS	D	Change 58 km density to	0.368E-03, and
			change 57 km density to	0.415E-03

TABLE B-1 (Cont.)

5803041930FC	5	4+	5	4	5	4	4	3+	4	+58.73	6407160243WD	1	0+	1	0+	0	0+	0+	0	1	-31.11	
5803211807FC	2	4+	4	3+	3+	3	3	3	5	+56.73	6407209027WD	2	2	1+	1	1	1	1	0+	0+	-31.11	
5803242208FC	2	3+	4	3+	3+	5	5	5	4	+56.73	6409170917WD	2	1	0	3	3	3	2	2	2	-31.11	
5807152008FC	7	1+	1+	2	1+	1+	2	1	2	+56.73	6410150938WD	2	1	0	0+	1	2+	2	1	2+	-31.11	
5810150109FC	1	2	1	2	3+	2	2	2	3	+56.73	6411210000WD	2	1	1	1+	2+	3+	2	1	-31.11		
5810202201FC	1	2	1	2	3+	2	2	2	3	+56.73	6422021026WD	3	3	3+	3+	3	3	2	1	-31.11		
5810311958FC	3	4+	3	3+	3	2	4	2	+58.73	6412101026WD	1	1	1	1	1	1	1	1	0+	-31.11		
5811232202FC	0	1+	1	2	3	3	2	1	1	+56.73	6505020957WD	1	2	3	2	1	0	1	1	1	-31.11	
6010172178FC	7	3	1	2	2	2	1	2	2	+58.73	6503300930WD	1	2	2	1	0	0	0	0	1	-31.11	
6212040705FC	0	0	1	1	1	1	0	0	3+	+58.73	4703071823WS										+32.38	
6212060543FC	1	1	2	2	2	2	2	2	3	+58.73	4808040137WS										+32.38	
6302202334FC	1	1	1	2	2	2	2	3	4	+58.73	4909251658WS	1	0+	1	2+	2	2	2	2	1+	+32.38	
6302282148FC	1	1	2	1	2	3	1	0	3	+58.73	5005112300WS	4	3	2	3	3	4	3	3	2+	+32.38	
6303050001FC	4	3	5	5	4	4	4	3	3	+58.73	5005112300WS	4	3	2	3	3	4	3	3	2+	+32.38	
6302750417FC	2	2	1	2	1	3	3	4	4	+58.73	5011211718WS	2	1	1	0	0	0	0	0	0	+32.38	
6402130430FC	2	3	4	3	3	2	1	2	1	+58.73	5107071800WS	2	3	1	2	3	2	2	2	2	+32.38	
6404180539FC	4	4	3	2	3	2	2	2	0	+56.73	5205150114WS	1	1	1	1	1	0	0	1	1	+32.38	
6408080400FC	3	3	3	2	2	2	2	2	1	+58.73	5212173478WS	2	1	3	3	2	2	2	2	1	+32.38	
6408180115FC	3	2	1	1	1	1	1	1	0	+58.73	5304221933WS	4	4	4	5	4	3	4	3	4	+32.38	
5811211406G	2	2	1	1	1	1	1	1	2	+13.62	5309292050WS	2	1	1	1	1	1	1	2	2	-1	+32.38
5811151801GM	2	2	3	2	1	1	1	1	0	+13.62	5305250505WS	2	1	1	1	1	1	1	2	2	-1	+32.38
5811220957GM	2	2	0	0	1	1	1	2	2	+13.62	5312011529WS	1	1	1	0	1	1	0	0	0	+32.38	
5811221708GM	2	2	0	0	2	1	1	1	0	+13.62	5512220015WS	0	0	2	1	1	1	1	1	2	0	+32.38
5811241727GM	2	1	1	0	0	2	1	0	1	+13.62	6100221703WS	0	0	1	0	0	1	0	1	1	-32.38	
5006201540HA	1	2	1	1	0	1	1	1	2	+32.85	6106051245WS	2	3	3	2	1	2	2	1	2	+32.38	
5109131137HA	4	5	4	3	5	6	5	4	3	+32.85	6102523305WS	5	4	4	4	4	4	5	5	5	+32.38	
5210221421HA	5	5	5	3	1	2	1	1	1	+32.85	6306061430WS	0	1	0	0	0	1	0	1	1	+32.38	
6103171445HA	3	3	1	1	2	2	5	4	3	+32.85	6307061704WS	2	2	3	2	3	3	2	2	2	+32.38	
6103311443HA	2	1	1	0	0	1	1	1	1	+32.85	6311041000WS	3	2	0	2	4	1	2	2	2	+32.38	
6104201443CHA	1	2	3	2	3	2	3	1	1	+32.85	6311050000WS	1	2	2	2	2	1	2	1	0	+32.38	
6104211443CHA	1	2	3	2	3	2	3	1	1	+32.85	6402182150WS	1	0	0	2	2	1	2	1	2	+32.38	
6104221443CHA	1	2	3	2	3	2	3	1	1	+32.85	6402182150WS	1	0	1	1	0	0	1	1	0	+32.38	
6104231443CHA	1	2	3	2	3	2	3	1	1	+32.85	6407250930WS	0	1	0	0	1	1	1	1	1	+32.38	
6104241443CHA	1	2	3	2	3	2	3	1	1	+32.85										+32.38		

APPENDIX C

TABLE C-1

PROGRAM TO EDIT DATA AND ADD JULIAN DATES

```

C INITIALIZE COUNTERS FOR NO. OF RECORDS PER ALTITUDE. SET LOCATION CODES
  INTEGER I, COUNT(500)/500*3/
  REAL KY, KW, KC
  DATA AQ, AI, AS, CA, EG, FE, GM, HI, HA, KY, KW, MC, PM, SA, SB, SC, SD, SE, SF, SG,
  1 SH, TH, WI, WS, 30/'AQ', 'AI', 'AS', 'CA', 'EG', 'FE', 'GM', 'HI', 'HA', 'KY',
  2 'KW', 'MC', 'PM', 'SA', 'SB', 'SC', 'SD', 'SE', 'SF', 'SG', 'SH', 'TH', 'WI',
  3 'WS', 'WO' /
  REAL LSGM, LSH, LAD
C DIMENSION STATEMENT CONTAINS FIELDS FOR READ RECORD
----- DIMENSION D(4), B(14), A(21) -----
  INTEGER D, RN/0/, IFR/0/
  DATA BL2, BL3/' ', ' ', ' ' /
C READ ONE RECORD - STEP 1
  301 READ(8, 100, END=99) (D(I), I=1, 5), A(1), B(1), D(6), B(2), A(2), A(3), A(4),
  1 (B(I), I=3, 8), A(5), B(9), A(6), B(10), C, B(12), A(7), B(13), (A(I), I=5, 1
  28), B(14), A(19), B(15), A(20), B(16), A(21)
  RN = RN + 1
  100 FORMAT(5I2, A2, A3, I3, A2, 3A3, 3A4, 3A3, A2, A4, 2A2, F6.2, A4, A2, 10A4,
  1A4, A3, A4, 3A2)
C LOOK FOR MISSING VARIABLES - STEP 2
  DO 101 I=1, 3
  IF(A(I).EQ.0) GO TO 105
  101 CONTINUE
  DO 102 I=1, 21
  IF(A(I).EQ.BL2.OR.A(I).EQ.BL3) GO TO 105
  102 CONTINUE
  IF(C.LT.0.0.OR.C.GT.24.0) GO TO 105
C FIND JULIAN DAY AT THE FIRST OF GIVEN YEAR - STEP 3
  IDY = 72 - D(1)
C GET NO. OF QUADRI-YEARS BEFORE 1972
  IQD = IDY/4
C GET NO. OF YEARS BEFORE FIRST QUADRI-YEAR
  IYD = IDY - 4*IQD
C CALCULATE JULIAN DAY NO. AT 1ST. OF YEAR... = 41317 IS JULIAN DAY 01/01/72
  JD = 41317 - 1461*IQD - 365*IYD
C FIND JULIAN DAY AT FIRST OF GIVEN MONTH - STEP 4
  K = D(2) - 1
  IF(K.EQ.0) GO TO 108
  DO 108 I=1, K
  IF(I.EQ.4.OR.I.EQ.6.OR.I.EQ.9.OR.I.EQ.11) GO TO 30
  IF(I.EQ.2) GO TO 28
  JD = JD + 31
  GO TO 108
  28 IF(IYD.EQ.0) GO TO 29
  JD = JD + 28
  GO TO 108
  29 JD = JD + 29
  GO TO 108

```

TABLE C-1 (continued)

```

30 JD = JD + 30
109 CONTINUE
C INCLUDE DAY OF THE MONTH, HR., MIN. OF THE DAY TO GET CURRENT JULIAN
C DAY (MEAN AT GREENWICH) - STEP 5
109 JD = JD + D(3) - 1
GMH = FLOAT(D(4)) + FLOAT(D(5))/60.
GMD = JD + GMH/24.
C COUNT NO OF RECORDS FOR EACH ALTITUDE - STEP 6
K = D(6)
ICOUNT(K) = ICOUNT(K) + 1
C GET CURRENT JULIAN DAY (LOCAL APPARENT) - STEP 7
C A FIND LOCAL STD. TIME DIFFERENCE FROM GMT
COM = A(1)
IF(COM.EQ.EG.OR.COM.EQ.FC.OR.COM.EQ.SC) GO TO 906
IF(COM.EQ.WI) GO TO 905
IF(COM.EQ.AQ.OR.COM.EQ.HA.OR.COM.EQ.WS) GO TO 907
IF(COM.EQ.AI) GO TO 900
IF(COM.EQ.WO) GO TO 9
IF(COM.EQ.HI) GO TO 5
IF(COM.EQ.KW) GO TO 12
IF(COM.EQ.MC) GO TO 11
IF(COM.EQ.SB.OR.COM.EQ.SD.OR.COM.EQ.SE.OR.COM.EQ.SH.OR.COM.EQ.TH)
1 GO TO 904
IF(COM.EQ.CA) GO TO 8
IF(COM.EQ.GM) GO TO 10
IF(COM.EQ.BS) GO TO 910
IF(COM.EQ.SF.OR.COM.EQ.SG) GO TO 903
IF(COM.EQ.PM) GO TO 908
IF(COM.EQ.KY) GO TO 4
IF(COM.EQ.SA) GO TO 911
GO TO 106
906 LSGM = -6.
GO TO 200
905 LSGM = -5.
GO TO 200
907 LSGM = -7.
GO TO 200
900 LSGM = 0.
GO TO 200
9 LSGM = 9.5
GO TO 200
5 LSGM = 5.
GO TO 200
12 LSGM = 12.
GO TO 200
11 LSGM = 11.
GO TO 200
904 LSGM = -4.

```

TABLE C-1 (continued)

```

GO TO 200
8 LSGM = 9.
GO TO 200
10 LSGM = 10.
GO TO 200
910 LSGM = -10.
GO TO 200
903 LSGM = -3.
GO TO 200
908 LSGM = -8.
GO TO 200
4 LSGM = 4.
GO TO 200
911 LSGM = -11.
C 3 GET LOCAL STD. TIME
200 LSH = GMH + LSGM.
IF(LSGM.GT.0.0) GO TO 201
C C FOR LOCATIONS WEST CORRECT JULIAN DAY IF NECESSARY
IF(ABS(LSH-C).LT.1.4) GO TO 205
JD = JD + 1
LSH = LSH + 24.
IF(ABS(LSH-C).GE.1.4) GO TO 107
C D FOR LOCATIONS EAST CORRECT JULIAN DAY IF NECESSARY
201 IF(ABS(LSH-C).LT.1.4) GO TO 205
JD = JD - 1
LSH = LSH - 24.
IF(ABS(LSH-C).GE.1.4) GO TO 107
C E GET LOCAL APPARENT, CURRENT JULIAN DAY
205 LAD = JD + C/24.
C WRITE OUT RECORD
WRITE(9,300) (D(I),I=1,5),A(1),B(1),D(6),B(2),A(2),A(3),A(4),
1(B(I),I=3,8),A(5),B(9),A(6),B(10),C, B(12),A(7),B(13),(A(I),I=3,1
28),B(14),A(19),B(15),A(20),B(16),A(21),GMD,LAD
300 FORMAT(5I2,A2,A3,I3,A2,3A3,3A4,3A3,A2,A4,2A2,F6.2,A4,A2, 12A3,
1A4,A3,A4,3A2,2F12.4)
GO TO 301
C**ERROR AND STOP MESSAGES*****
105 WRITE(6,400) RN
400 FORMAT(1H0,'THE',I6,'TH RECORD IS NOT COMPLETE')
421 WRITE(6,401) (D(I),I=1,5),A(1),B(1),D(6),B(2),A(2),A(3),A(4),
1(B(I),I=3,8),A(5),B(9),A(6),B(10),C, B(12),A(7),B(13),(A(I),I=3,1
28),B(14),A(19),B(15),A(20),B(16),A(21)
401 FORMAT(1H0,5I2,A2,A3,I3,A2,3A3,3A4,3A3,A2,A4,2A2,F6.2,A4,A2,12A3,
1A4,A3,A4,3A2)
IER = IER + 1
IF(IER.LE.600) GO TO 301
WRITE(6,490)
490 FORMAT(1H0,'600 ERRORS ENCOUNTERED')

```


TABLE C-1 (continued)

STOP

~~106 WRITE(6,410) RN~~

~~GO TO 411~~

~~410 FORMAT(1H0, 'THE LOCATION IS NOT IDENTIFIED ON THE', I6, 'TH RECORD')~~

~~107 WRITE(6,420) RN~~

~~GO TO 411~~

~~420 FORMAT(1H0, 'THE LOCAL STD. TIME DISAGREES WITH THE LOCAL APPARENT
TIME ON THE', I6, 'TH RECORD')~~

~~99 WRITE(6,425)~~

~~425 FORMAT(1H0, '///1H0, 30X, '*****FILE IS COMPLETE*****')~~

C WRITE FREQUENCY DISTRIBUTION FOR ALTITUDES

WRITE(6,500)

500 FORMAT(1H1, 20X, 'NO. OF ACCEPTABLE RECORDS AT EACH ALTITUDE'///3X,
1'ALTITUDE', 3X, 'NO. OF RECORDS'//)

DO 502 I=1,500

IF(ICOUNT(I).NE.0)WRITE(6,501) I,ICOUNT(I)

502 CONTINUE

501 FORMAT(2X, I5, 8X, I7)

STOP

END

TABLE C-2
 FORMAT OF THE DATA TAPE

The sorted atmospheric density data has been stored in alphanumeric form on magnetic tape. Each record on this tape represents one observation (one altitude from one sounding). The records are stored in a fixed length blocked format with a record length of 164 bytes and blocksize of 3280 bytes. The format for the 164 character records is presented below.

<u>COLUMNS</u>	<u>DATA</u>	<u>FORMAT</u>
1 and 2	Year of Sounding	I2
3 and 4	Month of Sounding	I2
5 and 6	Day of Sounding	I2
7 and 8	Hour of Sounding	I2
9 and 10	Minute of Sounding	I2
11 and 12	Code for Location of Sounding	A2
14	Code for Observation Technique	I1
16 to 18	Altitude (km)	I3
19 to 29	Density (kg/m ³)	E11.4
50 to 54	Solar Flux (1 day lag)	F 5.2
55 to 60	Solar Flux (current day)	F 6.2
61 to 66	Local Apparent Time of Observation	F 6.2
67 to 72	Sub-Solar Angle	F 6.1
73 to 81	Shadow Height (km)	E 9.2
82 to 84	Geomagnetic Index (24 hour lag)	"
85 to 87	" (21 hour lag)	"
88 to 90	" (18 hour lag)	"
91 to 93	" (15 hour lag)	"
94 to 96	" (12 hour lag)	"
97 to 99	" (9 hour lag)	"
100 to 102	" (6 hour lag)	"
103 to 105	" (3 hour lag)	"
106 to 108	" (0 hour lag)	"
109 to 115	Latitude of Observation	F 7.2
126 to 137	GMT Modified Julian Day *	E12.4
138 to 149	LAT " " "	E12.4
150 to 161	Modified Julian Day At * the start of the Year	E12.4

* The modified Julian day is the Julian day less 2,600,000.5 days.

TABLE C-3

STEPWISE MULTIPLE REGRESSION PROGRAM

```

C 360 STEPWISE MULTIPLE REGRESSION PROGRAM, 3/14/66
C PHASES 1 AND 2 CAN BE OVERLAID TO CONSERVE CORE. THE STEPS TO
C READY PHASES 1 AND 2 FOR OVERLAY ARE:
C 1. SET UP A COMMON AREA CONSISTING OF RIJ,XBAR,SIGMA,FIN,
C FOUT,OBS,NVAR,NOBS,NINDV.
C 2. SET SIGMA AND DATA EQUIVALENT IN PHASE 2.
C 3. REMOVE STATEMENT 101-2 FROM PHASE 1 AND INSERT IT
C BEHIND DIMENSION COMMENTS CARD IN PHASE 2.
C TO MODIFY THE PROGRAM TO OPERATE ON A DISK SYSTEM MAKE THE
C FOLLOWING CHANGES TO THE SOURCE DECK:
C 1. REMOVE STATEMENT 630 PLUS 1.
C 2. REMOVE THE C1 FROM COMMENT C1.
C 3. REMOVE THE C2 FROM COMMENTS CARD C2 AND INSERT IT
C FOLLOWING STATEMENT 101.
C 4. REPLACE STATEMENT 870 WITH COMMENTS CARD C3 AFTER
C REMOVING THE C3.
C 5. REPLACE STATEMENT 610 WITH COMMENTS CARD C4 AFTER
C REMOVING THE C4.
C 6. REPLACE STATEMENT 67 PLUS 2 WITH COMMENTS CARD C5 AFTER
C REMOVING THE C5.
C DEFINE FILE 1(10000,60,U,IFA)
C PHASE 1. TRANSFORM ORIGINAL DATA, COMPUTE AND PRINT MEANS,
C STANDAPD DEVIATIONS, AND SIMPLE CORRELATION COEFFICIENTS.
C DIMENSIONS
C DIMENSION SIGMA(58)
C COMMON/TRERM/ DATA(58),CONST(12),ITRAN(60),JTRAN(60),KTRAN(60),
C LTRAN(60),MTRAN(60),II,JJ,KK,LL,MM,KYR,OLOC,ALTU,DETE(58)
C COMMON/GBED/ RIJ(58,58),XBAR(58),AID(18),I,J,OBS
C DIMENSION SIGB(58),B(58),ID(60)
C EQUIVALENCES
C EQUIVALENCE (SIGMA(1),DATA(1))
C STATEMENT LABEL 101 IS NOT REFERENCED. IT MARKS THE FIRST
C EXECUTABLE STATEMENT OF THE SOURCE PROGRAM.
C ICOM IS FIXED DECIMAL REPRESENTATION OF ALPHABETIC COMMA.
C EXTERNAL DEBG
C CALL FRRSET(209,30,10,2,DEBG,209)
101 ICOM=1799372864
C IFA=1
C READ I.O.
C READ(5,1)(AID(I),I=1,18)
1 FORMAT(18A4)
C READ CONTROL CARD
C READ(5,2)NFIN,NVAR,NOBS,NTRAN,NCONS,FIN,FOUT,IFRS
2 FORMAT(2I2,14,2I2,2F6.3,1I)
C IF(FIN-FOUT)1020,690,690
690 IF(NTRAN)1000,730,700
C READ TRANSFORMATION CARDS
700 READ(5,71)(ITRAN(I),JTRAN(I),KTRAN(I),LTRAN(I),MTRAN(I),I=1,NTRAN)

```


TABLE C-3 (continued)

```

C      COMPUTE STANDARD DEVIATIONS*SQRT ROUTE (OBS-1)
      DO 120 I=1,NVAR
120  SIGMA(I)=(PIJ(I,I)-XBAR(I)*XBAR(I)/OBS)**.5
C      COMPUTE CORRELATION MATRIX
      DO 130 I=1,NVAR
      DO 130 J=1,NVAR
130  PIJ(I,J)=(PIJ(I,J)-XBAR(I)*XBAR(J)/OBS)/(SIGMA(I)*SIGMA(J))
C      COMPUTE MEANS AND STANDARD DEVIATIONS
      DO 140 I=1,NVAR
      XBAR(I)=XBAR(I)/OBS
140  SIGMA(I)=SIGMA(I)/(OBS-1.0)**.5
C      SKIP TO NEW PAGE, WRITE I.D., AVERAGES, STANDARD DEVIATIONS,
C      AND SIMPLE CORRELATION MATRIX.
      WRITE(6,65)(AID(I),I=1,18)
65  FORMAT('1',1PA4)
      WRITE(6,51)
51  FORMAT('0 AVERAGES')
      WRITE(6,52)(I,XBAR(I),ICOM,I=1,NINDV),NVAR,XBAR(NVAR)
52  FORMAT(4(' VAR(',I2,')=',F10.3,A1))
      WRITE(6,53)
53  FORMAT('0 STANDARD DEVIATIONS')
      WRITE(6,52)(I,SIGMA(I),ICOM,I=1,NINDV),NVAR,SIGMA(NVAR)
      WRITE(6,55)
55  FORMAT('0 SIMPLE CORRELATION COEFFICIENTS')
      DO 150 I=1,NINDV
150  WRITE(6,56)(I,J,PIJ(I,J),ICOM,J=1,NINDV),I,NVAR,PIJ(I,NVAR)
56  FORMAT(4(' VARS(',I2,',' ,I2,')=',F7.3,A1))
C      PHASE 2. PERFORM STEPWISE CALCULATIONS AND PRINT RESULTS.
C      DIMENSIONS
      INITIALIZE
      DO 190 I=1,NVAR
      SIGB(I)=1.0
190  X(I)=1.0
      NENT=0
      DE=OBS-1.0
      NSTEP=-1
C      TRANSFORM SIGMA VECTOR FROM STANDARD DEVIATIONS TO SQUARE
C      ROOTS OF SUMS OF SQUARES.
      DO 310 I=1,NVAR
310  SIGMA(I)=SIGMA(I)*(OBS-1.0)**.5
C      BEGIN STEP NUMBER NSTEP.
200  NSTEP=NSTEP+1
      STDEF=((PIJ(NVAR,NVAR)/DE)**.5)*SIGMA(NVAR)
      DE=DE-1.0
      IF(DE)1010,1010,205
205  VMIN=C.0

```

TABLE C-3 (continued)

```

VMAX=0.0
NIN=C
C FIND MINIMUM VARIANCE CONTRIBUTION OF VARIABLES IN REGRESSION
C EQUATION. FIND MAXIMUM VARIANCE CONTRIBUTION OF VARIABLES
C NOT IN REGRESSION EQUATION.
DO 300 I=1,NINDV
IF(RIJ(I,I)-.001)300,300,210
210 VI=RIJ(I,NVAR)*RIJ(NVAR,I)/RIJ(I,I)
IF(VI)240,300,220
220 IF(VI-VMAX)300,300,230
230 VMAX=VI
NMAX=I
GO TO 300
240 NIN=NIN+1
ID(NIN)=I
C COMPUTE REGRESSION COEFFICIENT AND ITS STANDARD DEVIATION.
B(NIN)=RIJ(I,NVAR)*SIGMA(NVAR)/SIGMA(I)
SIGB(NIN)=(STDEF*RIJ(I,I)**.5)/SIGMA(I)
IF(VMIN)250,260,1000
250 IF(VI-VMIN)300,300,260
260 VMIN=VI
NMIN=I
300 CONTINUE
IF(NIN)1000,460,400
C COMPUTE CONSTANT TERM.
400 BSUBO=XBAR(NVAR)
DO 410 I=1,NIN
J=ID(I)
410 BSUBO=BSUBO-B(I)*XBAR(J)
IF(NENT)1000,480,420
C OUTPUT FOR VARIABLE ADDED
420 WRITE(6,57)NSTEP,K
57 FORMAT('STEP NUMBER ',I2,10X,'ENTER VARIABLE ',I2)
425 WRITE(6,58)STDEF
58 FORMAT(' STANDARD ERROR OF ESTIMATE=',E15.4)
R=(1.-RIJ(NVAR,NVAR))**.5
WRITE(6,59)R
59 FORMAT(' MULTIPLE CORRELATION COEFFICIENT =',F6.3)
IDFN=OBS-DF-2.0
IDFD=DF+1.0
F=(SIGMA(NVAR)**2-(STDEF**2)*(DF+1.0))/((OBS-DF-2.0)*STDEF**2)
WRITE(6,60)IDFN,IDFD,F
66 FORMAT(' GOODNESS OF FIT,F(I',I4,',',I4,',')=',E8.4)
WRITE(6,60)BSUBO
60 FORMAT(' CONSTANT TERM=',E12.4)
WRITE(6,61)
61 FORMAT('QVAR COEFF STD DEV T VALUE BETA COEFF')

```


TABLE C-3 (continued)

```

SUBROUTINE TRANX
COMMON/TRERM/ DATA(58),CONST(12),ITRAN(60),JTPAN(60),KTRAN(60),
ILTRAN(60),MTRAN(60),II,JJ,KK,LL,MM,KYR,OLDC,ALTI,DETF(58)
REAL EQUI(21)/79.23,79.47,79.71,78.95,79.19,79.43,79.68,78.92,79.1
16,79.40,79.64,78.89,79.13,79.37,79.61,78.86,79.10,79.35,79.59,78.8
24,79.08/
DATA WS/'WS'/
KF = II - 9
GO TO(100,110,120,130,140,150,160,170,180,190,200,210,220,230,240,
1250,260,270,280,290),KF
100 JYR = KYR - 45
A = (DETF(JJ) - DETF(KK) - EQUI(JYR))/365.24
NUL=IABS(LL)
DATA(MM) = SIN(CONST(NUL)*A*6.2832)
IF(DETF(16).LE.0.0.AND.LL.GE.0) DATA(MM) = -DATA(MM)
RETURN
110 A = (DETF(JJ) +CONST(LL))/24.0
DATA(MM) = SIN(A*6.2832)
RETURN
120 IF(OLDC.EQ.WS) DETF(16) = 32.28
JYR = KYR - 45
SLAT = 23.5*SIN((DETF(JJ) - DETF(KK) - EQUI(JYR))*6.2832/365.24)
DATA(MM) = COS((DETF(16) - SLAT)*6.2832/360.0)
RETURN
130 DATA(MM) = COS((DETF(JJ) + CONST(LL))*6.2832/360.0)
RETURN
140 DATA(MM) = 0.0
CH = DETF(JJ) + CONST(LL)
IF(CH.GE.350.0)DATA(MM) = 1.0
RETURN
150 JYR = KYR - 45
A = (DETF(JJ) - DETF(KK) - EQUI(JYR))/365.24
NUL=IABS(LL)
DATA(MM) = COS(CONST(NUL)*A*6.2832)
IF(DETF(16).LE.0.0.AND.LL.GE.0) DATA(MM) = -DATA(MM)
RETURN
160 A = (DETF(JJ) +CONST(LL))/24.0
DATA(MM) = COS(A*6.2832)
RETURN
170 A = (DETF(JJ)-4.0)/25.0 - AINT((DETF(JJ)-4.0)/25.0)
DATA(MM) = SIN(A*6.2832)
RETURN
180 A = (DETF(JJ)-4.0)/25.0 - AINT((DETF(JJ)-4.0)/25.0)
DATA(MM) = COS(A*6.2832)
RETURN
190 IF(OLDC.EQ.WS) DETF(16) = 32.28
JYR = KYR - 45

```


APPENDIX D
TABLE D-1
RESULTS OF SECOND ANALYSIS

Altitude = 40 km

R = .732

<u>VARIABLE</u>	<u>COEFFICIENT</u>	<u>F SCORE</u>	<u>CRITICAL F VALUES</u>	
			<u>F₉₅</u>	<u>F*₉₅</u>
Constant term	.317X10 ⁻²			
Latitude difference (cos)	.866X10 ⁻³	117.	3.8	9.8
Annual (sin)	.221X10 ⁻³	27.0	3.8	9.7
Latitude difference (sin)	.156X10 ⁻³	19.5	3.8	9.6
Annual (cos)	-.179X10 ⁻³	8.1	3.8	9.6
Semi-annual (sin)	-.125X10 ⁻³	11.2	3.8	9.5
Shadow height	-.178X10 ⁻³	10.0	3.8	9.4
Semi-annual (cos)	considered not significant	6.2	3.8	9.3
Remaining Variables	considered not significant	<2		

Altitude = 65 km

R = .822

Constant term	.105X10 ⁻³			
Latitude difference (cos)	.596X10 ⁻⁴	327.	3.8	9.8
Sub-solar angle (cos)	.480X10 ⁻⁴	14.4	3.8	9.7

TABLE D-1
(Continued)

Altitude = 65 km

R = .822

<u>VARIABLE</u>	<u>COEFFICIENT</u>	<u>F SCORE</u>	<u>CRITICAL F VALUES</u>	
			<u>F₉₅</u>	<u>F*₉₅</u>
Diurnal (cos)	.315X10 ⁻⁴	29.4	3.8	9.6
Solar flux reciprocal (current day)	considered not significant	4.4	3.8	9.6
Geomagnetic index (24 hours lag)	considered not significant	3.3	3.8	9.5
Annual (cos)	considered not significant	3.4	3.8	9.4
Remaining Variables	considered not significant	<2.5		

Altitude = 100 km

R = .474

Constant term	.677X10 ⁻⁶			
Latitude difference (cos)	-.322X10 ⁻⁶	11.3	4.1	11.4
Geomagnetic index (6 hours lag)	considered not significant	3.3	4.1	11.3
Solar flux reciprocal (current day)	considered not significant	2.5	4.1	11.2
Remaining variables	considered not significant	2.5	4.1	11.2

TABLE D-2
RESULTS OF THIRD ANALYSIS

Altitude = 30 km

R = .758

<u>VARIABLE</u>	<u>COEFFICIENT</u>	<u>F SCORE</u>	<u>CRITICAL F VALUES</u>	
			<u>F₉₅</u>	<u>F*₉₅</u>
Constant term	.145X10 ⁻¹			
Latitude difference (cos)	.319X10 ⁻²	69.9	3.9	10.3
Latitude difference (sin)	.123X10 ⁻²	29.0	3.9	10.3
Annual (sin)	.885X10 ⁻³	18.5	3.9	10.2
Annual (cos)	-.107X10 ⁻²	11.6	3.9	10.2
Semi-annual (sin)	-.734X10 ⁻³	9.8	3.9	10.1
Sub-solar angle (cos)	considered not significant	7.3	3.9	10.0
Geomagnetic index (21 hours lag)	considered not significant	3.8	3.9	9.9
Remaining variables	considered not significant	<2.5		

Altitude = 40 km

R = .717

Constant term	.311X10 ⁻²	117	3.8	9.8
Latitude difference (cos)	.823X10 ⁻³	27.0	3.8	9.7

TABLE D-2
(Continued)

Altitude - 40 km

R = .717

<u>VARIABLE</u>	<u>COEFFICIENT</u>	<u>F SCORE</u>	<u>CRITICAL F VALUES</u>	
			<u>F₉₅</u>	<u>F*₉₅</u>
Annual (sin)	.259X10 ⁻³	19.5	3.8	9.6
Latitude difference (sin)	.163X10 ⁻³	8.1	3.8	9.6
Annual (cos)	-.159X10 ⁻³	11.2	3.8	9.5
Semi-annual (sin)	-.133X10 ⁻³	10.0	3.8	9.4
Shadow height	considered not significant	6.2	3.8	9.3
Semi-annual (cos)	considered not significant	<2		
Remaining variables	considered not significant			

Altitude = 60 km

R = .716

Constant term	.159X10 ⁻³			
Latitude difference (cos)	.156X10 ⁻³	250	3.8	10.0
Annual (cos)	.944X10 ⁻⁵	13.9	3.8	9.9
Latitude difference (sin)	.161X10 ⁻⁴	10.6	3.8	9.8
Remaining steps lost due to computational error				

TABLE D-2
(Continued)

Altitude = 65 km		R = .822		
VARIABLE	COEFFICIENT	F SCORE	CRITICAL F VALUES	
			<u>F₉₅</u>	<u>F*₉₅</u>
Constant term	.105X10 ⁻³			
Latitude difference (cos)	.596X10 ⁻⁴	327.	3.8	9.8
Sub-solar angle (cos)	.480X10 ⁻⁴	14.4	3.8	9.7
Diurnal (cos)	.315X10 ⁻⁴	29.4	3.8	9.6
Solar flux reciprocal (current day)	considered not significant	4.4	3.8	9.6
Geomagnetic index (24 hours lag)	considered not significant	3.3	3.8	9.5
Annual (cos)	considered not significant	3.4	3.8	9.4
Remaining variables	considered not significant	<2.5		
Altitude = 75 km		R = .703		
Constant term	.180X10 ⁻³			
Latitude difference (cos)	.136X10 ⁻³	13.7	3.9	10.4
Annual (sin)	-.985X10 ⁻⁵	13.2	3.9	10.3
Shadow height	considered not significant	7.6	3.9	10.2

TABLE D-2
(Continued)

Altitude = 75 km

R = .703

<u>VARIABLE</u>	<u>COEFFICIENT</u>	<u>F SCORE</u>	<u>CRITICAL F VALUES</u>	
			<u>F₉₅</u>	<u>F*₉₅</u>
Geomagnetic index (18 hours lag)	considered not signi- ficant	3.9	3.9	10.1
Solar flux (24 hours lag)	considered not signi- ficant	3.5	3.9	10.1
Solar flux (current day)	considered not signi- ficant	3.1	3.9	
Remaining variables	considered not signi- ficant	<3.2		

Altitude = 100 km

R = .474

Constant term	.677X10 ⁻⁶			
Latitude difference (cos)	-.322X10 ⁻⁶	11.3	4.1	11.4
Geomagnetic index (6 hours lag)	considered not signi- ficant	3.3	4.1	11.3
Solar flux recipro- cal (current day)	considered not signi- ficant	2.5	4.1	11.2
Remaining variables	considered not signi- ficant	2.5	4.1	11.2

TABLE D-2
(Continued)

Altitude = 110 km

<u>VARIABLE</u>	<u>COEFFICIENT</u>	<u>F SCORE</u>	<u>CRITICAL F VALUES</u>	
			<u>F₉₅</u>	<u>F*₉₅</u>
Solar flux reci- procal (current day)	*	2.2	4.3	13.3
Solar flux (24 hours lag)	*	5.8	4.4	13.3
Geomagnetic index (9 hours lag)	*	2.6	4.4	13.3

Remaining variables

* no variables can be considered significant

TABLE D-3
RESULTS OF FOURTH ANALYSIS

Altitude = 30 km

R = .775

<u>VARIABLE</u>	<u>COEFFICIENT</u>	<u>F SCORE</u>	<u>CRITICAL F VALUES</u>	
			<u>F₉₅</u>	<u>F*₉₅</u>
Constant term	.107X10 ⁻¹			
Latitude difference (cos)	.622X10 ⁻³	69.9	3.9	11.0
Latitude X annual (cos)	-.119X10 ⁻³	39.6	3.9	10.9
Semi-annual (sin)	-.796X10 ⁻³	19.6	3.9	10.9
Latitude difference (sin)	.381X10 ⁻²	13.4	3.9	10.8
Sin latitude X annual (cos)	.678X10 ⁻²	7.5	3.9	10.8
Solar flux linear (1-day lag)	considered not signi- ficant	6.8	3.9	10.8
Solar flux recipro- cal (1-day lag)	considered not signi- ficant	7.9	3.9	10.7
Sin latitude X annual (sin)	considered not signi- ficant	3.7	3.9	10.7

Altitude = 35 km

R = .819

Constant term	.817X10 ⁻²			
Latitude X annual (sin)	.616X10 ⁻⁴	136	3.8	10.8

TABLE D-3
(Continued)

Altitude = 35 km

R = .819

<u>VARIABLE</u>	<u>COEFFICIENT</u>	<u>F SCORE</u>	<u>CRITICAL F VALUES</u>	
			<u>F₉₅</u>	<u>F*₉₅</u>
Latitude difference (sin)	.389X10 ⁻³	44.0	3.8	10.7
Latitude (absolute value)	-.122X10 ⁻⁴	25.6	3.8	10.7
Latitude X annual (cos)	-.471X10 ⁻⁴	14.2	3.8	10.6
Semi-annual (sin)	-.288X10 ⁻³	15.7	3.8	10.5
Sin latitude X annual (sin)	-.308X10 ⁻²	10.6	3.8	10.4
Sin latitude X annual (cos)	.281X10 ⁻²	9.3	3.8	10.4
Semi-annual (sin)	considered not signi- ficant	1.9	3.8	10.3
Geomagnetic index (6 hours lag)	considered not signi- ficant		3.8	10.3

Altitude = 40 km

R = .827

Constant term	.392X10 ⁻²			
Latitude X annual (sin)	.412X10 ⁻⁴	225	3.8	10.6

TABLE D-3
(Continued)

Altitude = 40 km

R = .827

<u>VARIABLE</u>	<u>COEFFICIENT</u>	<u>F SCORE</u>	<u>CRITICAL F VALUES</u>	
			F ₉₅	F* ₉₅
Latitude difference (sin)	.209X10 ⁻³	26.8	3.8	10.6
Latitude (absolute value)	-.685X10 ⁻⁵	39.7	3.8	10.5
Sin latitude X annual (sin)	-.200X100 ⁻²	24.0	3.8	10.5
Latitude X annual (cos)	-.241X10 ⁻⁵	11.1	3.8	10.4
Annual (cos)	considered not significant	6.9	3.8	10.4
Latitude difference (sin)	considered not significant	4.7	3.8	10.3
Semi-annual (sin)	considered not significant	4.8	3.8	10.3
Latitude difference (cos)	considered not significant		3.8	10.2

Altitude = 45 km

R = .747

Constant term	.169X10 ⁻²			
Latitude X annual (sin)	.238X10 ⁻⁴	206	3.8	10.6

TABLE D-3
(Continued)

Altitude = 45 km

R = .747

<u>VARIABLE</u>	<u>COEFFICIENT</u>	<u>F SCORE</u>	<u>CRITICAL F VALUES</u>	
			<u>F₉₅</u>	<u>F*₉₅</u>
Sin latitude X annual (sin)	$-.131 \times 10^{-2}$	58.6	3.8	10.6
Latitude difference (cos)	$.209 \times 10^{-3}$	18.2	3.8	10.5
Latitude X annual (cos)	$-.180 \times 10^{-5}$	16.8	3.8	10.5
Annual (sin) not adjusted for hemisphere	considered not signi- ficant	10.4	3.8	10.4
Latitude (cos)	considered not signi- ficant	7.5	3.8	10.4
Solar flux linear (1-day lag)	considered not signi- ficant	6.6	3.8	10.3
Semi-annual (sin)	considered not signi- ficant	4.5	3.8	10.3
Semi-annual (cos)	considered not signi- ficant	4.6	3.8	10.2
Sin latitude X annual (cos)	considered not signi- ficant	3.5	3.8	10.2
Sub-solar angle (sin)	considered not signi- ficant	4.75	3.8	10.2

TABLE D-3
(Continued)

Altitude = 50 km

R = .745

<u>VARIABLE</u>	<u>COEFFICIENT</u>	<u>F SCORE</u>	<u>CRITICAL F VALUES</u>	
			<u>F₉₅</u>	<u>F*₉₅</u>
Constant term	.784X10 ⁻³			
Latitude X sin annual (sin)	.185X10 ⁻⁴	202	3.8	10.6
Sin latitude X annual (sin)	-.107X10 ⁻²	27.8	3.8	10.6
Latitude difference (cos)	.229X10 ⁻³	41.5	3.8	10.5
Latitude difference (sin)	.483X10 ⁻⁴	20.3	3.8	10.5
Latitude X annual (cos)	considered not signi- ficant	6.0	3.8	10.4
Subsolar angle (cos)	considered not signi- ficant	5.1	3.8	10.4
Shadow height	considered not signi- ficant	6.3	3.8	10.3
Diurnal (sin)	considered not signi- ficant	5.4	3.8	10.3
Semi-annual (sin)	considered not signifi- cant	3.3	3.8	10.2
Solar flux reci- procal (1-day lag)	considered not signifi- cant	3.3	3.8	10.2

TABLE D-3
(Continued)

Altitude = 55 km

R = .771

VARIABLE	COEFFICIENT	F SCORE	CRITICAL F VALUES	
			F ₉₅	F* ₉₅
Constant term	.407X10 ⁻³			
Latitude X annual (sin)	.114X10 ⁻⁴	233	3.8	10.6
Sin latitude X annual (sin)	-.660X10 ⁻³	35.8	3.8	10.6
Latitude difference (cos)	.144X10 ⁻³	47.1	3.8	10.5
Latitude difference (sin)	.247X10 ⁻⁴	13.0	3.8	10.5
Diurnal (sin)	-.122X10 ⁻⁴	7.9	3.8	10.4
Latitude X annual (cos)	considered not signi- ficant	6.9	3.8	10.4
Annual (sin)	considered not signi- ficant	4.7	3.8	10.3
Geomagnetic index (12 hours lag)	considered not signi- ficant	3.6	3.8	10.3

Altitude = 60 km

R = .777

Constant term	.939X10 ⁻⁴			
Latitude difference (cos)	.181X10 ⁻³	250	3.8	10.6

TABLE D-3
(Continued)

Altitude = 60 km

R = .777

VARIABLE	COEFFICIENT	F SCORE	CRITICAL F VALUES	
			F ₉₅	F* ₉₅
Latitude difference (sin)	.101X10 ⁻³	27.9	3.8	10.6
Latitude X annual (sin)	.776X10 ⁻⁶	42.7	3.8	10.6
Latitude X annual (cos)	-.272X10 ⁻⁶	16.3	3.8	10.5
Latitude (absolute value)	considered not significant	6.7	3.8	10.5
Latitude difference (sin)	considered not significant	4.6	3.8	10.4
Annual (sin)	considered not significant	7.1	3.8	10.4
Diurnal (sin)	considered not significant	6.0	3.8	10.3
25 day(sin)	considered not significant	3.7	3.8	10.3

Altitude = 65 km

R = .867

Constant term	.237X10 ⁻³			
Latitude difference (cos)	-.562X10 ⁻⁴	327	3.8	10.6

TABLE D-3
(Continued)

Altitude = 65 km

R = .867

VARIABLE	COEFFICIENT	F SCORE	CRITICAL F VALUES	
			F_{95}	F^*_{95}
Latitude X annual (sin)	$.408 \times 10^{-5}$	25.7	3.8	10.6
Sin latitude X annual (sin)	$-.204 \times 10^{-3}$	29.0	3.8	10.5
Latitude sin	$-.761 \times 10^{-4}$	27.1	3.8	10.5
Subsolar angle (cos)	$.333 \times 10^{-4}$	12.5	3.8	10.4
Diurnal (cos)	$.202 \times 10^{-4}$	8.7	3.8	10.4
Diurnal (sin)	considered not signi- ficant	6.0	3.8	10.3
Latitude difference (sin)	considered not signi- ficant	4.6	3.8	10.3
Annual (sin)	considered not signi- ficant	4.3	3.8	10.3
Latitude difference (sin ²)	considered not signi- ficant	4.8	3.8	10.2

Altitude = 70 km

R = .825

Constant term	$.843 \times 10^{-4}$			
Latitude X annual (sin)	$.195 \times 10^{-5}$	256	3.9	11.0

TABLE D-3
(Continued)

Altitude = 70 km

R = .825

<u>VARIABLE</u>	<u>COEFFICIENT</u>	<u>F SCORE</u>	<u>CRITICAL F VALUES</u>	
			<u>F₉₅</u>	<u>F*₉₅</u>
Latitude (sin)	$-.152 \times 10^{-4}$	23.6	3.9	10.9
Sin latitude X annual (sin)	$-.999 \times 10^{-4}$	15.4	3.9	10.9
Shadow height	considered not signi- ficant	8.1	3.9	10.8
Geomagnetic index (18 hours lag)	considered not signi- ficant	4.7	3.9	10.8
25 day period (sin)	considered not signi- ficant	4.8	3.9	10.8
Annual (sin)	considered not signi- ficant	2.9	3.9	10.7
Geomagnetic index (15 hours lag)	considered not signi- ficant	3.0	3.9	10.7

Altitude = 75 km

R = .824

Constant term	$.365 \times 10^{-4}$			
Latitude X annual (sin)	$.105 \times 10^{-5}$	206 .	3.8	10.8
Sin latitude X annual (sin)	$-.558 \times 10^{-4}$	21.5	3.8	10.7

TABLE D-3
(Continued)

Altitude = 75 km

R = .824

<u>VARIABLE</u>	<u>COEFFICIENT</u>	<u>F SCORE</u>	<u>CRITICAL F VALUES</u>	
			<u>F₉₅</u>	<u>F*₉₅</u>
Geomagnetic index (18 hours lag)	$-.878 \times 10^{-7}$	12.7	3.8	10.7
Semi-annual (sin)	$.140 \times 10^{-5}$	10.7	3.8	10.6
Subsolar angle (cos)	considered not signi- ficant	3.9	3.8	10.5
25 day period (sin)	considered not signi- ficant	4.0	3.8	10.4

Altitude = 80 km

R = .696

Constant term	$.161 \times 10^{-4}$			
Latitude X annual (sin)	$.519 \times 10^{-6}$	94	3.9	11.0
Sin latitude X annual (sin)	$-.291 \times 10^{-4}$	15.7	3.9	10.9
Solar flux linear (current day)	considered not signi- ficant	3.9	3.9	10.9
25 day period (sin)	considered not signi- ficant	2.9	3.9	10.8
Latitude difference (sin)	considered not signi- ficant		3.9	10.8

TABLE D-3
(Continued)

Altitude = 85 km

R = .333

<u>VARIABLE</u>	<u>COEFFICIENT</u>	<u>F SCORE</u>	<u>CRITICAL F VALUES</u>	
			<u>F₉₅</u>	<u>F*₉₅</u>
Constant term	.699X10 ⁻⁵			
Sin latitude X annual (sin)	.126X10 ⁻⁵	12.7	3.9	11.2
25 day period (sin)	considered not signi- ficant	6.9	3.9	11.1
Latitude X annual (cos)	considered not signi- ficant	5.9	3.9	11.0
Solar flux linear (1-day lag)	considered not signi- ficant	4.2	3.9	11.0
Annual (sin)	considered not signi- ficant	6.1	3.9	10.9
Geomagnetic index (9 hours lag)	considered not signi- ficant	1.8	3.9	10.9

TABLE D-3
(Continued)

Altitude = 90 km

R = .404

<u>VARIABLE</u>	<u>COEFFICIENT</u>	<u>F SCORE</u>	<u>CRITICAL F VALUES</u>	
			<u>F₉₅</u>	<u>F*₉₅</u>
Constant term	.282X10 ⁻⁵			
Geomagnetic index (6 hours lag)	.200X10 ⁻⁷	5.4	4.0	11.6
Geomagnetic index (9 hours lag)	-.155X10 ⁻⁷	6.5	4.0	11.5
Semi-annual (sin)	considered not signi- ficant	5.0	4.0	11.4
Annual (cos)	considered not signi- ficant	4.5	4.0	11.4
Semi-annual (cos)	considered not signi- ficant	2.1	4.0	11.4

Altitude = 95 km

R = .735

Constant term	.332X10 ⁻⁵			
Latitude difference (cos)	-.183X10 ⁻⁵	16.6	4.0	12.0
Latitude difference (sin)	-.142X10 ⁻⁵	11.0	4.0	11.9
Annual (sin)	-.204X10 ⁻⁶	10.0	4.0	11.9
Geomagnetic index (24 hours lag)	-.695X10 ⁻⁸	8.8	4.0	11.8
Geomagnetic index (0 hours lag)	considered not signi- ficant	3.9	4.0	11.8
Semi-annual (sin)	considered not signi- ficant	3.2	4.0	11.7

TABLE D-3
(Continued)

Altitude = 100 km

R = .474

<u>VARIABLE</u>	<u>COEFFICIENT</u>	<u>F SCORE</u>	<u>CRITICAL F VALUES</u>	
			<u>F₉₅</u>	<u>F*₉₅</u>
Constant term	.677X10 ⁻⁶			
Latitude difference (cos)	-.322X10 ⁻⁶	11.3	4.1	12.3
Latitude difference (sin ²)	considered not signi- ficant	5.8	4.1	12.3
Geomagnetic index (6 hours lag)	considered not signi- ficant	3.9	4.1	12.2
Latitude difference (sin)	considered not signi- ficant	1.3	4.1	12.2

Altitude = 105 km

Constant term				
Latitude difference (sin ²)	*	7.4	4.1	12.5

* not considered significant

TABLE D-3
(Continued)

Altitude = 105 km

<u>VARIABLE</u>	<u>COEFFICIENT</u>	<u>F SCORE</u>	<u>CRITICAL F VALUES</u>	
			<u>F₉₅</u>	<u>F*₉₅</u>
Subsolar angle (sin)	*	2.4	4.1	12.4
Latitude X annual (sin)	*	1.6	4.1	12.4

* no variables can be considered significant

Altitude = 110 km

Constant term

Latitude X annual (cos.)	*	5.3	4.3	14.2
Semi-annual (cos)	*	4.2	4.3	14.2
Sub-solar angle (sin)	*	6.2	4.3	14.2
Latitude difference (sin)	*	2.8	4.3	14.2

* no variables can be considered significant